1-1-2003

Evaluation of driver visual demand in complex two dimensional rural highway alignments

Chandi D. Ganguly
Ryerson University

EVALUATION OF DRIVER VISUAL DEMAND IN COMPLEX TWO DIMENSIONAL RURAL HIGHWAY ALIGNMENTS

By

Chandi D Ganguly, P.Eng
B.C.E. (Jadavpur University, India, 1985), M.Tech (Indian Institute of Technology, Kharagpur, India, 2001)

A thesis

Presented to Ryerson University

In partial fulfillment of the requirement of degree of

Master of Applied Science

In the Program of

Civil Engineering

Toronto, Ontario, Canada, 2003

National Library of Canada
Bibliothèque nationale du Canada

Acquisitions and Bibliographic Services
Acquisisitons et services bibliographiques

395 Wellington Street
Ottawa ON K1A 0N4
Canada

395, rue Wellington
Ottawa ON K1A 0N4
Canada

Your file Votre référence
ISBN: 0-612-87155-X
Our file Notre référence
ISBN: 0-612-87155-X

Author's Declaration

I hereby declare that I am the sole author of the thesis.

I authorize Ryerson University to lend this thesis to other institutions or individuals for the purpose of scholarly research.

Signature

I further authorize Ryerson University to reproduce this thesis by photocopying or by other means, in total or part, at the request of other institutions or individuals for the purpose of scholarly research.

Signature

Borrowers

Borrowers undertake to give proper credit for any use made of the thesis. Ryerson University requires the signatures ofall persons using or photocopying this thesis.

Please sign below and give address and date

Name	Signature of Borrower	Address	Date

Evaluation of Driver Visual Demand in Complex Two Dimensional Rural Highway Alignments

By

Chandi D Ganguly, P.Eng

Master of Applied Science in Civil Engineering

Department of Civil Engineering

Ryerson University, Toronto

April 2003

Abstract

Transportation has proven to be one of the most important infrastructures in the economic development of any country. Safe and effective traffic operations support growth of the economy and help in future developments. Highway alignment design plays a crucial role in implementing safer traffic operation and management. Road accidents not only jeopardize safety, but also have a major effect on the national economy. These accidents can be divided in three classes, grouped according to their severity. Statistics in North America and Europe show that one of the major reasons for such road accidents is driver error. Wrong decisions during navigation may be the primary reason for such errors. Wrong decisions occur when a driver is unable to process the range of visual information available in a complex highway situation.

Drivers need to have sufficient visual information in guiding and controlling vehicles along the correct path. Drivers scan the roadway to collect visual information. This visual information consists mainly of the traffic situation, roadway signs, and the

information from the highway alignment itself. The information from the highway alignment plays a major role in decision-making during maneuvering. All drivers, therefore, need sufficient visual information for perfect navigating, and for guiding and controlling their vehicles on the road.

The main focus of this research study was on evaluating visual demands on two-dimensional highway alignments with an emphasis on determining the effect of complex curves on visual demand. Complex curves are defined as combinations of simple, compound, and reverse curves in a series. Eighteen hypothetical alignments for two-lane rural highways have been developed following the standard guidelines of the Transportation Association of Canada (TAC) and American Association of State Highway Transportation Officials (AASHTO). These alignments were simulated in a low-cost driving simulator. A series of experiments was carried out using the visual occlusion method.

Nine subject drivers drove in the simulator, and the output data related to visual demand information and positioning of the subject vehicle were collected. The data relating to visual demand information and lateral positioning on curves and tangents were processed using Microsoft Excel™ and analyzed using SAS, a statistical software. The turning directions, characteristics of preceding elements, and the combination of curve to curve, tangent to curve, or curve to tangent have been considered as nominal variables and analyzed as independent variables with visual demand.

It has been observed that visual demand varies widely with the inverse of radius of curvature of the preceding and current elements, and the characteristics of the combination of the current and the preceding element. The statistical significance of some preceding element characteristics, e.g., the radius of the preceding curve, indicates that complex curves have a considerable effect on visual demand. Visual demand also varies on identical tangents, depending on the deflection angle, inverse of radius, and turning direction of the preceding curve. The standard deviation of lateral positioning of the subject vehicle was evaluated with respect to the centre-line of the driving lane. This was supposed to have a considerable impact on visual demand evaluation, but it has been observed that this does not bear any significant relationship to visual demand. Hence, the investigation on lateral positioning was not carried out any further. However, models to evaluate the visual demand on complex curves and intermediate tangents have been developed. In developing these models, it became clear that preceding curves in compound and reverse curves have a huge effect on the visual demand on the following curves. In addition to curves, tangents, as preceding elements have an immense impact on visual demand evaluation on following curves. Besides, visual demand on tangents has also been observed as highly dependent on the preceding curve and their turning directions.

Acknowledgements

I would like to thank my supervisor, Dr. Said Easa, for his total support, research freedom, and his excellent guidance and advice at each individual step in this research project. He has not only given advice but also provided most effective suggestions and innovative concepts in developing the final modeling in my thesis. My deepest gratitude goes to Professor Paul Milgram, of the Mechanical and Industrial Engineering Department of University of Toronto, for his active help, guidance, and support in carrying out the entire simulator experimentation. I am also grateful to Dr. Kathryn Woodcock and Dr. Ali Mekky, members of my thesis defence committee, for their thoughtful and diligent comments on my thesis.

I am grateful to Dr. Alison Smiley for allowing me to carry out the experimentation, using the driving simulator at University of Toronto, to accomplish the research objectives. Humble thanks and acknowledgement to my colleagues and friends in the Civil Engineering Department of Ryerson University for their contributions in accomplishing the objective of this research study.

There are not enough words to express my gratitude to my wife and my son for sacrificing their needs and time and for supporting me throughout the successful completion of this research project. Finally, I would like to express my deep feeling of joy to almighty God for the spirit and courage to accomplish this research work during one of the crucial phases in my career.

Dedication

Dedicated to my Parents, who are watching all this from "Holy Abode"

Table of Contents

List of Tables

List of Figures

Chapter 1 INTRODUCTION

1.1 Project Description

Transportation Engineering plays an important role in daily life around the world. The highway and road transportation network is one of the most reliable means for mass movement in both North America and Europe. To meet the extensive demands on the transportation network, it has become mandatory to implement the highest possible range of safety and efficiency practices. The statistics show that most road crashes (approximately 90%) are caused by driver error. It is anticipated that the primary reason for such driver error is the workload imposed by different highway geometric features. These highway geometric features were built based on the standards set by statutory authorities like the American Association of State Highway Transportation Officials (AASHTO) of the United States since 1937.

Organizations such as AASHTO and the Transportation Association of Canada (TAC) from time to time furnish new guidelines to maintain minimal standards in the provision of geometric features. The fact that the guidelines change is one of the main reasons for the varying standards in providing geometric features. These varying standards result in inconsistencies in highway design. Both AASHTO and TAC, in their latest guidelines, have emphasized the importance of consistent highway design. Different studies have evaluated highway design consistency in terms of i) operating speed, ii) alignment indices, and iii) driver workload. However, there has been very little evaluation of driver workload, probably because of the difficulty of measuring this workload directly.

This research emphasizes analyzing human factors involvement as a reason for driver error. The principal cause of mental workload generation for any driver relates to the visual information conveyed by the road. Mental workload builds up, while driving, through these steps: scanning of visual information, processing of all such information, making decisions, and then implementing such decisions.

In this research, an attempt has been made to evaluate visual demands made on drivers while they negotiate different geometric features. This research also attempts to evaluate performance in terms of the lateral position of the subject's vehicle while maneuvering in a two-dimensional (2D) highway alignment. Its focus is the effect of complex curves, i.e., the combination of simple curves, compound curves, and reverse curves in a stretch, on visual demand. In addition, a model has been developed to evaluate maximum visual demand during lane extrusion.

This research work was undertaken as partial fulfillment of a Master's degree. It was intended to conceptualize the evaluation of visual demand in a two-dimensional highway alignment. The change in visual demand effected by varying geometric features will be used to measure design inconsistencies. This concept should be applied to rectify such inconsistencies so that visual demand on consecutive elements varies only within a prescribed limit.

1.2 Research Motivation and Objectives

The geometric design of highways has been a primary issue ever since the inception of the automobiles. Highway design standards and methods were introduced in 1937, as a result of the work of a special committee on Administrative Design Policy under AASHO. The committee was to formulate administrative policies aimed at stimulating uniform practices of effective highway design to maximize safety and usefulness.

Since then, a number of policies have been framed, amended, changed, and improved in highway geometric design practices to improve the efficiency, safety, and performance of traffic operation. However, there exists a gap in bridging the changing standards; as a result, inconsistencies crop up among the published standards. Recently, AASHTO and TAC have emphasized providing consistent geometric design for highways to promote safety throughout the transportation network.

One of the best ways to arrive at this goal is to develop a set of design standards, as per the highway users'/ drivers' choice, or to verify the existing design by the same. Research has been conducted to evaluate human factors implementation in such design and to formulate theories with emphasis on driver behaviour (Kahneman 1973). Consistent design features play an important role in the safety of highway driving. The comparison of overall fatalities shows that the highest percentage of fatalities comes from road accidents, most of which are caused by human error, and more specifically by driver error. An in-depth study to analyze why these situations occur and to recommend appropriate counter measures has long been needed.

The primary reason for driver error is the sudden change in visual information as have been seen by researchers. The sudden change occurs when the expectations of the driver are violated. The dissimilarity in geometric features in adjacent sections of the same highway represents one such violation of driver expectation, resulting in higher perception reaction time of the driver. In turn, the increased perception/reaction time increases the overall time needed to implement a judgment to control the vehicle.

It has been understood that the more complex the information presented, the higher the probability of driver error. The quantity of such information sometimes exceeds the driver's processing capacity. The probability of accident becomes much higher where the workload exceeds this capacity.

Currently, there is much research into estimating driver workload. The focus of such work is to arrive at a method whereby driver workload can be applied in developing consistency in highway design. Most of this work has correlated driver workload to highway design features, primarily degree of curvature or radius of horizontal curve. Some work on highway design consistency has also been done to apply operating speed concepts. However, since most of the accidents are related to human error, it has become mandatory to develop a valid method to ensure highway design consistency related to human behaviour.

The principal objective of this research was to evaluate the impact of complex curves (reverse and compound curves) on visual demand and to develop an aggregated model to evaluate such visual demand for a two-dimensional highway alignment using a driving simulator study. In addition, an attempt was made to develop another model to evaluate visual demand with respect to the lateral positioning of the subject vehicle within the driving. This model was supposed to help determine the threshold of visual demand on a given geometric element. The pilot study had been carried out in two phases. The first phase, to check the variability of mental workload with respect to geometric features, was carried out on Don Valley Parkway, a freeway in Toronto, Canada. This phase was intended to verify the usefulness of the National Aerospace and Space Administration Task Load Index Scale (NASA TLX), which can assess mental workload with a multidimensional scale. The second phase was carried out in a driving simulator in the Ergonomics in Tele-operation Research and Control (ETC) Laboratory, situated at University of Toronto, in Toronto, Canada. This phase was intended to verify the effectiveness of the methodology adopted for the purpose of accomplishing the principal objective of the thesis. The thesis work has been carried out as per the flow chart given in Figure 1.

- Literature Review: This chapter deals with an in-depth study of related materials in the scope of highway design and with some attention to ergonomics. Emphasis has been placed on human behaviour as it relates to highway design, design consistency evaluation procedures in practice or under research development, and workload related subjects. All the literature used is grouped under corresponding headings. The workload portion of the literature review covers all established and recognized procedure of measuring such variable.

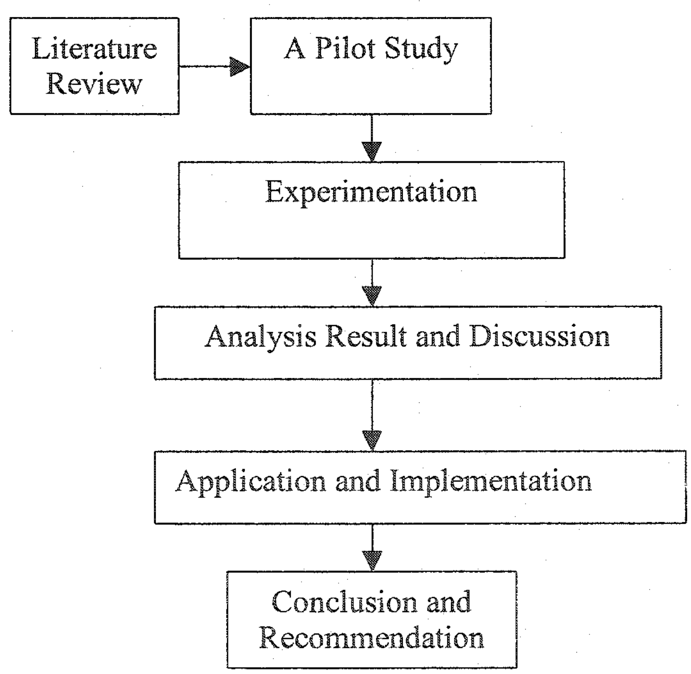

Figure 1 Flow Chart on Thesis Report

Papers related to mental demand and visual demand with respect to highway design have been reported in detail along with the adopted methodology and analysis.

- Pilot Study: Studies were carried out in two phases as to obtain information used in this research. The first of them evaluated mental workload directly using the NASA TLX scale. This study was carried out on an expressway, the Don Valley Parkway (DVP), within the jurisdiction of the City of Toronto. The evaluation of mental workload (MWL) with respect to the highway design parameters was done using NASA TLX.

  The second study was conducted to confirm the visual occlusion methodology and the design of experiments adopted in this research study. This study showed that the experimentation procedure adopted for this research was ideal. The considered output variables, which form the main database for analysis, were also found to be appropriate for evaluating visual demand.

- Experimentation: Experimentation forms the core of this thesis. The evaluation of mental workload in terms of visual demand in relation to highway design parameters depended on a successful experimentation procedure and correct methodology. This chapter deals with the details of the methodology adopted, the design of experiments, the individual steps involved in carrying out the research experimentation using a driving simulator (STISIM) developed by System Technology Incorporated, and the collection and storing of data.

- Analysis, Results, and Discussions: This chapter deals with the procedure adopted to extract data from the STISIM database. Data interpretation, aggregation, and analysis have been discussed, step by step. The development of statistical models is discussed and includes an explanation of the statistical significance of different variables.

- Application and Implementation: This chapter deals the application of the developed model in estimating the design consistency of any given alignment. A comparative study using operating speed consistency, the alignment indices consistency, and visual demand consistency method has been carried out.
- Conclusion and Recommendation: This chapter concludes with gross findings and their acceptability, adoptability, and applicability in real world situations. Further developments, which need to be incorporated in future studies, are recommended.

1.3 Final Outcome

An effective model for measuring visual demand in a 2D environment has been developed. The effect of complex curves and the impact of the preceding element on visual demand have been evaluated. The estimation of visual demand with respect to lateral placement of the subject vehicle also forms a part of the research study.

Chapter 2 LITERATURE REVIEW

2.1 Background

The geometric aspects of a highway include features that affect or relate to its operational quality and safety. These features, which are visible to the driver and affect driving performance, include elements of the roadways, ramps, and roadside. Roadways have features related to: roadway curvature (horizontal and vertical alignment); intersections and interchanges; cross sections (e.g., number of lanes and lane width, presence of shoulders and curbs); channelization and medians; and other miscellaneous elements (e.g., driveways, bridges). Ramps have features related to: type (e.g., freeway, arterial, entrance, and exit); configuration (e.g., diamond, loop, trumpet, etc.); length; curvature; and other miscellaneous elements (e.g., speed-change lanes). Physical features of the roadside include: barriers (e.g., guide rails); obstacles (e.g., noise barriers, trees, and signs); and other miscellaneous features (e.g., embankment slopes, ditches)

The evolution of geometric design standards and criteria dates back to the late 1930s. The American Association of State Highway and Transportation Officials (AASHTO) has been the source of most of the design values and criteria used in geometric highway design. Although most states and agencies have developed their own standards, the design approach and design values in the AASHTO policies are accepted by consensus and form the basis for individual state design practices. In addition, the Federal Highway Administration (FHWA) has adopted AASHTO policies for design and construction and major reconstruction of Federal-aid highways. The most recent AASHTO design policy reference was published in 2001, "A Policy on Geometric Design of Highways and Streets."

AASHTO highway design policies for sight distance, horizontal and vertical alignment, and associated traffic control devices are based on the following driver performance characteristics: detection and recognition time, perception reaction time, decision and response time, time to perform brake and accelerator movements, maneuver time, and (if applicable) time to shift gears. However, these design standards have typically been based on driving performance (or surrogate driving measures) of the entire driving population, or have been formulated from research biased toward younger (college-age) as opposed to older driver groups. The models underlying these design standards therefore have not, as a rule, included variations to account for slower reaction time or other performance deficits that are consistently demonstrated in research on older driver response capabilities.

In particular, diminished visual performance (e.g. contrast sensitivity), physical capability (e.g. strength to perform control movements), cognitive performance (e.g. attention deficits in choosing reaction time unpredictable stimuli), and perceptual abilities (e.g. accuracy of processing speed-distance information) combine to make the task of negotiating the highway design elements more difficult and less forgiving for older drivers.

Application of human factors in highway design is essential; the driving tasks of control, guidance, and navigation, therefore, needed to be considered in design. Control tasks include the driver's interaction with the vehicle and the lateral and longitudinal control of the vehicle through the steering wheel, accelerator, and brake.

Guidance tasks include the driver's performance in selecting an appropriate and safe path on the highway, as well as driver evaluation of immediate conditions and decisions for control actions relating to lane changes, headway, overtaking, and speed change. Navigation includes the driver's execution of a trip along the course of the highway, using information from maps, guides and signs, and landmarks.

2.2 Consistency of Highway Design

Design and operating speed form the vital part in developing any alignment or in measuring the consistency of design. AASHTO (2001) suggest the following criteria to select design speed:

- Assumed design speed should be a logical one with respect to the topography, the adjacent land use, and the functional classification of the highway.
- Except for local streets where speed controls are frequent and intentional, every effort should be made to use as high a design speed as practicable, to attain a desired degree of safety, mobility, and efficiency within the constraints of environmental quality, economics, aesthetics, and social or political impacts.
- The design speed chosen should be consistent with the speed a driver would like to adopt. Where a difficult condition is obvious, drivers are more apt to accept lower speed operation than when there is no apparent reason for it.
- A highway of higher functional classification may justify a higher design speed than a less important facility in similar topography. This is particularly relevant where the savings in vehicle operation and other operating costs are sufficient to offset the increased cost of right-of-way and construction. A low design speed should not be assumed for a secondary road where the topography is such that

drivers are likely to travel at high speed. Drivers do not adjust speed to the importance of the highway, but to their perception of physical limitations and traffic on the highway.

- The speed selected for design should fit the travel desires and habits of almost all the drivers. A cumulative distribution of vehicle speeds has the typical S pattern when plotted as percent of vehicles versus operating speed. The design speed chosen should have high percent value in this speed distribution curve.
- A pertinent consideration in selecting design speeds is the average trip length. The longer the trip, greater the desire for expeditious movement.

A consistent roadway alignment should meet the expectations of a driver, who can correctly predict the driving path while devoting little visual information capacity (Woodridge et al. 2000). With a consistent roadway alignment, the driver can pay more attention to obstacle avoidance and to navigation. If the geometry of the road ahead does not match expectations, a driver may not have allocated sufficient mental resources to the guidance task. Sight distance limitations and inability to assess features complexity may further add to the demand for mental resources.

Polus et al. (1987) mentioned the following factors that increase or decrease the design consistencies:

- A horizontal curve at the end of a tangent, i.e., a tight curve immediately at the end of a tangent or any curve at the end of a long tangent. In both these cases, the consistency declines markedly.
- Large variation in radii: A curve of higher radius followed by a much lesser radius in a horizontal alignment decreases the design consistency.

- Smaller radius in comparison to average radius of curves also reduces design consistency.

A combined geometric and spectral statistical model was developed for evaluating design consistency.

Lamm et al. (1988) proposed a measure of design consistency of horizontal design as defined by operating speed and accidents expected and emphasized operating speed to evaluate design consistency. The maximum and minimum limits for the length of tangents along any highway had been suggested in relation to operating speed (Lamm et al. 1988). Control of total acceleration/deceleration capability of driver was taken into consideration during the time in which the driver negotiates two corresponding curves. The relation of the tangent length to the average 85th percentile speed, and the difference between these operating speeds while negotiating such curves one after another, was developed. The transition length was quantified based on simple laws of motion and on acceleration/deceleration.

Statistical models were developed to express the speed reduction as a function of geometrics, pavement condition, prevailing terrain, and posted speed variables (Al-Masaeid et al. (1995). The data collected were split into groups according to categories of curves and the preceding or following tangents. The speed reduction model was found to provide a sound statistical characteristic specifically for continuous and reverse curve. It was concluded that, in addition to the degree of the horizontal curve, the length of vertical curve within the horizontal curve, gradient, and pavement condition have a significant effect on consistency of horizontal alignment. Speed reduction as a measure of alignment consistency was greatly affected by the degree of curves.

Krammes (2000) recommended four areas to ensure consistent design, i.e., selection of an appropriate design speed, revision to the design-speed concept to improve operating speed consistency, uniformity of horizontal curve design, and a curve information system for drivers. An appropriate speed, it was suggested, must consider safety aspects. It was recommended that the traditional concept of 85th percentile speed be revised, and a higher percentile was suggested for consideration to arrive at safer and more consistent design. The operating speed was concluded to be reviewed with an emphasis to be made on developing guidelines for major rehabilitation projects.

Also to be reconsidered, they recommended, was the maximum superelevation rate (the rate of road banking at curves) and its application policy, which includes application of equal superelevation of all curves having equal radius independent of design speed. It was assumed that such an arrangement would help drivers fix the path selection for any curve. It was suggested that curve information be supplied with accuracy so that drivers could select an appropriate speed for the safest path to travel.

2.3 Evaluation Measures to Design Consistency

Gibreel et al. (1999) categorized the area of design consistency into three main areas. These areas were: speed consideration, safety consideration, and performance consideration. Speed consideration addresses the effects of different design parameters on the prediction of operating speed. Safety consideration addresses the design parameters on highway safety. It was suggested that special attention be given to superelevation and side friction design on vehicle stability and to the low cost improvement to highway safety. Performance consideration addresses the effect of design parameters on driver workload and driver expectation. Hence, evaluation of design consistency has been divided into the following categories:

i) Evaluation with respect to operating speed along the alignment under consideration.

ii) Evaluation with respect to change in highway geometric features along the stretch under consideration.

iii) Evaluation with respect to change in driver workload along the alignment.

2.3.1 Discussions on Operating Speed

Many factors affect prediction of operating speed, such as radius of horizontal curve, length of the horizontal curve, sight distance, superelevation rate, side friction factor, and pavement condition (Gibreel et al. 1999). Implementation of the design speed concepts evolves two steps (Krammes et al. 1992). First, a design speed is selected "consistent with the speed a driver likes to adopt/expect," based on the functional classification of the highway, development environment, and topography. Then all the pertinent features should be related to the design speed to obtain a balanced design. The design speed concept does not provide sufficient coordination among individual geometric features along an alignment, since it has no meaning on a tangent; however, the speed on the tangent becomes the approach speed to a curve, where this feature violates driver ad hoc expectancy and exhibits undesirable operating-speed profiles.

Geometric design consistency was evaluated using an operating-speed profile to identify undesirable large speed differentials (Leisch et al. 1977). The suggested procedure estimates average running speed for passenger cars and trucks on horizontal curves and tangents including truck speeds on vertical grades. The speed estimating procedures are derived from AASHTO design policies of 1965 and 1973. Researchers recommended a three part, 10-mph rule:

- Average automobile speeds along an alignment should vary by not more than 10-mph.
- Design speed reduction should not exceed 10-mph.
- Average truck speeds should differ from average automobile speeds by no more than 10-mph.

Lamm et al. (1988) developed a regression model to evaluate the operating speed parameter with respect to highway geometry and the traffic volume (vpd). The model, as follows, has a R^2 value = 0.842 and SEE = 2.814:

$$V_{85} = 34.7 - 1.005*DC + 2.081*LW + 0.174*SW + 0.0004*AADT \qquad (1)$$

where

V_{85} = 85 percentile operating speed,

DC = Degree of curve,

LW = Lane width,

SW = Shoulder width,

AADT = Traffic volume expressed in vehicles per day,

R^2 = Coefficient of Determination, and

SEE = Standard error of estimate (mph).

The operating speed model was developed with respect to the degree of curvature and posted speed ((Lamm et al. 1988). In addition, an estimated accident rate model was developed in relation to degree of curvature and posted speed. Monograms were developed for evaluating operating speed and accident rate with respect to the degree of curvature and the posted speed.

Choureiri et al. (1994) suggested the use of curvature change rate (CCR) to predict operating speed and to locate speed inconsistency on horizontal alignments. The CCR is defined as the absolute sum of the angular changes per unit length of a highway section and is expressed in metric units as:

$$CCR = \frac{57300}{L_J}\left(\sum_i \frac{L_{ci}}{r_i} + \sum_j \frac{L_j}{2r_i}\right) \tag{2}$$

where

CCR = curvature change rate (degrees/Km),

L_{ci} = length of circular curve i (m),

L_j = length of spiral curve j (m),

r_i = radius of circular curve i (m), and

L_J = total length of the section.

Using linear regression, relationships between the 85th percentile operating speed V85 and design parameters were established for different lane widths (Choureiri et al. 1994). For example, a lane width of 3.65 meter produces a model that is given as follows:

$$V_{85} = 95.780 - 0.076 * CCR \tag{3}$$

$$V_{85} = 96.152 - \frac{2803.769}{r} \quad (4)$$

where CCR and r have the same meaning as detailed above. The relationship between V_{85} and horizontal curve character had been further studied by them and resulted in the following equations:

$$V_{85} = 94.398 - \frac{3188.656}{r} \quad (5)$$

The following operating speed model has also been given (Lamm 2000):

$$V85 = \exp(4.561 - 0.000527*CCR_s) \quad (6)$$

where CCR_s = curvature change rate in gon/km.

The development of regression models on speed reduction for different vehicle characteristics with respect to simple circular curves to evaluate design consistency parameters were undertaken by Al-Masaeid et al. (1995). They are as follows:

$$\Delta V_P = 3.64 + 1.78 * DC \quad (7)$$

$$\Delta V_L = 2.0 * DC \quad (8)$$

$$\Delta V_T = 4.32 + 1.44 * DC \quad (9)$$

$$\Delta V_A = 3.30 + 1.58 * DC \quad (10)$$

where ΔV_P, ΔV_L, ΔV_T, ΔV_A are speed reduction from tangent and curve for passenger cars, light trucks, trucks and all vehicles. DC represents the degree of curve, which may be defined as the angle subtended at the centre of the curve by a 30m long arc. In addition, other equations for the change in speed were developed with respect to parameters of highway combined (vertical & horizontal) alignment, which are as follows:

$$\Delta V_A = 1.84 + 1.39 * DC + 4.09 * PC + 0.07 * G^2 \tag{11}$$

$$\Delta V_A = 1.45 + 1.55 * DC + 4.00 * PC + 0.00004 * V_C^2 \tag{12}$$

where

ΔV_A = reduction of speed of all vehicles with respect to DC (degree of curve)

PC = pavement condition (For PSR ≥ 3, PC=0, otherwise 1),

G = gradient in %, average slope between the points of speed measurements on the tangent and the curve centre, and

V_C = vertical curve length within the horizontal curve.

In addition, regression equations for continuous curves and common tangents had also been developed. These regression equations are as follows:

$$\Delta V_P = \frac{5708}{R_2} - \frac{5689}{R_1} \tag{13}$$

$$\Delta V_L = \frac{4957}{R_2} - \frac{4888}{R_1} \tag{14}$$

where R_2 and R_1 represents the radius of the 1st and 2nd curves. The equations relating to tangents are as follows:

$$\Delta V_T = 99.30 - \frac{3099}{LT} - 0.75 * \left(\frac{DF_1 * DF_2}{DF_1 + DF_2} \right) \tag{15}$$

$$\Delta V_A = 108.30 - \frac{3498}{LT} - 0.71 * \left(\frac{DF_1 * DF_2}{DF_1 + DF_2} \right) \tag{16}$$

$$\Delta V_P = 115.0 - \frac{3722}{LT} - 0.70 * \left(\frac{DF_1 * DF_2}{DF_1 + DF_2} \right) \quad (17)$$

$$\Delta V_L = 106.0 - \frac{3391}{LT} - 0.73 * \left(\frac{DF_1 * DF_2}{DF_1 + DF_2} \right) \quad (18)$$

where

ΔV_i = reduction of speed occurs to i^{th} category vehicle;

LT= length of common tangent;

DF_i = deflection angles for i^{th} curve.

Kanellaidis et al. (1986) studied speed behaviour of drivers on horizontal alignments of two-lane highways. Their equation is as follows:

$$V_{85} = 129.88 - 623.1 / r^{1/2} \quad (19)$$

Anderson et al. (1999) examined geometric design consistency for two-lane rural highway alignments with respect to five candidate measures: speed reduction on a horizontal curve relative to preceding tangent or curve, average radius along the alignment, ratio of maximum radius to minimum radius, average rate of vertical curvature, and ratio of individual curve radius to average radius. An accident prediction model was developed in relation to AADT, length of horizontal curve (CL) and speed reduction (SR) from adjacent tangent to the curve. The equation stands as follows:

$$Y = \exp^{(-7.1977)} * (AADT)^{0.9224} * (CL)^{0.8419} * \exp^{(0.0662*SR)} \quad (20)$$

Ottesen et al. (2000) assumed speeds on curves are constant and acceleration or deceleration occurs only on the tangents. Three cases depending on the occurrence of maximum 85^{th} percentile speed were formulated, i.e., drivers accelerate uniformly between the curves and thus the maximum 85 percentile speed occurs at the end of tangent, the tangent is long enough for some acceleration but not long enough for the drivers to reach and sustain their desired speed at normal acceleration or deceleration rate, and the tangent is long enough to make the driver reach and for some distance sustain the desired speed. The concept of critical tangent length was developed, and is given as follows:

$$TL_c = (2V_t^2 - V85_1^2 - V85_2^2)/ (25.92*a) \quad (21)$$

where

TL_c = critical tangent length

V_t and $V85_i$ = desired speed (km/h) on the tangent and i^{th} curve respectively, and

a = rate of acceleration/ deceleration (0.85 m/s^2).

Using speed data on rural two-lane highways in Alberta, a model was developed on V_{85} (km/h) on horizontal curve to the degree of curve (Morrall et al. 1994), as follows:

$$V_{85} = \exp^{(4.561-0.0058DC)} \quad (22)$$

where DC is the degree of curve, i.e., central angle subtended by a 100m arc of the curve. The database used to develop this model belongs to level terrain and is related to simple horizontal curve with constant lane and shoulder width.

Operating speed was modeled based on observation of a specific highway in Ontario (Hassan et al. 2000). The 85^{th} percentile speed was used to predict the profile of operating speed, and obtained operating speed from the developed model was compared to field measurement. Sight distance was developed using a three-dimensional approach during both daytime and nighttime. The obtained operating speeds were checked with respect to vehicle stability, whereas the maximum allowable speeds were determined with respect to stability. Models were developed to account for the tire to tire friction variation and interaction between longitudinal and side friction.

2.3.2 Discussions on Geometric Features

The design consistency with respect to geometric elements mainly produces safe traffic operation and efficient driving performance. Pignataro (1975) studied the relationship between accident rate and cross-section design. The results show that the total accident rate per million vehicle miles on two-lane rural highways decreased from 5.5 to 2.4 as the pavement width increased from 5.0m to 7.5m. It was also found that the accident rate decreased by 22% for the two-lane rural road with low traffic volume and by 47% for the two-lane rural highway with high traffic volume when the pavement width was widened from 5.5 to 6.7 meters.

Design consistency was evaluated by developing some geometric models (Polus et al. 1987) as follows:

$$L_c = \frac{l_c}{l_c + l_T}; R_R = \frac{R_{min}}{R_{max}}; R_D = \frac{R_{avg}}{R_{vd}} \tag{23}$$

where

L_c = ratio between the length of the curves to the total length of the same section,

l_c = length of the curved sections

l_t = length of the straight sections,

R_R= ratio of minimum (R_{min}) to maximum radius (R_{max}) of the existing or proposed curves, and

R_D= ratio of average radius (R_{avg}) to minimum radius required for design speed (R_{VD}).

Design consistency on geometric features of any alignment is explained as follows (Lamm et al. 1988):

Case 1: (Good Design) – Range of change in degree of curve: $\Delta DC \leq 5^0$;Range of change in operating Speed: $\Delta V_{85} \leq$ 6mph (10Km/h).

Case 2: (Fair Design) – Range of change in degree of curve: $5^0 < \Delta DC \leq 10^0$; Range of change in operating Speed: 6mph $< \Delta V_{85} \leq$ 12mph (20Km/h).

Case 3: (Poor Design) – Range of change in degree of curve: $\Delta DC > 10^0$;Range of change in operating Speed:$\Delta V_{85} >$ 12mph (20Km/h).

The relation of tangent length to the average 85th percentile speed and the difference between the operating speeds while negotiating curves one after another has been developed (Lamm et al. 1988). The transition length was quantified as follows:

$$TL = \frac{\overline{V_{85}} * \Delta V_{85}}{1{,}302} \tag{24}$$

where

TL= Length of the transition in feet (Tangent Length), and

V_{85} = 85th percentile of operating speed in mph.

Fink et al. (1995) carried out research work to evaluate accident rate with respect to tangent length and sight distance on and along two-lane highways. They found that occurrence of accidents is mainly a function of excessive workload. The excessive workload generally caused by any geometric features results in loss of control and guidance of the vehicle. The prime causes are either availability of very small perception reaction time (PRT), and/or the vehicular stability on that particular feature. It has been found that the accident rates rise with increasing degrees of curvature.

In a review of design consistency, it is stated that turnings with a radius of less than about 150 meters, following a straight section longer than 400 meter, generates loss of control accidents (Brenac 1996). A sharp turning with partial visibility on a steep downgrade produces an ad hoc expectancy where the drivers generally assume a higher radius curve than the existing one and ends in loss of control crashes. Researchers concluded the following:

- The conventional concept of design speed and the associated design practice do not seem sufficient to ensure consistency of the design horizontal alignment and the safety of curves.
- Introducing the expected actual speeds (necessary in other respects, e.g., to verify sight distance condition) is positive but not sufficient to complete the conventional approach.
- The introduction of consistency rules concerning the succession of the different elements of the horizontal alignment seems necessary from a safety point of view.
- The use of complex curves containing a succession of circular curves and same direction transition curves may generate safety problems, so may be better avoided.

Passetti et al. (1999) worked on the operating speed of passenger cars on circular curve and preceding and following spirals. The study emphasized the actual requirement of providing transition curves or spirals before circular curve. It has been a long-standing recommendation to provide spirals at the location of circular curves. Previous studies that examined vehicle operations on spiral transitions had not used field data collected, but data were simulated through simulation software (HVOSM). It was concluded that the lateral acceleration was as much as 50% greater on circular curves, and that such spiral transition curves allow drivers to follow an easier path than circular curves do (Segal et al. 1979). Using the same software, HVOSM, another researcher concluded that in all cases, the presence of a spiral reduces the friction demand from a value much higher than the design "f" (Glenon et. al. 1984). A regression model for predicting operating speed was developed (Passetti et al. 1999), as follows:

$$V_{85} = 103.9 - 3020.5*(1/R). \quad (25)$$

The findings of the research show:

- For the range of data analyzed, spiral transition did not significantly affect the speed at which passenger cars traversed a horizontal curve on two-lane rural highways.
- Speed prediction models to estimate 85^{th} percentile speeds of passenger cars on horizontal curves do not have to account for the presence of transition curves.
- Inclusion of spiral curves does not produce significant operational benefits for passenger cars.

Several alternative methods for measuring the design consistency of a roadway alignment based on alignment indices have been proposed (Fitzpatrick et al. 1985). Alignment indices are quantitative measures of a general character of a roadway segment's alignment. A common example is at terrain transitions from level to rolling or mountainous, and the alignment correspondingly changes from gentle to more severe.

Alignment indices have several advantages for use in the design consistency evaluation (Fitzpatrick et al. 1985), i.e., alignment indices are easy to use by designers to understand and explain, alignment indices are a function of horizontal and or vertical alignment elements, alignment indices attempt to quantify the interaction between the horizontal and vertical alignment, a design strategy that is currently missing from design policy. The alignment indices could be divided into 1) average radius, 2) ratio of maximum radius to minimum radius, and 3) average rate of vertical curvature, for evaluation of design consistency.

Anderson et al. (1999) developed the following models to evaluate design consistency in terms of predicted number of accidents:

- $Y = \exp^{(-7.845)} * (AADT)^{0.995} * (\ln(\text{Section Length}))^{1.108} * \exp^{(-0.000137*\text{Average Radius})}$ (26)
- $Y = \exp^{(-7.859)} * (AADT)^{0.988} * (\ln(\text{SectionLength}))^{1.058} * \exp^{(0.0043*(\text{Maximum / Minimum Radius})}$ (27)
- $Y = \exp^{(-8.297)} * (AADT)^{1.052} * (\ln(\text{Section Length}))^{1.167} * \exp^{(-0.0028*\text{Average Vertical Curvature Rate})}$ (28)

A more successful parameter was suggested (Lamm et al. 2000) to explain much of the variability of operating speed and accident rate is the curvature change rate of a single curve CCR and is calculated as follows:

$$CCR_s = \frac{63700\left(\frac{L_{c/1}}{2R} + \frac{L_{cr}}{R} + \frac{L_{c/2}}{2R}\right)}{L} \quad (29)$$

where

CCR_s = curvature change rate in gon/km,

L_{cr} = length of the circular curve,

$L_{c/1}$ and $L_{c/2}$ = lengths of the spiral preceding and following the circular curve respectively

R = radius of circular curve, and

L = length of the curve and spirals in meters.

In addition to sight distance, highway horizontal alignments should account for vehicle dynamics on the curve. Design takes care of passenger comfort and vehicle stability while designing horizontal curves. The formula relating to design of the horizontal curve is as follows:

$$R = \frac{V^2}{127(e+f)} \tag{30}$$

where

R = radius of the circular curve,

e = rate of superelevation, and

f = coefficient of side friction.

AASHTO considers mass of the vehicle as a point mass. In fact, this should be considered the mass in a 3D perspective. Hassan et al. (2000, 2001) carried out a study on design consistency on a two-lane highway. Operating speed on each of tangent, spiral before the circular curve, curve, and tangent and spiral after the circular curve were recorded by field measurements. Available sight distances, applying the three-dimensional concept, were estimated both for daytime and nighttime and compared with the standard values prescribed with two dimensional analysis. It was found that 2D values of sight distances are higher than that of 3D during nighttime where a sag curve overlaps with a horizontal curve or where a crest vertical curve overlaps with a horizontal curve at cut section during daytime. On the other hand, it was noted that 2D values are lower than that of 3D values during daytime where a sag curve overlaps with a horizontal curve at cut sections or a crest curve overlaps with a horizontal alignment at a fill section. Design consistency was evaluated using profiles of predicted operating speed and allowable speed with respect to 3D perspective.

2.4 Fundamental Concepts

2.4.1 Driver Workload

Driver workload may be defined as the load imparted on a driver while driving a vehicle on a roadway. This load generally relates to the psychological load/ stress involved in collecting different information from the roadway ahead, processing those observations, making necessary decisions and implementing those decisions, one by one, in controlling the movement of the vehicle. It is clearly understood that the information may be relevant or irrelevant to driving perspective. Drivers must always decide whether the information is relevant or irrelevant. As a result, driver workload can be divided into direct workload and indirect workload. Some of the available information, which is relevant to navigate and control the vehicle in motion, causes the direct workload on the driver, while the irrelevant information causes indirect workload.

The direct workload, however, is much more vital to driving, and this should lie between a well-defined lower limit and an upper limit to arrive at the best performance. It is understood that a direct workload level lower than a particular level distracts the driver, which results in bad driving performance. It is also understood that a direct workload beyond a maximum level involves so many alternative decisions that driving performance declines.

The indirect workload builds up from processing irrelevant information and distracts drivers from the main task of driving. Hence, all the roadways need to be designed in such a way that each driver is kept busy processing relevant up to a distinct level of workload. Driver workload varies all the time. The variation of this stress is a function of the complexity of the relevant information. The complexity of the total information, when processed in the brain, generates a number of alternative ways to handle the situation and to control maneuvering. The volume of information is expressed in bits. For example, if any information has only one alternative to implement, it is enumerated as zero bits of information. In the case of information that has eight alternatives to implement, it is enumerated as 3 bits of information. Hence, the relation of bits of information to the number of alternative decisions could be given as 2^x= Number of alternatives, where x is the bit of information.

AASHTO (2001) has used the above relationship for the quantities of such information and the reaction time. However, the reaction time again relates to feature/ information that is different from the expectation of the driver. AASHTO described the driving task as a combination of three levels: control, guidance, and navigation. These activities are ordered on scales of complexities and importance for safety. Of these three major components, highway design and traffic operations have the greatest effect on guidance. Design should emphasize the guidance task component, which should be a governing principle for the highway designer who wants to aid to driver performance.

Workload has been defined as "a measure of the 'effort' expended by a human operator while performing a task, independently of the performance of the task itself" (Senders 1998). Another definition of workload was given as the answer to two questions: "How much attention is required?" and "How well will the operator be able to perform additional tasks?" (Knowles 1987)

Driver workload has been examined by many researchers. The definition of driver workload has also been given in many ways. The following section deals with the definitions developed by the previous researchers: Driver workload is defined as the time rate at which driver must perform a given amount of work or driving tasks (Krammes et al. 1992). This definition relates to that developed by Messer et al. (1979), which states driver workload increases with increasing geometric complexities and as the time available to perform a given amount of work decreases because of the increase in speed or decrease in available sight distance.

A research on simulator-based assessment of driver workload was carried out in South Korea (Cha et al. 1997). The research paper describes driver workload as: "Although there is no universally accepted definition of the mental workload, the basic notion is related to the difference between the amount of resources available within a person and the amount of resources demanded by the task situation." Therefore, altering either the amount of resources available within the person or the demands made by the task on the person can change the mental workload (McCormick et al. 1992). Another definition considers that mental workload is the ratio of the task demands to the average of maximal capacity of each individual. It must be noted that individual maximal capacity is variable. Generally, as the task demand increases, so does the workload (Pauzie et al. 1995). Driver workload was suggested as a function of highway characteristics and vehicle operation (Heger 1998).

Different researchers have emphasized visual demand as it relates to driving efficiency. Perception of the visual environment is, by far, the most important clue that guides both driving in general, and speed estimation while driving. It is widely believed that 90% of the information necessary for driving is derived from the visual environment. In contrast, only 10% is considered to originate from the auditory and proprioceptive senses, and from monitoring information sources, such as the speedometer (Hartman 1970, Rockwell 1972, Hills 1980, Lay 1986, Olson 1993). However, it had been argued that while the information relevant to driving is predominantly visual, it is premature to conclude that it amounts to 90% of the information used" (Sivak 1996).

Drivers' awareness of their travel speed is often based primarily on subjective estimates from the environment rather than from the use of the speedometer. This is especially so during speed-sensitive vehicle maneuvers (Denton 1969, Recarte et al. 1996). The direction and velocity of the arrays of the optical flow is known as the motion perspective. The relative velocities of these vectors are governed by motion parallax (Gordon 1965). That is, if looking straight ahead when moving, the velocities of elements in an observer's visual field are inversely proportional to the distance they are from the observer. This also holds when looking in any direction while moving, since near objects change their angular direction more than distant objects (Gibson 1950). This fact has been well established empirically.

According to the original capacity model by Kahneman (1973), the human information processing system consists of a resource pool of limited capacity. The limit of this capacity determines the limit of information that can be stored, processed, and transmitted at a particular time. Different tasks impose different demands on this resource pool, with more difficult tasks imposing a greater demand. When the supply of attention capacity (or resources) cannot meet the demands, performance will either deteriorate or fail completely. For example, a driver may be performing two tasks simultaneously, such as maintaining a specific headway distance (primary task) whilst engaging in a mobile phone conversation (secondary task). If resource demands of both tasks combined reach the limit of the resources available, allocating more resources to the primary driving task, either to improve its performance, or to maintain its performance when it is made more difficult, should only occur at the expense of a reduced performance on the secondary task.

This strict undifferentiated capacity model, where all processes draw on a single resource pool, however, cannot always account for empirical data (Wickens 1984). This led researchers to propose the concept of independent multiple pools from which tasks can draw resources; this concept is known as multiple resource theory (Navon et al. 1979). According to this model, each specific resource pool has its own capacity, and can be shared by a number of processes concurrently. However, different tasks may also use different resource pools. Thus, if concurrent tasks do not demand resources from any of the same pools, it should be possible to perform them in parallel without decrement. However, tasks are generally considered to use resources from a number of pools. A concurrent task may use some of the same resource pools, whilst not sharing others. Researcher had also elaborated on the non-specific multiple resource theory of Navon and Gopher (1979) with a model containing specific resource pools for specific tasks (Wickens 1984).

Driving and mental workload was described as follows: "Driving is a complex task, although it is often considered by drivers to be a non-strenuous activity (Shinar 1978). While driving, attention needs to be directed towards longitudinal control (velocity and headway), lateral control (lane position and curve negotiation), navigation, monitoring and operating the vehicle, predicting, recognizing, and reacting to hazards, and often but less importantly, attending to communications with passengers, mobile phones, and the radio (Schlegel 1993). To enable driving to continue at the same level of control, an increase in workload in any of these areas requires more attention resources to be directed towards that area.

Mental workload while driving can be higher than usual for a number of reasons. These include heavy traffic conditions (Brown et al. 1961, Zeitlin 1995), built-up surroundings and kinesthetic (Zeitlin 1995), sleep deprivation, time of the day (Lenne 1997), use of a mobile phone and car radio (Briem et al. 1995), increasing curvature of horizontal curves (McDonald et al. 1975), decreased lane width (DeWaard et al. 1995), and importantly, faster driving speeds (Alm et al. 1994, Brown et al. 1961, McDonald et al. 1975, DeWaard et al. 1995).

For example, driving through a village, instead of on an open road (Harms 1991), increases workload because it requires more attention to be directed towards hazard detection. A narrower lane will increase workload as it increases the amount of attention that needs to be directed towards lateral control (DeWaard et al. 1995). Thus, in these two situations (village and narrow lane widths), there is less mental capacity available for the driver to concentrate on other driving tasks. As drivers can choose where to direct their attention, it can be speculated that attention resources will be withheld from those aspects of the driving task which have the least dangerous consequences from a less than optimal performance. These may include reducing speed and ignoring the radio or conversations with passengers or mobile phones (although other personal motivations can also influence where a driver directs attention away from). Therefore, in addition to shedding non-driving tasks, it had been suggested (with supporting evidence) that drivers primarily compensate for increased attention demands by reducing their speeds (DeWaard et al. 1995).

Federal Highway Authority of United States (FHWA) has been developing geometric design software, Interactive Highway Safety Design Model (IHSDM), which implements design consistency and roadside safety. In one research paper relating to "Evaluation of Design Consistency Method for Two Lane Rural Highways." the author relates visual demand to driver workload (Fitzpatrick et al. 2000). Visual demand has been measured through the visual occlusion process on different types of alignments e.g., straights, unidirectional curves, reverse curves, and straight alignments. The visual demand obtained by this process was plotted to measure driver workload.

In the research work carried out by FHWA to develop the IHSDM, the researcher commented on measuring the effect of driver workload by measuring physiological responses that resulting from the stress developed in the driver during changes in driving demand (Fitzpatrick et al. 2000). Using an approach initially reported by Senders et al. (1998) design consistency was examined for horizontal curves using vision occlusion to determine the effective workload on the driver. Drivers wore an occlusion device that provided fixed-length glimpses of the roadway in response to presses of a switch. Recording the frequency and location of requested glimpses provided a measure of the amount of information needed to successfully traverse the roadway. It was found that workload increased linearly as the degree of curvature increased, increasing on the approach to and peaking near the beginning of horizontal curves. No effect was found for deflection angle.

In another work, FHWA analyzed driver workload relating to attention demand on the drivers (Dingus et al. 1996). In their opinion, drivers should not be overloaded at critical times during driving tasks. The critical times, again, had been referred to as the time of negotiating critical sections of alignments. In the review of different literatures, different researchers concluded: It had been reported that subjects using complex navigation devices drove more slowly than those using less complex devices (Walker et al. 1994). These effects were also more prevalent in older drivers (55 years and older) than in younger drivers. If the driver was traveling at a faster speed or on a less complex road (i.e. fewer curves), shorter viewing times of any display will be required as compared to traveling at a slower speed or on less complex turns (Senders et al. 1966).

It was reported that driving attention demands for older drivers increase because of decreased capacity. It was suggested that presentation of auditory information instead of visual information proves much easier and effective media for conveyance, since auditory information does not increase visual demand, leaving the workload factor much less overstressed.

2.4.2 Perception Reaction Time (PRT)

Different researchers have adopted different measures to evaluate driver workload. The primary concept behind all such measures is evaluation of "Perception Reaction Time" (PRT). Again, PRT varies with the expectancies of the drivers. This expectancy becomes most effective to regular drivers. Regular drivers, due to their experience in driving, frame their own expected features, especially when negotiating areas along roads where available sight distance is a constraint. Hence, the review of previous work could be divided into different sectors for a better understanding of the measures that could be applied to evaluate driver workload.

Researchers concluded that PRT covers four steps (Cleveland et al. 1985), which are:

i) Detection of obstacle,

ii) Identification of the obstacle as hazard,

iii) Decision to stop, and

iv) Application of brakes.

A surprise situation has been described as the most important situation. The concept of object contrast has also been discussed in relation to PRT. It has been agreed that the lesser the contrast of the object with its background, the higher the PRT. This concept conveys the same criteria of bits of information, as has been discussed, and adopted by AASHTO (2001).

Neuman et al. (1983) also discussed four important factors in evaluating stopping sight distance (SSD). The concept describes the applicable modification of the highway geometrics to fixing such SSD. The applicable modifiers cite driver ability and driver state as the prime factors. Moreover, the visibility of the driver has also been focused on determining the required parameter. It was concluded that the determination of PRT varies with the type of road obstacles with respect to the expectancy of the driver and with the mental condition of the driver.

In other research related to developing new models on SSD, assumptions concerning driver behaviour, as well as vehicle and roadway characteristics in relation to operational model parameters, had been emphasized. PRT, vehicle type, driving behaviour, and available pavement-tire friction were among the parameters of interest. In developing this functional model, Neuman (1989) stressed varying assumptions for determination of PRT. The prime factors of these assumptions relate to driver state of mind and complexity of information present, depending on the kinesthetic of the area under consideration. PRT was found to vary from 4.0 seconds to 7.0 seconds, depending on the type of highway and the existing or proposed constrained conditions.

In another work on determining safety effects of limited sight distance on crest vertical curves, the researchers came up with some vital conclusion which indirectly indicates the importance of unexpected features (Urbanik II et al. 1989). These include the existence of a sharp horizontal curve hidden by a crest vertical curve and a hidden intersection beyond a crest curve. These features clearly violate the expectancy of the driver, and so the PRT values increase in relation to the increase in the numbers of alternatives for guiding and controlling the vehicle.

2.4.3. Expectancy

The workload, as defined above, again varies with the expectancy of the driver. In general, we can easily comment that experience with the roadway is a function of the number of times a driver has driven a particular road, the similarity of the traits of the road to those of others in the driver's experience, and the accuracy of predictions about the unseen characteristics of the road according to the driver's judgment. Collectively, this experience has been referred to as expectancy. An operational definition of expectancy with regard to transportation has been given by Ellis (1975): "Driver expectancy relates to the observable, measurable features of the driving environment, which increases a driver's readiness to perform a driving task in a particular manner, causes the driver to continue in the task until it is completed or interrupted." Alexander and Lunenfeld (1986) provided a similar definition: "Expectancy relates to a driver's readiness to respond to situations, events, and information in predictable and successful ways."

Lunenfeld and Alexander (1986) described expectancy in two forms: i) A-Priori and ii) Ad hoc. A-priori expectancy is relatively long-term and widely held expectancies, based on collective previous experience that drivers bring to the driving task. Unusual geometric features (e.g., a one-lane bridge), features with unusual dimension (e.g., very long or very sharp horizontal curve), and features combined in unusual ways (e.g., an intersection hidden beyond a crest vertical curve) may violate a-priori expectancies. On the other hand are short-term expectancies the drivers formulated during a particular trip; they are based on site-specific practices and situations encountered in transit. Geometric features whose dimensions differ significantly from upstream features (e.g., a horizontal curve significantly sharper than upstream curves) may violate ad hoc expectancies.

Researchers had described expectancy on a roadway as a culmination of experience earned by a driver on that road stretch. A driver always expects the path and roadway geometry to be consistent when the sight distance is restricted (Woodbridge et al. 2000). A consistent highway design ensures that successive geometric elements act in a coordinated way, so that those successive geometric elements produce a harmonized driver performance without surprising events (Gibreel 1999).

In general, the research area on design consistency can be divided into the following areas: vehicle operations-based consistency, roadway geometrics-based consistency, and driver workload consistency. Researchers also sought to examine issues related to driver tolerance for workload change. Expectancy dictates the level of mental resources allocated to the visual search task. If the future geometry of the roadway is consistent with expectancy or predictions, then mental capacity can be allocated to driving and other tasks. It is extremely difficult to quantify a limit to acceptable workload levels (Wierwille et al. 1993).

2.4.4. Attention

A driver's attention level also influences the successful performance of driving tasks. "Drivers allocate sufficient attention to maintain a perceived level of driving safety" (Messer et al. 1979). Most rural highways require low attention levels. Geometric inconsistencies, however, demand more attention than is normally required. If sight distance to an inconsistent feature is adequate, drivers have sufficient time to increase their attention levels and perform necessary vehicle control actions; if sight distance is not adequate, some drivers may not have time to react properly, and accidents may result.

Ford Motor Company and General Motors Corporation (Ford Motors 2000) created the Crash Avoidance Metrics Partnership (CAMP) in 1995 to conduct joint pre-competitive projects to accelerate the deployment of future crash avoidance measures. This had been an attempt to develop practical, repeatable driver workload metrics and procedures for both visual and cognitive demands that can realistically assess which types of driver interface tasks are appropriate to perform while a vehicle is in motion. The main background of the research is that the use of an in-vehicle system imposes demands on drivers. If those demands exceed the driver's capacity (e.g. on input modalities, output modalities, or cognitive processing resources), then driver performance on the primary task of driving may be degraded or affected in some way.

If the degradation or interference is significant, and if it co-occurs with other contributing factors (such as traffic or unexpected roadway objects), a crash (or near miss) may result. This is the logic that underlies Driver Workload. The research was, however, mainly concerned with causes of crashes relating to driver distraction; hence, it could provide only an idea in the area of driver workload.

2.4.5. Risk

The influence of risk on driving has been theorized about in several, often quite similar, models (see Organization for Economic Cooperation and Development [OECD] 1990, for a review). Risk is defined as the product between the probability of an accident and the expected accident severity, per unit of time (Janssen et al. 1988). Drivers will compare experienced risk with their personal level of acceptable risk, and if they do not match, the discrepancy is eliminated by adjusting their behaviour. The level of risk that is acceptable to a driver is determined by the maximized difference between the expected benefits and costs of a given level of mobility.

The most prominent of these is Wilde's risk homeostasis theory (Wilde 1982, 1988). This model has received the greatest amount of international attention, and so will be the focus for this section. The origin of risk homeostasis theory (RHT) is from evidence that some road safety measures do not always lower the accident rate. This may occur even when, from a traditional engineering approach, the driving environment is made safer through the implementation of external controls and restrictions that limit the opportunity of drivers to take a particular risk. According to RHT, accidents are not reduced because drivers continuously adjust their behaviour to accommodate situational fluctuations in the amount of risk they experience.

Therefore, when drivers perceive an increase in safety (from a safety measure), they respond by either putting less effort into the driving task, or by increasing the difficulty of other aspects of the driving task that are not targeted by the countermeasure, such as by driving faster (Naatanen et al. 1974). This is known as behavioral adaptation, or homeostasis (OECD 1990), and it results in no gain in road safety. This is the essence of RHT. Therefore, perceptual counter measures (PCM) and other safety measures, while reducing speed or other dangerous driving behaviours, may not actually increase safety.

2.5 Measures to Evaluate Driver Workload

There are four ways to measure workload for the task of driving: performance on the primary driving task itself, performance on a secondary task while driving, physiological measurements, and subjective workload questionnaires.

These four methods of measuring workload are described below:

I. The first is through measuring performance on specific aspects of the primary driving task itself. The most common measures used include the number of steering wheel reversals, the variation of the steering wheel angle, and lateral variation. When other driving tasks are more difficult and more effort is given to them, or when the driver has a reduced capacity (such as from fatigue), less attention may be directed towards lane-keeping behaviour. This results in the driver making fewer steering corrections, leading to smaller steering variation and fewer steering wheel reversals, but larger lateral variation. When more effort is directed towards lateral control, drivers make more steering wheel corrections, so the steering wheel angle will change more often. This produces larger steering wheel angle variation, more steering reversals, and smaller lateral variation.

II. The second method is by measuring performance on a secondary task while driving. Examples of these tasks include mental arithmetic, comprehension, and self-paced generation of random digits, delayed recall of random digits, simple and complex recognition, and digit span (Alm et al. 1994). When workload demands for driving increase, performance on secondary tasks should deteriorate. However, if the driver has spare mental capacity, this may be utilized without impairment to the secondary task.

III. The third method for measuring workload is through physiological measurements. These include pulse rate extractions, incorporating sinus arrhythmia (inter-heart beat variability), mean pulse rate, and the spectral energy of inter-heart beat intervals (Meshkati et al. 1988).

IV. The fourth measure is the use of subjective workload questionnaires. These measure the level of workload that a driver associated with the driving task and, as such, may not always accurately reflect objective workload.

There are three criteria by which a workload technique can be measured to access its usefulness and validity. First, it should be sensitive to changes in workload and not influenced by fluctuations in non-mental workload variables. Second, a technique should indicate the origin of workload variations. Finally, a workload measurement technique should not interfere with the primary task (Eggmeier 1988). Each of the above four techniques have weaknesses as well as strengths in these areas, and so it is often argued that relying on workload measures from one area only can be misleading. Instead, a more comprehensive and reliable estimate of mental workload appears when more than one area is measured (Schlegel 1993).

2.5.1 Primary Task Measures

Primary task measures of workload are often considered to be the most attractive approach of the four methods of measuring mental workload because they measure the actual task that the investigator is interested in, that is, driving. Measurement is also simple, especially in a simulator, and importantly, they cannot interfere with the task at hand.

The most useful primary task measures are related to lateral control, as these are required for safe driving at all times. There are various measures, including steering wheel reversals, lateral deviations (measured by the standard deviation of lateral placement from the centreline, edge line, or lane centre), the root mean square error of lateral position (measured from the centre of the lane), steering wheel angle variation, and yaw deviations. These measures assume that if there is enough mental capacity available, then the lateral position of a vehicle should remain fairly steady within a lane.

However, when demand for resources by other tasks increases, the number of steering corrections will be reduced (leading to smaller steering deviations and less reversals), so variation within the driving lane and heading direction tends to increase (leading to larger lateral and yaw deviations respectively). When more effort is directed towards lateral control, drivers make more steering wheel corrections, so the steering wheel angle will change more often. This produces larger steering wheel variations, more steering reversals, and smaller lateral and yaw deviations.

Other primary task workload measures originate from longitudinal control, such as speed variation. However, variations in speed, while showing greater workload, cannot be assumed to be a primary goal when driving. As such, the use of speed variation as a workload measure is appropriate only in tasks where the driver is told to maintain a constant velocity (Godley 1999).

Visual occlusion has been another method used to measure driver workload. This technique measures how long a driver is prepared to continue driving without being able to see where he or she is driving. However, this may be more associated with risk and driver control than mental workload. Primary measures tend to be independent of non-workload variables. For example, McLean and Hoffmannn (1975) found that steering wheel reversals are associated with steering task difficulty (measured by steering deviations), but do not correlate with absolute steering angles. Hicks et al. (1979) compared five measures of workload for a simulated driving task, where difficulty was manipulated by wind gusts appearing at different locations relative to the vehicle, either at the front (difficult), or in the middle (easy).

The most sensitive workload measures were related to lateral control, namely steering wheel reversals and yaw deviations, followed by a subjective rating scale, and then lateral deviation. Other measures, however, were not sensitive, including an occlusion task, inter-heart beat variability, and secondary tasks. However, their results may be specific to their independent variable, since manipulation of wind gusts would be expected to have a large effect on lateral control. A similar experiment by Wierwille et al. (1978), which varied task difficulty by vehicle dynamics as well as wind, found that multiple primary task measures (steering reversals, high pass steering deviations, yaw deviations, and lateral deviations), provided substantially greater information and insight than the single secondary task. Each individual measure also showed sensitivity to different difficulty manipulations.

Therefore, primary task workload measurements are especially sensitive to particular manipulations that directly affect those measurements, but not necessarily the overall level of mental workload experienced by drivers. Another shortcoming is that it can be difficult to make comparisons across tasks, especially when the various primary measures are affected, to a varying extent, by different types of workload manipulations (Schlegel 1993). Typically, they will also show a high level of sensitivity only when the amount of resources demanded for driving exceeds the amount available.

If there is residual mental capacity (that is, driving does not utilize all available capacity, as would be expected except for highly demanding situations), an increase in driver workload can change motivation levels of the driver who responds by directing more resources to those tasks whose difficulty has increased. These result in the various aspects of driving still being performed at their full potential, with no change in the primary task measure recorded (Schlegel 1993). This is often seen as a weakness of primary task measures, especially compared to secondary task measures.

The basic approach suggested by Smiley (1989) has been quoted as:

- Primary task measures: as the task becomes more difficult, performance deteriorates.
- Secondary task measures: while performing a primary task, the driver also performs a secondary task such as doing mental arithmetic or discriminating audio or visual signals; the more difficult the primary task, the poorer the performance on the secondary task.
- Physiological measures: as the primary task increases in difficulty, physiological arousal increases.
- Subjective measures: as the primary task increases in difficulty, so does the driver's estimate of his/her own workload.

However, Smiley (1989) has suggested the following five main criteria in addition to the fundamental feeling for measuring such workload:

- Sensitivity: the measure should have a high signal/noise ratio.
- Diagonisticity: the measure should be an indicator of the type of resource that is being stressed, e.g., physical vs. mental, visual vs. auditory, etc.
- Selectivity: the measure should not be confounded with physical or emotional stress.

- Obtrusiveness: the measure should be as transparent to the driver as possible. Ideally, the driver should not know he/she is being assessed, although this is normally unavoidable given human subject guidelines and requirements. The only countermeasure is sufficient acclimatization (a judgment call) to minimize interference effects from being a subject.
- Compliance: the measure should track changes in workload rapidly enough to capture transient phenomena.

Another criterion often identified is transferability: the measure should be applicable in a variety of operational situations. Thus, the most direct way of determining the moment-to-moment mental load being placed on the driver is to simply ask him or her, in some structured way, how busy they are. But this process is quite cumbersome and impractical in getting unbiased results (Wierwille et al. 1993).

Primary task performance, i.e., driving the vehicle at the control and guidance levels of performance, can be measured to assess workload. If the driver is overtaxed, his or her performance will suffer. Up to some critical level, the driver will adapt and shed off secondary tasks, and no differences will show up even though the geometric design of the roadway is considerably varied (McDonald et al. 1975). Hence, secondary task performance is a better choice to demonstrate shifting of mental resources in response to such roadway variations. It takes considerable ingenuity to devise realistic secondary tasks as opposed to arbitrary ones, such as working arithmetic problems or responding to extraneous signals on a cathode ray tube.

It has been found by different researchers that higher level of mental workload is required for safe driving with a high speed (De Waard 1995). Driving at higher speed requires higher rate of information processing per unit time. Hence, higher speed represents an increase in task difficulty. Driving in areas having high traffic concentration causes more workload than areas having low traffic concentration. Therefore, the speed of driving in dense traffic automatically becomes lower than that with lesser concentration. Thus, it can be inferred that criteria for highway design in denser areas needs to be a little different than areas having lower traffic density. The lane width bears a direct influence on driving speed. De Waard et al. (1995) have shown the driving speed reduces in narrow lane width since much attention is paid to lateral control of the vehicle. Since lateral control poses a primary workload, the other half of the same workload needs to be reduced in lowering the driving speed.

2.5.2 Secondary Tasks

Mental workload on a primary task is often measured indirectly by performance on a secondary task. There have been various secondary tasks successfully used with driving, including mental arithmetic, comprehension, self-paced generation of random digits, delayed recall of random digits, simple and complex recognition, and digit span (Zeitlin 1995). Assuming a single global attention resource pool, as the driving task becomes easier, there is more attention resource left over to process the secondary task, so it is achieved relatively successfully. However, when the driving task is difficult, there will be relatively few resources left over, so, provided that the secondary task requires more resources than available, performance should deteriorate (assuming that driving is kept at the same level).

However, multiple resource theory postulates a weakness in this approach. Secondary tasks that are not very similar to the driving task (e.g. auditory and verbal tasks) should not compete for many of the same resources. Thus, some secondary tasks can be insensitive to workload changes. This can affect the ability of secondary tasks to demonstrate which aspects of driving are demanding more attention, although secondary tasks are generally considered to be reflective of specific workload changes. In addition, the overall level of a driver's workload needs to be high for performance trade-offs to occur between driving and the secondary task. However, the secondary task often performs the function of increasing overall workload to capacity levels. As such, secondary tasks may record workload increases which, under normal driving conditions, would not be of significant concern to the driver.

When measuring driver workload with secondary tasks, performance on the driving task should not be affected by the addition of such tasks. Zeitlin (1995) found that delayed digit recall and random digit generation secondary tasks did not interfere with the primary driving task, but this is not always so. For example, Wierwille and Gutmann (1978) found a visual digit reading secondary task interfered with simulator driving for low workload conditions, but not for heavy conditions. This still occurred even though participants were told they would not be paid in full if they did not keep the vehicle under full control. However, interference is made more probable when using a secondary visual task rather than an auditory task from the predictions of multiple resource theory (Wickens 1980, 1984).

Brown (1965) found that the time taken to complete a driving route was longer when drivers also performed a secondary task of detecting odd-even sequences of randomly presented digits, than it was when no secondary task was present. He also found that changes in speed were correlated with performance on this secondary task.

Similarly, it was also found that a secondary task involving listening to music, compared to a silent condition, led to more time taken to complete a circuit in heavy traffic.

However, in light traffic, the secondary task decreased only the amount of accelerator and brake activity, and not speeds. This suggests that the higher level of workload in heavy traffic was needed to reach the driver workload threshold (so the speed drivers could cope with was influenced). Thus, both of these studies suggest that an increased workload led to slower speeds. However, Brown (1965) also found a secondary task, consisting of listening to spoken prose, had no effect on speed even when a comprehension test was included at the end of the drive. It was therefore suggested that his secondary music task may have had an effect of lowering frustration and stress in heavy traffic, rather than increasing workload.

McDonald et al. (1975) measured mental workload while driving with a secondary task involving a bonnet-mounted digit display. They argued that, while traveling through curves, workload increased when participants were asked to travel at faster speeds. However, this visual stimulus secondary task may have interfered with driving ability, especially since close visual tracking of the road is required while negotiating curves.

On a motorway, Senders et al. (1966) measured the amount of time drivers were prepared to have their view of the road occluded at different driving speeds. It was found that the faster the required driving speed, the more time drivers spent looking at the road; that is, drivers were prepared to have their view of the visual scene occluded for less time. In addition, driving speeds were measured with variable occlusion times. Similarly, it was found that the shorter the observation period given or the less frequent the observations were, the slower the participants drove. Thus, it was suggested that more visual attention needs to be directed towards the driving scene with faster driving speeds.

In a simulator experiment, Harms (1991) varied the difficulty of up to three simultaneous secondary tasks while measuring driving speed (with participants asked to drive as they would normally). Two of the tasks were visual, originating from the simulator screen (a colour detection task and a name detection task), and one task was auditory (mental arithmetic). It was found that when the task load of the name-task increased (from one target name and two names presented simultaneously to two targets and four names presented simultaneously), driving speed decreased from 98.8 to 64.5 km/h, and performance deteriorated on the auditory task. This suggests that the increased workload of the name-task left fewer attention resources available, and which were insufficient for fast driving, so driving speeds had to be reduced.

In another study in the same simulator using a secondary reaction time task, Alm et al. (1994) found that using a hands-free mobile phone led to increased workload. When driving was on an (easy) mainly straight road, phone use was associated with speed reduction. However, when driving was on a (challenging) winding road, this increase in workload affected only lateral position and not speeds. They concluded that this latter result might reflect a change in the priority participants gave to the driving sub-tasks and non-driving tasks.

2.5.3 Physiological Measures

Changes in mental workload lead to certain changes in some parts of a person's physiology, which can be measured as an index of workload. There are various physiological measures of mental workload, some more reliable than others, but very few are reliable enough to be used as a sole measure of workload. Physiological measures that have been used include pupil dilation, eye blinks, and the P300 component of event-related brain potentials, pulse rates, and respiration rate. The most commonly used measures for driving are pulse rate extraction including sinus arrhythmia, which is a measure of inter-heart beat variability (HRV), mean pulse rate, and the spectral energy of inter-heart beat intervals (De Waard et al. 1995).

Physiological measures tend not to be disruptive to driver ability to perform the primary driving task. The only possible intrusion is from operator distraction or discomfort from the recording equipment (Eggemeier 1988). Most criticisms of physiological measures are that these can be insensitive to changes in task difficulty, and are generally considered to be less precise than secondary task measurements of workload (Schlegel 1993). It can also be difficult to determine what aspect of a task is increasing workload, as all task aspects tend to influence physiological measures similarly.

More importantly, these can also be affected by non-mental workload changes. The most prevalent extraneous influences are from stress from the task, physical activity, and the emotional state of the participant. This can lead to the problem of not being able to separate the effects of these extraneous influences from the influence of metal workload (Meshkati et al. 1988). For example, respiratory rate, motor activity, and thermo-regulation also affect HRV. Thus, these need to be kept constant across driving conditions.

Researchers found that HRV within this spectrum was still affected by respiration, arguing that respiration needs to also be measured with HRV to control for this. However, this is seldom measured in workload studies. Wierwille and Eggemeier (1993) identify the most widely used measurements to be heart rate (HR), heart rate variability (HRV), brain activity, and eye activity (the last measure has aspects of performance assessment about it). Heart rate changes with workload have long been documented as a general index of arousal and/or physical work. Changes in heart rate variability, i.e., the variance in the beat-to-beat interval (cardiac arrhythmia) have been found to reliably discriminate among various types of tasks relevant to driving. As workload increases, HRV decreases, while HR tends to increase with physical effort. Both statistical and spectral analysis techniques have been employed to analyze electro-cardio graphic records.

Heart rate measures are fairly unobtrusive once the electrodes are placed (only three or four are required for HR or HRV), and good results can be obtained by measuring and processing tidal blood volume changes in appendages such as an earlobe. Brain activity measurement presents a much more complex recording and data interpretation situation. Event-related potentials (ERP) have been shown to relate to inferred levels of demand in a variety of flight simulator tasks and in driving. Specific events give rise to changes in cortical activity that can be correlated if the specific events leading to the ERP can be identified. Continuous tasks, in particular control tasks, do not lend themselves well to ERP analysis using the present state-of-the-art.

Eye, body, and heart potentials pose a distinct problem because the evoked brain potentials are so small (10 to 20 micro volts). Electrodes are rather obtrusive and require careful placement for retention on the scalp of drivers' heads.

Eye activity measurements have been in use for many decades. Eye blinks, eye movements, and pupillary responses have all been studied for application to workload assessment. Eye blink frequency and duration have both been shown to have a direct relationship with visual workload: blink rate decreases as workload increases, as does blink duration. Under stress, drivers tend to blink less, stare more, and minimize time that their eyes are closed during each blink. But eye blink measurements do not correlate well with other types of cognitive tasks or those involving other sensory modalities. Pupillary responses have also been studied; they relate more to general arousal of the driver. As arousal increases, the pupil tends to dilate, if light levels are held constant. Infrared reflection, direct imagery, and electro-oculographic techniques have all been used to study blinking and pupil responses.

As synthesized by Johannsen (1992), workload consists of several different attributes: input load, operator effort, and performance. Several studies have used the vision occlusion method of assessing perceived visual information requirements for individual geometric features (Alexander et al. 1986). The vision occlusion method involves allowing a driver to observe the roadway ahead only when the driver perceives the need to update information for guidance and control purposes. Assuming no lane excursions occur, this process can produce a simple estimate of visual information needs.

This measure has been referred to as visual or mental workload (WL). The complement of this measure (1-WL) has been referred to as spare visual capacity (Krammes et al. 1995, Shafer 1994). Texas Transportation Institute (TTI) has conducted a number of studies of workload and roadway geometry using the vision occlusion approach. The approach varies somewhat among researchers, but the basics are the same. The driver is assumed to need to attend to the roadway for only part of the total driving time. Glimpses of the roadway serve to confirm hypotheses about the task immediately ahead. As the roadway ahead becomes increasingly less predictable, for whatever reason, the driver spends more time looking at the cues that tell him or her how to guide the vehicle in the next few seconds. A pair of goggles or another similar device is equipped to blank out the driver's view of the road.

Senders et al. (1967), in a study using five drivers, found that drivers requested more glimpses of the roadway as the complexity of the roadway increased, but did not find a direct relationship between roadway curve characteristics and glance frequency. In this study, speed was also examined. Subjects directly controlled their speed while experimenters controlled glimpse frequency. Speeds were found to be lower in more complex portions of the roadway, indicating the trade-off between selected speed and glimpse frequency. In a study using 24 drivers, TTI examined vision occlusion at a fixed speed. The findings suggest that the frequency of glimpses (and hence the percentage of the total time that vision is not occluded) goes up as the degree of curvature increases, the inference being that workload is also increasing.

A study of driver responses in a wide variety of driving environments found that driver workload is significantly affected by the geometric properties of roadway curves. The general pattern was for the visual demand to begin to rise about 90 m from the beginning of the curve, peak near the beginning, remain level or slightly drop through the curve, and then gradually return to the baseline level after the end of the curve.

Driver workload increases linearly with the inverse of radius. That is, as radius becomes smaller, driver workload increases. This finding is supported by the variety of measures and techniques used to evaluate driver workload. Both subjective and objective measures of driver workload indicated similar trends (the Modified Cooper-Harper rating, a scale by which multidimensional mental workload can be measured, is a subjective measure, while visual demand is an objective measure). The effect of deflection angle was persistent but small in overall influence and practical significance for driver workload. Analyses examining subjective and objective measures indicated a modest increase in workload with increased deflection angle, although the subjective measure provided a clearer indication of the influence of deflection angle on workload.

When vision was not occluded in occlusion test sessions, drivers primarily looked ahead, searching for points where roads curved; they generally ignored edge markings in the near field. The point on which drivers focused depended upon the curve direction (left or right) and how sharp the curve was. The sharper the curve, the more likely drivers were to look at the outside lane line (versus the inside lane line). This may have implications for delineation placement (i.e., providing enhanced outside lane line treatments for sharp curves).

The examination of paired curves revealed that neither type of curve pair (i.e., broken-back or S-curve) nor curve pair separation greatly influenced VDL; however, the influence was statistically significant. Somewhat contradictory results were found, indicating different responses depending on the run. An interaction between separation and pair type indicated that closely spaced S-curves resulted in significantly higher workload than closely spaced broken-back curves when 1st run results were examined. Run 2-6 results indicated that widely spaced curves resulted in higher VDL than closely spaced curves. Both of these findings were unexpected. It was anticipated that S-curves would be more consistent with driver expectations (and be associated with lower workload) and that more closely spaced curves would impose a greater workload through carry over from the previous curve. The VDL changes observed were relatively small, however, and further research should be conducted to confirm or extend these results.

The test track, on-road, and simulator studies all produced generally the same results with regard to changes in workload, as did a previous test track study. Predicting overall workload proved elusive, with significant differences apparent in the various studies; these differences, however, do not diminish the utility of being able to predict the level of workload change between features. Improvements in the roadway markings used on and within 100 m of curves or other test features would be expected to reduce this intercept difference.

In a fatigue study by a researcher in Institute for Research in Safety and Transport reported, driver workload has been defined as "the demand that a task imposes on the operator's limited resources. The workload imposed on the operator is influenced by factors such as the person's capabilities, motivation and operator mood." The researchers referred to a number of research works and hypotheses made by different researchers in relation to driver workload/ fatigue with respect to additional information systems through introducing IVHS.

2.5.4 Subjective Workload Measures

Rating scales completed by drivers are the easiest way to measure workload. The scales can be direct, asking for estimates of actual workload, or indirect, asking for estimates on a number of scales (Meshkati et al. 1988). These ratings procure the subjective impact that the task has on the driver, and integrate the effects of many workload contributors. Other workload measurement techniques fail to do this (Hart et al. 1988) but, as such, it was not specified precisely what is responsible for a change in workload or when it occurred. Applied after the task is completed, these are not intrusive to the primary driving task (Eggmeier 1988).

There are, however, considerable individual differences associated with how people score ratings. This poses a problem for the comparison of different tasks when they are completed by different participants, but poses no such problem in a repeated measures design. Ratings completed after the task do not always procure all of the relevant workload information available to the participant and may include contributions of irrelevant information. This can occur because people do not normally quantify, remember, and verbalize experiences of workload, and because memories of experiences at each moment are replaced by the following experiences (Hart et al. 1988). More specific information on workload can be achieved by ongoing ratings, but these have a major problem of interference with the primary task.

If one task is done at a time, with a rest-break in between tasks, however, these problems can be minimized if ratings are completed immediately after each task is finished. It has also been reported that subjective workload is accurate only when a person's mental capacity is not exceeded. If it is exceeded, workload begins to be rated as declining with increasing objective workload. Thus, subjective ratings are not appropriate for extremely demanding tasks.

There have been a number of subjective workload scales devised and developed. De Waard et al. (1995) found support for increasing workload with speed from heart rate variability measures (lower power in the 0.10 Hz component, and a lower variability component). This was from driving on a real road involving special edge markings and centrelines with a reduced lane width. It was suggested that the narrower lane width increased driver mental workload because more attention was needed for lateral control. Furthermore, this happened disproportionably (i.e., non-linearly) with increasing speed, leading to their conclusion that driving speed is dependent on available mental capacity.

Zeitlin (1995) tested commuters using secondary tasks in a long-term field study. By observing drivers, he found that speed adjustment seemed to be the primary means of maintaining a comfortable workload. It was concluded that speed choice was determined by a combination of road characteristics and traffic density, both of which affected workload.

NASA Task Load Index (NASA-TLX) was developed by Hart and colleagues, and the final development was reported by Hart et al. (1988). This is a well-respected and widely used scale, which has been subjected to a thorough development, evaluation, and validation by a number of investigations on a variety of tasks, from simple discrete tasks to motion-based pilot simulations. The final version of the scale is based on six sub-scales, namely mental demand, physical demand, temporal demand, performance, effort, and frustration level. To overcome any bias from various sub-scales having more importance for some tasks over others, weightings are used. These are based on an additional rating of each of the sub-scales by each participant with respect to its subjective importance to them for the tasks they completed.

In a research work by Doo-Won Cha et al. (1997) relating to "Development of Human Factor Evaluation System for Car Navigation System," the mental workload has been assessed as a function of mental workload, visual demand, auditory demand, temporal demand, difficulty in driving, and difficulty in understanding information. The researchers proposed to measure driver workload using a scale developed by National Aerospace and Space Administration, and which is known as RNASA-TLX (Revision of National Aerospace and Space Administration – Task Load Index). This scale was described as more acceptable than NASA-TLX or SWAT (Subjective Workload Assessment Technique) or MCH (Modified Cooper-Harper Scale). All these scales are used to measure multidimensional mental workload. The dimensions are related to mental, physical, or temporal workload, and include other parameters.

When using subjective measures, what is actually measured is perceived workload, rather than objective workload per se. Furthermore, the level of task difficulty experienced subjectively can be different from the level gauged objectively from performance levels. This can result from three subjective qualities upon which perceived workload depends. The first is the long term memory ability of the measured experience, as well as of similar tasks used for comparison. Second, perceived workload is influenced by participant background factors, such as personality, habits, attitudes and expectations. Finally, it is affected by the momentary state of the participant, including emotional state, fatigue, and motivation (Meshkati et al. 1988). Several excellent subjective rating techniques have been used by a number of researchers. TTI (Texas Transportation Institute) has used various forms of the Cooper-Harper Scale for much different continuous control. Other good scales include the Subjective Workload Assessment Technique (SWAT) and the NASA Task Load Index (TLX). The methods are thought to be "globally sensitive," i.e., they have the "capability to reflect variations in different types of resource expenditures or factors that influence workload. The ratings can be elicited before, after, and in the case of the Cooper-Harper Scale, by an experienced rater, during the actual loading. SWAT and TLX are multi-dimensional, and thus are more diagnostic than the Cooper-Harper Scale.

2.6 Evaluating Design Consistency Using Driver Workload

2.6.1 Highway Geometry and Driver Workload

Roadways should be designed or redesigned in a manner such that the workload demands of their component features do not exceed the tolerance for demand change of the typical driver. If the characteristics of this tolerance variable are known, it then becomes a matter of measuring the workload values associated with various geometric features and specifying the maximum amount that successive features on a roadway could vary without exceeding the tolerance limit. The approach for assessing this tolerance limit value was the method of limits.

Messer et al. (1979) use driver workload to evaluate geometric design consistency. Workload is estimated based on

- Criticality of and availability of sight distance of individual geometric features, and
- Consistency and spacing between successive features.

Criticality ratings were developed for 10 geometric features: horizontal curves, crest vertical curves, bridges, divided highway transitions, lane drops, intersections, railroad grade crossings, shoulder width changes, lane-width reductions and cross-road overpasses. The workload for a feature is calculated as follows:

$$WL_n = R_f \text{ X } S \text{ X } E \text{ X } U + C \text{ X } WL_{n-1} \quad (31)$$

where

WL_n = workload value for feature n,

R_f =workload potential rating for feature n,

S = sight distance factor,

E = feature expectation factor,

U = driver unfamiliarity factor,

C = feature carry over factor, and

WL_{n-1} = workload value for the preceding feature, n-1;

The workload potential rating (R_f) represents the criticality of an individual feature. The rating was based upon evaluation of features by design, traffic, and human factors engineers on a seven point scale (0 = no problem and 6 = critical problem). Features criticality depends on the feature type and its relative frequency of occurrence, basic operational complexity, and overall accident experience.

The sight distance factor (S) increases from 0.6 to 1.8 as the sight distance to the feature decreases from approximately 1400 to 400 feet. The feature carry over factor (C) increases from 0 to 1 as the separation distance between features decreases from approximately 2000 to 0 ft. The feature expectation factor (E) equals to 1 if the feature n is not similar to the preceding feature n-1, and equals (1-C) if the feature n is similar to n-1. The driver unfamiliarity factor (U) increases with the percentage of drivers unfamiliar to the roadway from 0.4 for a rural local road that has mostly familiar drivers to 1.0 for a rural principal arterial road that has many unfamiliar drivers. The first term of equation suggests that the workload value for a particular feature (n) is a function of:

(a) Criticality of the feature itself

(b) Sight distance to the feature

(c) Similarity of the feature n to the previous n-1st feature

(d) Familiarity of the driver with the roadway.

For a feature with given criticality, the workload value decreases as the sight distance to the feature increases. That is, the shorter the sight distance, the less time available for drivers to adjust their attention level, process the information presented, and initiate the necessary control actions to traverse the feature and, therefore, the higher the workload. If the preceding feature (n-1) is similar, it creates an ad hoc expectancy that reduces the workload for feature n. The workload value increases with the percentage of unfamiliar drivers.

The second term of the equation accounts for the effect of the preceding features on the workload value for feature n. The contribution of the preceding feature on the workload value increases as the separation distance in between the features decreases. That is, the more closely spaced are the features, the less is the time available for processing the information presented by the features and to initiate the required control actions associated with the features – and therefore the higher the workload. Messer et al. (1979) provides level of consistency criteria that are similar in concept and application to the level of service criteria used in highway capacity analysis. The levels are given in Table 1.

Krammes et al. (1992) has developed concept of effective workload values for a particular stretch of road. The work developed by Messer et al. (1979) produces different workload values when applied to evaluate a stretch of road section, since the concept developed by Messer to measure workload was feature-wise. In this work, the concept of considering workload value for a specific road stretch was developed as the highest of those values for existing features. An equation establishing the concept of mean workload value had been developed and given as follows:

$$\mu_{EWL} = \frac{\Sigma(l_i)(EWL_i)}{\Sigma l_i} \tag{32}$$

where

μ_{EWL} = Mean effective workload,

EWL_i = Effective workload rating for any feature I, and l_i = Length of the feature i.

The mean workload value thus developed had been used to establish a statistical relationship between workload and number of accidents using a non-linear regression.

If drivers are able to successfully negotiate a given geometric feature at some workload level determined by the vision occlusion method,

Table 1 Driver Workload-Based Level of Consistency

Level of Consistency	Workload Value (WL_n)	Likely Driver Response
A	≤ 1	No Problem Expected
B	≤ 2	Smallest Surprise Possible
C	≤ 3	Smaller Surprise Possible
D	≤ 4	Small Surprise Possible
E	≤ 6	Problem Expected
F	>6	Big Problem Possible

they have established their perceived level of needed visual information. If decreasing the allowed glances at the roadway artificially reduces this level of information availability, there will be a point at which lane excursion will occur. This level will define the minimum mental workload required by the feature. The difference, then, between the perceived workload levels can be taken as an approximation of the tolerance for change in workload value that could be managed when the next geometric feature on the roadway is encountered.

Woodridge et al. (2000), in their experimentation, suggested measuring visual demand as follows:

$$VD = \frac{t_{glancelength}}{t_{request} - t_{last\ request}} \qquad (33)$$

where VD = Visual demand and t represents time for glance. They found that the VD value is strongly correlated with two of the horizontal curve parameters, i.e., radius (r) or 1/r of the curve and the deviation angle Δ or 1/Δ. They concluded as follows:

- Driver workload has great potential as a design consistency rating measure.
- The vision occlusion method is sensitive to changes in road geometry and is a promising measure of effectiveness.
- The preferred method for computing visual demand for a horizontal curve is over a relatively short, fixed-length portion of roadway after the beginning of the curve to eliminate confounding between the summary measure used and the length of the curve.

This calculation provides a measure of the percentage of time a driver observes the roadway at any point along the roadway. It can readily be seen that a given observation's value increases as the time between successive glances grows shorter and decreases as the interval between glances increases. The more information the driver needs to carry out his or her control function in driving, the more often the scene ahead must be sampled, i.e., the workload increases.

The visual demand rating for a given feature of the roadway is simply the sum of the individual observations that occurred during a set distance in or before the feature divided by the number of those observations, i.e., the mean visual demand during the distance in question:

$$VD_{avg} = \frac{\sum VD_t}{N} \qquad (34)$$

The practical limits on this assessment of visual demand range from a maximum of approximately 1 (assuming a glance duration of 0. 5 s and the driver's request for a glance almost instantaneously with the close of the glance interval) to a minimum of 0.08, reflecting a given observed time of 6 s between glances (obtained on a tangent section of track). The circuit does not reset for the next glance request until the previous glance period has elapsed, and requires at least 0.1 s between successive presses to reset. The result obtained from statistical analysis shows that both VD_L (visual demand for the entire length) and VD_{30} (visual demand for the 1st 30 m length) increase with increases in curvature, i.e., 1/R.

2.6.2 Operating Speed and Driver Workload

The most common vehicle operations-based consistency measure is operating speed, although other methods such as conflicts and accidents have been suggested by different researchers. A method for using operating speed as a consistency check is to predict speed using a speed profile model. Roadway geometrics-based consistency focuses on evaluating the consistency of the design using only information that would be typically available from a set of roadway plans. Driver workload assumes that there is a relationship between the effort required to perform a task and the roadway geometrics presented during that performance. Checklists largely consist of reminders to designers to examine design features for possible expectancy violations.

Narrower lane widths cause slowing down of driving speed. The reasons behind this phenomenon have been explained in different studies. The first explanation is that driving is perceived as riskier in narrower lanes. Lower safety ratings were found by Fildes et al. (1987), and the longer headway distances were found by Vey et al. (1968) for narrower roads. Both suggest that motorists feel less safe on narrower roads and in narrower lanes. Thus, as predicted from RHT, driving behaviour is modified by reducing speed to keep the risk that the driver experienced at an acceptable level.

A second explanation originates from De Waard et al. (1996), and involves mental workload and total lateral clearance (TLC). First, faster speeds require higher mental effort, and narrower lanes require more mental effort to keep the vehicle in the lane. Therefore, if a driver is mentally occupied enough to be near or at his or her mental capacity level, some attention must be taken away from speed if the driver wishes to ensure that his or her vehicle remains within the lane (assuming performance on other concurrent tasks is maintained). However, even if overall mental demand does not require all of a driver's attention capacity, according to the utility model (extension of RHT), drivers may not be prepared to provide the extra steering effort required for driving in a narrower lane at the same speed because of comfort considerations (in terms of physical and mental workload). In such a circumstance, the driver who wishes to remain within the lane may reduce his or her driving speed.

De Waard et al. (1996) also provided evidence for these ideas. It was found that speed reductions on narrower lanes were associated with higher workload levels (from physiological workload measures), and more effortful lane tracking shown by smaller lateral variation. Further evidence is provided by McLean and Hoffmann (1975). The researchers had participants drive an instrumented car on an airport runway with three lane widths (8, 10, and 12 feet/2.4, 3.0, and 3.7 m), and at three speeds (30, 40, and 50 mph/48.3, 64.4, and 80.5 km/h). Similarly, it found an increase in high frequency steering movements with increasing speed and decreasing lane width. Moreover, they found less accurate steering for the narrowest lane (2.4 m) compared to the two wider lanes, but only at the fastest speed (80.5 km/h).

The third possible explanation why travel speeds are slower on narrower roads originates from the speed perception findings of other research. This research suggests that speed estimation is faster on narrower roads. However, this explanation may be applicable only to road narrowing, and may not translate to lane narrowing. This is because their speed perception findings were probably a result of increased peripheral visual stimulation and/or a faster moving visual scene through the observer's peripheral vision. This is because the landscape on the side of the road was closer when the road was narrower. However, if a wider road contains narrower lanes (through not utilizing the entire road width for driving), the side of the road scenery will not necessarily be closer to the driver, as such, enhanced speed perception is unlikely to occur.

Aspects of the actual road infrastructure that influence speed choice include lane and road width, road shoulder width, radius of road curvature, length of curves, delineator type and number, delineator spacing, condition of delineators, pavement markings, intersecting roads or driveways, and the roadway grade. Empirical evidence shows that driving speeds tend to be slower when roads have a walled surrounding, such as from buildings or a forest, and faster when they have flat, featureless roadside terrains. For instance, researchers asked participants to travel at 60 mph (96.6 km/h) on two straight sections of the same two-lane rural highway, one tree-lined, and the other with open surroundings. It was found that produced speeds were slower on the tree-lined section than on the open section by 7 mph (11.3 km/h). Similarly, on urban roads it was reported a positive correlation exists between how far back houses were from the roadside and travel speed.

Chapter 3 PILOT STUDY

The literature review of recent research into driver workload shows a complicated methodology of measuring driver workload. The portion related to workload reflects the deficit of ideal scale to measure mental workload. However, among all the available methods, NASA TLX scale and visual occlusion procedure appeared to be more relevant and capable of measuring multidimensional human sensations with weightage and visual demand respectively, as a direct input from subjects. This thesis includes findings from research undertaken in a two-phase pilot study. The first phase was done on road, using a defined stretch of the Don Valley Parkway (DVP) in Toronto, and the second one was done using a driving simulator at ETC Lab in University of Toronto The first phase has been done to assess mental workload using NASA TLX scale, while the second one was done to verify the visual occlusion method used, and to evaluate workload in terms of visual demand. The studies have been reported separately as follows.

3.1 Field Pilot Study

3.1.1 Methodology

The basic methodology of the on road study comprises:

- Collecting highway geometric data related to the highway alignment on the considered stretch of Don Valley Parkway (DVP).
- Evaluating mental workload using NASA TLX multidimensional scale.

- Establishing a statistical correlation between the exogenous variable of mental workload and the endogenous variables related to highway design alignments.

3.1.2 Collection of Alignment Data

The stretch of alignment considered for the pilot study extended from the York Mills exit at the North and the Bay-Bloor exit at the South. The entire study was carried out on southbound DVP, from the entry ramp of York Mills meeting DVP, to the exit from DVP to the Bay-Bloor ramp. The highway alignment data of the said length has been extracted from the available maps of 1:1000 and 1:5000 scales.

Emphasis was on data pertaining to horizontal and vertical geometry of the section. The horizontal radii of curvatures were calculated from the available plans, including the numbers and arrangements of compound curves and reverse curves. The lengths of the tangents were also calculated from the same plans. The vertical elevations of points distributed all along the said alignment has been considered to calculate vertical grades and also to use the K values to the vertical curvatures. However, because of the complexity of the information, grade was not considered. The dataset which has been extracted relates to the following considerations and are tabulated and furnished in Appendix A.

- Geometric Features
  - Lane width
  - Width of shoulder
  - Right of way width
  - Roadside features (kinesthetic)
- Horizontal Curvature

    - Deflection angle
    - Radius of curvature
    - Length of tangents
    - Position of lateral obstruction (continuous)
- Kinesthetic along the road stretch, evaluated with a rating scale of 0 to 6

3.1.3 Data Collection and Evaluation of Mental Workload

The entire alignment along Don Valley Parkway, undertaken to carry out the pilot study, comprises four stretches as follows, the entire data extracted was from the entry ramp to the exit ramp, and the highway geometric features were considered from the end of the acceleration lane to the start of the deceleration lane:

- York Mills exit to Lawrence (East) exit,
- Lawrence exit to Eglinton (East) exit,
- Eglinton exit to Don Mills (South) exit, and
- Don Mills exit to Bay and Bloor exit.

The subject selection criteria were as follows:

- The age of each driver should be greater than 18 years, and
- All the subjects should have a valid driving license and more than 3 years driving experience.

Ten drivers were selected at random, depending on their availability and willingness. The population of subjects was a well-defined mix of age, ranging from 24 years to 46 years. The rating scales, which stand as follows, were explained to all the subjects. The rating scales are related to the following:

- Mental demand (in a scale of 0 to 10)

- Physical demand (in a scale of 0 to 10)
- Temporal demand (in a scale of 0 to 10)
- Performance (in a scale of 0 to 10)
- Effort (in a scale of 0 to 10)
- Frustration level (in a scale of 0 to 10)
- Riskiness (in a scale of 0 to 10)

These seven rating scales were explained to all the subjects. Zero in the demand scale shows the least demand, whereas ten in the same scale represents the highest demand. Similarly, on the performance scale, a rating of zero shows the poorest performance, and a zero on the frustration level and riskiness scales shows the minimum level. Again, all these variables were given a separate weightage in a scale of zero to seven. These rating scales, used here, constitute the NASA TLX scale, which has been mentioned earlier.

All the drivers were given a clear concept of the entire experiment and the demand/ performance rating scale was described to them with the specific criteria of intake of their sensations. The subjects were also informed of the start and end of the experiments, during which they were supposed to note the demands and to report their sensations after completing the particular stretch driven. The traffic operation parameters were also taken into consideration, e.g. the travel speed and the traffic volume.

The mental workload for each individual stretch was evaluated using the following formula:

$$\text{Mental Workload} = \text{Mental Demand*Weightage } (w_{md}) + \text{Physical Demand* Weightage } (w_{pd}) + \text{Temporal Demand* Weightage } (w_{td}) \quad (35)$$

All the data collected during the pilot study are given in Appendix A. The data were taken with respect to performance and frustration level. Riskiness was ignored, since there were ways to evaluate exact performance measures of the subjects. Moreover, this study had been carried out to oversee the possible correlation between mental workload (MWL), obtained using NASA TLX, and the highway geometric parameters as listed above. It has been considered that the total mental workload is a function of mental, physical, and temporal demand only, whereas performance rating is a function of performance, frustration level, and riskiness.

3.1.4 Mental Workload and Highway Geometric Parameters

All the inputs from the subjects, at every stretch along the entire alignment, with the individual geometric features of each stretch, have been analyzed to establish a statistical model to evaluate mental workload with respect to highway geometric features. A correlation analysis has also been done; this analysis shows that mental workload possesses a very good correlation with the radius of curvature, number of reverse/compound curvature, and total road width, including lane width, shoulder width, and kinesthetic along the road stretch. The entire correlation analysis and statistical analysis are appended in the Appendix A. However, the best relation obtained from the collected workload ratings (weighted) and the highway parameters is as follows:

$$\text{Log (MWL)} = 8.8828 - 0.0005R - 1.0247SW - 0.5121 \text{ Aesthetics} \quad (36)$$

where

R = Average Radius of the all the curves in one stretch,

SW = Shoulder Width, and

Aesthetics = a weighed discrete variable (considered as 0 and 1 for cut and fill section respectively).

3.1.5 Results and Discussions

All individual data relating to extracted geometric parameters and the mental workload rating of the subjects are given in Appendix A. These data are used to formulate statistical relations to weighted mental workload and highway geometric parameters; whereas it has been found that the mental workload possesses a good correlation with different highway geometric parameters. The distribution function of mental workload follows Poisson distribution, and the exogenous variables, as have been considered, show a statistically significant relation to the variability of mental workload.

The DVP study was carried out to determine the statistically significant exogenous variables that provide a good correlation with the endogenous variables of mental workload. It has been observed that mental workload inversely varies with the radius of curvature and possesses the highest correlation with each other. Previous studies show that mental workload varies only as a function of radius of curvature. But in the DVP study, we found that mental workload possesses a high correlation with the number of reverse curves as well as the number of compound curves. It has also been seen that mental workload is highly correlated with average available sight distance (AASD).

This finding supports the mental workload model developed by Messer et al. (1979). The findings showed that the higher the number of reverse or compound curves, the lower the mental workload, which shows the significance of the ad hoc expectancy factor of the driver. Similarly, the higher the available sight distance, the lower the mental workload, which supports the sight distance factor, as had been suggested by Messer et al. (1979).

The method of data collection using NASA TLX has been appreciated all over the world. However, the input from the subjects on mental, physical, and temporal demand appears to be unreliable, since the input has been provided by individual subjects at the end of each stretch run, but not during the driving sessions. Although this index reflects the sensations of the subject on specific alignments, it still raises questions on the reliability of the input.

In addition, the input given by the subjects on the different demands was also a function of the representation capacity of the subjects at the time of the input; this capacity could vary considerably from time to time. Moreover, this study emphasized getting input on mental workload (MWL) with respect to highway geometric parameters, and not on input relating to traffic operations. But since the study was carried out in normal traffic flow situations, the traffic operation impact on the input of MWL cannot be denied.

Hence, observing such discrepancies in carrying out the process of evaluation of mental workload, it was decided to switch the methodology of measuring the mental workload evaluation in such a way that the demand could be recorded electronically to arrive at a more reliable method. Thus, it was decided to switch the methodology of evaluating mental workload through visual demand on the subjects, using the **Visual Occlusion** method.

3.1.6 Conclusions

The DVP study leads us to two important conclusions on the "Evaluation of Highway Geometric Design Consistency with respect to Driver Workload." They are as follows:

I. Evaluation of Mental Workload using NASA TLX will be difficult, where we consider the direct verbal output of the subjects as input to the method. The reliability of this methodology may always remain ambiguous. Hence, an alternative method of evaluating mental demand should be considered. Since mental workload related to driving is always a function of visual information from the highway, the visual occlusion method may be a much better method than NASA TLX. The visual occlusion method is preferable since we can measure it with the help of electronic device, making it highly reliable and relevant. Hence, the rest of the research was carried out using visual demand as a dependent variable.

II. Recent research shows that visual demand varies only with the degree of curvature of any roadway alignment, but complex curvatures or stretches do not have any significant effect on visual demand. However, this phase of the pilot study shows that mental demand varies with reverse or compound curvatures and stretches, as well as with other parameters including available average sight distances.

Hence, it was decided to carry out experimentation in a driving simulator to evaluate driver visual demand with respect to highway geometric parameters.

3.2 Simulator Pilot Study

3.2.1 Methodology

The methodology designed for this study consists of the following:

- Developing hypothetical scenarios of highway alignments in the simulator and designing the operation of a visual occlusion spectacle.
- Collecting data on vision request and the lateral position of subject vehicle at a given interval.
- Analyzing data and formulating models relating to visual demand and highway geometrics.

The detailed methodology can be seen in the Experimentation chapter (see 4.1). This pilot study has been carried out to ensure correctness of the adopted methodology and to determine the effect of complex alignments, which include simple, compound, and reverse curves, on visual demand. The steps, as given above, have been described in the experimentation chapter (refer Chapter 4). Three subject drivers drove, the data collected and analyzed. These data have also been included in the main analysis of evaluation of visual demand.

3.2.2 Data Extraction

The data were collected in *.dat file format for each alignment and for individual subjects. Data were extracted one by one from those data files with the Microsoft Excel™ program, and a sample of data output in Excel has been provided in

Appendix B for ready reference. The whole file exceeds one sheet; therefore, only a part of the output data is shown therein.

Once the .dat file is opened in Excel, the information on vision request (VDI) shows clearly the binary pattern of saving data. As detailed in the previous chapter, this information shows *one* when no vision request has been made; otherwise, it shows *zero*. The area of interest within those data was seeing how many times the vision request were made by the subjects, including the point of time such requests were made. Thus, a filter option was used to segregate the zeros within the VDI column. The data showed that, once the switch has been pressed, the data shows up in a group of fives, to reflect the opening of each glass of the Plato Vision Spectacle for 0.5 seconds (500 milliseconds).

Visual demand (VD) was calculated as follows:

$$VD = \frac{0.5}{t_{request} - t_{last\_request}} \tag{37}$$

The first request or the first five zeros were not considered for evaluation of VD but the 1st request time has been considered as the time of last request. Hence, each of the 1st 1/10th second in 0.5 seconds got a value of visual demand, whereas the other four of 1/10th second data remained as zero. Again, the filter option was used to segregate the rows with the calculated values of visual demand to evaluate VD on a given element.

The visual demand has been calculated for the entire length (VDL) of each element, half of the lengths (VDH), and the first thirty meters (VD30) of individual components accommodated in the alignments. The visual demand for the first half and first thirty meters has been calculated using the principles followed in the research study of FHWA (Woodridge et al. 2000). Hence, all such VD in terms of VDL (VD_L), VDH ($VD_{0.5L}$), and VD30 (VD_{30}) have been calculated as above. The calculated data were grouped according to the individual curvatures of each curve and considering compound and reverse curves as segments with all other relevant highway design parameters, i.e., inverse of radius (1/R or INVR), lane width (LW), average available sight distance (AASD), the deflection angle (Delta), and turning direction (Turning).

3.2.3 Analysis

The data extracted have been aggregated in another Excel file for analysis. The experiments showed that most subjects requested more glimpses on tangents following curves than they did on straight tangents; in addition, a parameter of preceding element (PE) in terms of integer variable was considered for analysis. A correlation analysis was done for the whole set; the correlation analysis results show that INVR and PE possess a good correlation with VDL, VDH, and VD30. In particular, the correlation of PE to VDH was excellent. All the aggregated analysis data are included in Appendix C.

3.2.4 Results

Initially, data were processed for developing statistical relationships using Microsoft Excel. The developed models are annexed in Appendix C. The goodness of fit of the models developed with VDL, VDH, and VD30 showed statistical significance as far as simple regression is concerned. Hence, it became clear that some of the considered variables, such as INVR, PE, LW, and AASD relating to highway design parameters, possess a significant relationship individually with the VD parameter. The t-stat values for each individual independent variable have also been checked to confirm their statistical significance to VD. However, one of the best models obtained from the pilot study is given for ready reference:

$$VD_{0.5L}=0.489+0.089*PE-0.074*LW+23.367*INVR \quad (38)$$

(Adjusted R^2=0.58)

The other models obtained using different probability distribution functions have also showed a closer fit, such as:

$$VD = 0.4905 + 0.1131*PE - 0.0834*LW + 0.0500*TURNING$$

(Pearson ChiSq / DF =0.4168) (39)

where all the parameters are self-explanatory and described above.

3.2.5 Conclusions

The results enclosed in Appendix C show the significance of the variables considered and the accuracy of the methodology adopted. The results have also reflected that *preceding element (PE)* makes a considerable contribution in determining VD. Thus, it had also become more evident that complex curves, in terms of compound and reverse curves, have an impact in deciding VD. Since the goodness of fit was not that high, it was decided to apply other probability distribution functions to build the model on VD. The result of the pilot study proved to be encouraging and promising.

Chapter 4 SIMULATOR EXPERIMENTATION

Proposed research experimentation, to accomplish the final goal of evaluating mental workload in terms of visual demand, was carried out using a driving simulator. The emphasis was on simulating rural two-lane highway alignments consisting of horizontal curves with tangents.

The horizontal curves comprise simple, compound, and reverse curves. The research focused on evaluating the effect of compound and/or reverse curves on visual demand and on developing a disaggregate model on visual demand with respect to highway design parameters and the lateral positioning of the subject vehicle. The highway design parameters include radius of individual curve, and turning directions for curves, with preceding and following tangents for any segment.

The simulator STISIM (Figure 2), a low cost driving simulator, operates in the DOS operating system. It can develop and simulate any hypothetical or real highway alignment with given curvatures, lengths, and width of the road, including the width of each lane. The simulator is also capable of simulating any given constant speed of the subject vehicle. If no speed is specified, the speed of the subject vehicle can be controlled using the throttle (gas) and the brake pedal. Input files were developed, following the guidelines in the STISIM manual, to simulate any hypothetical scenario and also to take control of the subject vehicle. A photograph of the STISIM used for the experiment is included in this chapter.

The visual occlusion device, a spectacle, was developed by Translucent Technologies Inc. of Toronto, Ontario. In normal situations, both glasses of the spectacles remain opaque, preventing and the person from seeing through the glasses.

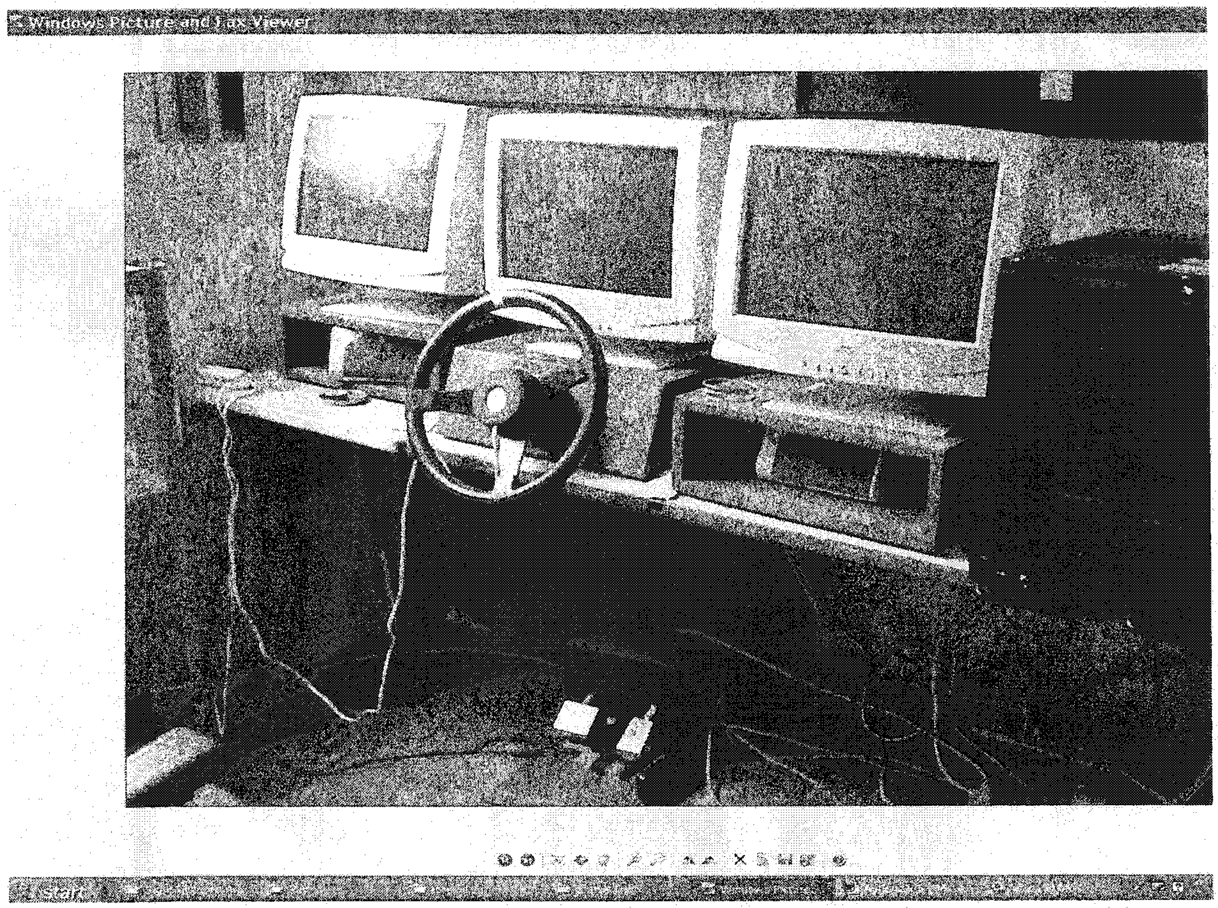

Figure 2 View of STSIM Simulator (ETC LAB University of Toronto)

Both glasses of the spectacles are connected to a control box through wire. The control box is comprised of two switches and a power cord.

Another arrangement in the box accommodates a 9V battery as an alternative power source. Once the power cord is connected with an electrical source, the box becomes active to individually control each of the glasses. Hence, to see when wearing the spectacles, one of the switches is pressed to make the corresponding lens clear; the lens returns to the opaque state once the switch is released. This process happens simultaneously for both the glasses, when a subject wearing the spectacles can see through both the glasses.

4.1 Methodology and Design of Experiments

The background for this research was developed through the literature review. Special emphasis was given to the literature related to similar experiments done by TTI and FHWA (Shafer M. 1996, Fitzpatrick et al, 2000). Both the TTI and FHWA research shows that visual demand (VD) is related only to curvature and, to some extent, to the deflection angle. Both reports show that neither compound curves nor reverse curves affect visual demand.

Thus, the emphasis of this research was on evaluating whether the preceding element has an impact on the following element of the alignment. Curves with the turning directions have been taken as integer variables *one* and *two* for right and left turnings respectively and the tangents have been taken as an integer variable *zero*.

4.1.1 Methodology

The method of this research study was a purely experimental one. The core methodology of scenario development comprised the following steps:

- Developing hypothetical alignment scenarios in a driving simulator.
- The type of alignments simulated comprised simple as well as complex scenarios.
- The simple scenarios were constituted of simple curves with preceding and following tangents. These alignments reflect visual demand on tangents and on the in-between curve as well.
- The simple scenarios with reverse and compound curves were constituted with one reverse or compound curve preceded and followed by a tangent. These

simple alignments reflect visual demand on curves that are preceded by either a tangent or another curve of either a different turning direction or curves of different radii having a common point of curvature.

- The average complex scenario was constituted of at least two reverse or compound curves, or compound and reverse curve in a series, connected by a tangent. Here, visual demand is expected to show a serious effect of the preceding element on the following element. In other words, a curve preceded by a tangent is supposed to have less visual demand than when it is preceded by another curve. Moreover, the direction of turning in the preceding curve and the direction of movement in the current curve should also show an effect on visual demand for the current element.
- The most complex scenario will have a number of reverse curves and compound curves in series and connected by tangents.

Individual elements in these scenarios followed the design standards as per TAC and AASHTO. The radii of curvatures were more than the minimum radius required for a given speed. The values for lateral friction and superelevation were considered as per standards established by TAC or AASHTO. The sight distance analysis for all such alignments was done using the standard software MARKH and incorporated in the visual demand modeling. Varying lane width is also incorporated in different alignments to evaluate the significance of lane width to visual demand.

Visual demand was evaluated using the visual occlusion principle. The visual demand equation is given in equation 26. The overall visual demand for any element was evaluated as an average of visual demand along the particular element. The visual demand was, however, evaluated for the whole length of the element, the half length of the same element, and for a length of the first 30 meters of the same element. Hence, visual demand (VD) of any element is expressed by VD_L (VDL), $VD_{0.5L}$ (VDH), and VD_{30} (VD30). The VD_{30} is calculated using same principle followed in the FHWA research study, i.e., if satisfactory demand is not found in the first 30 meters, visual demand is evaluated applying a proportional method.

The subject vehicle moved with a constant speed all along the given alignment. The primary responsibility of the subject was to keep the vehicle within the driving lane. The secondary responsibility of the subject was to take as few glances as possible while guiding the vehicle within the driving lane.

4.1.2 Design of Experiments

Design of experiment was developed following the methodology outlined above and the steps followed were similar to those in the experiments carried out by TTI and FHWA. As a reference, the flow chart on the design of the experiment is included (see Figure 2). The design of the experiment constitutes the following:

- All the alignments were designed for rural two-lane highways. No alignments have any intersections or any added complexity to require visual information.
- The speed was kept constant at 80 km/h. The constant cruising speed made it easier for the subject to concentrate on guiding the vehicle rather than diverting their attention to control speed.
- The radii of curves were kept greater than the minimum radius calculated for the given speed of 80 km/h. The superelevation rate and lateral friction was considered as stipulated in TAC and AASHTO.

- The length of each alignment was kept such that all subjects negotiate individual elements for a duration that is much higher than the PRT given by AASHTO.
- Eighteen alignments were considered for simulation to facilitate making each subject drive similar kinds of alignments more than once, whereas the complexity of these alignments varied from very simple to complex. Higher numbers of alignments helped the subjects to minimize visual demand as they got acclimatized.
- Request for vision was initiated by each subject, during driving, at their own discretion, as and when required. Hence, a switch was provided to all the subjects. The switch was located near the throttle or brake paddle, so that all the subjects could drive using both hands and concentrate totally on guiding the vehicle while driving along the individual alignment.
- The circuit was developed in such a way that, whenever the switch was pressed for visual information, the electronic pulse generated by pressing the switch traveled simultaneously to the visual occlusion device and the simulator.
- Immediately upon receipt of the pulse by the visual occlusion device, it provided a glimpse for the subject. The time when the request for vision was made was recorded at the simulator database simultaneously.
- The glimpse time was fixed as 500 milliseconds (0.5 seconds) and the pulse width was 600 milliseconds. Hence, there was a gap of at least 100 milliseconds between two corresponding vision requests. Therefore, in any scenario, the visual demand value will be less than 1.

- To establish the principle of as few visual demands as possible, all the subjects were given sufficient trial runs on the trial alignment, where each subject was provided with visual glimpses controlled by the experimenter. During such trial runs, the pulse width for opening the lens was kept much higher than 600 milliseconds.
- Once the subjects showed an acceptable limit (i.e., much more than 600 milliseconds) of their vision request, the experiment commenced and control of the vision request was transferred to the subjects.
- Upon successful completion of the experiment, visual demand would be evaluated based on the principle detailed in the methodology section. Then models relating to visual demand were evaluated with respect to highway design parameters.

4.2 Experimental Design

The entire scenario for the experiment involved in this study constitutes the following:

a) Developing hypothetical scenarios in the STISIM simulator.

b) Designing the control methodology for the Visual Occlusion spectacles.

c) Synchronizing registration of the electrical signal by both the visual occlusion device and the STISIM.

4.2.1 Developing Hypothetical Scenarios in STISIM

The STISIM simulator operation involves manipulating input files by the experimenter. The program files have been designed by the manufacturer of STISIM.

The input files required by STISIM are as follows:

a) GAINS File

b) STISIM.COL

c) Events File

4.2.1.1 GAINS FILE

The GAINS file is the primary configuration file in the STISIM. It allows all numerous program options and configurations to be specified. When the executable file for the simulation, STISIM.exe, is loaded, the program immediately searches the GAINS file in the same directory. If it does not find the file, the program immediately terminates. This input file has default values in all the fields, but to accomplish the intended simulation run, necessary inputs are made, changing the defaults.

The GAINS file contains several parameters that influence the vehicle dynamics. All these parameters are set in a manner to facilitate smooth functioning of STISIM. There are six GAINS files used in STISIM. The main file, GAINS, has seventy-two parameters, and all the other files have seventy-one parameters. The additional parameter in the GAINS file contains the name of the directory in which all output data are stored.

4.2.1.2 STISIM . COL File

The graphics card used for the simulation is a Texas Instrument Graphic Architecture (TIGA) board. Some of the modes that the TIGA board supports include 256 colours and resolutions of 1024 X 768 pixels. For these modes, the colours used for the objects displayed along the road scene are controlled by the experimenters themselves. All the

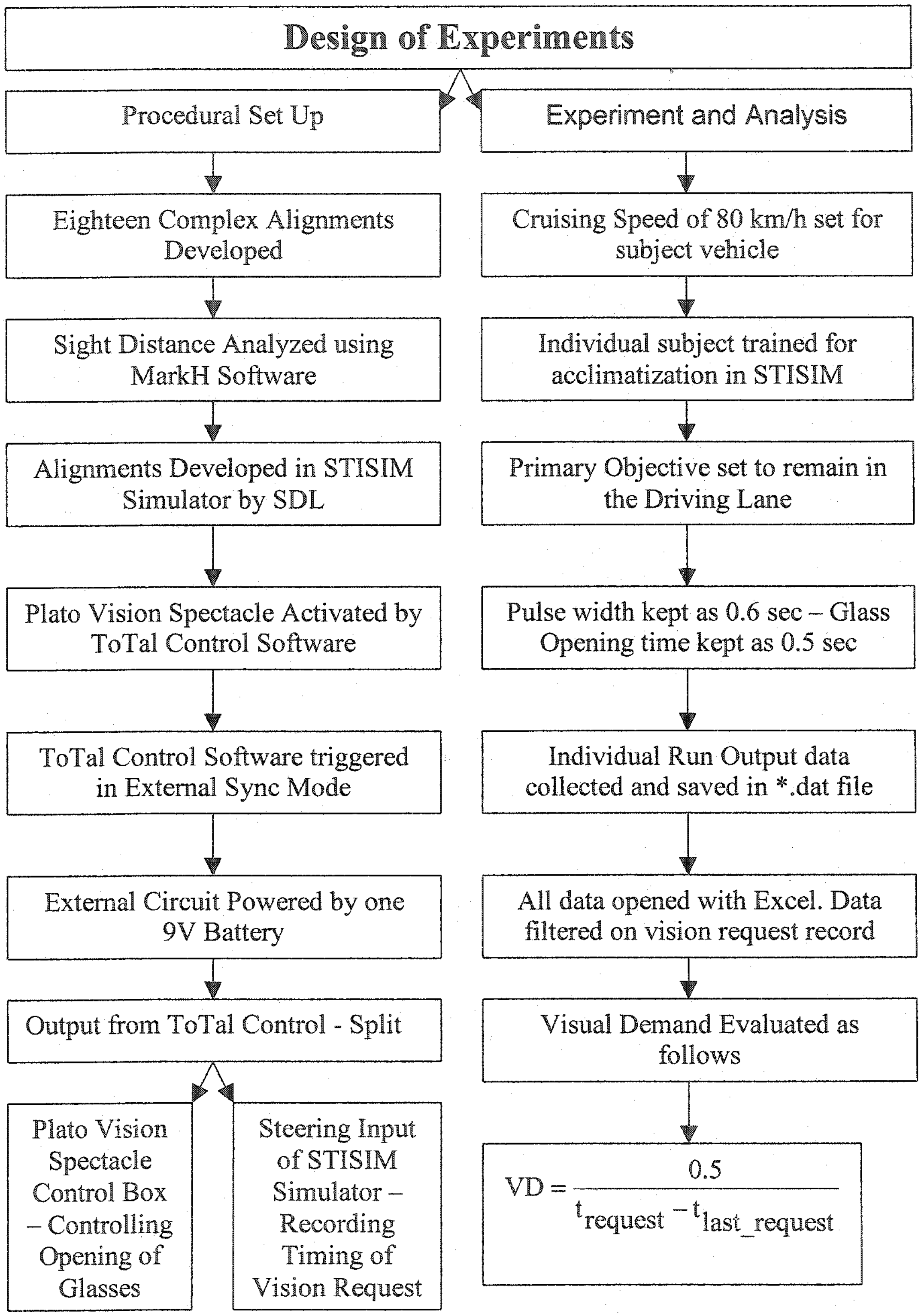

Figure 3 Flow Chart Showing Individual Step on Experimentation and VD Analysis

colours are defined in an ASCII text file. The colour of each display gives the user complete control over the display's appearance. The format and the parameter definitions are well explained in the STISIM manual so they are easy to manipulate.

4.2.1.3 Event File

This is the main file for developing the alignment scenario. The event file contains all the information that guides STISIM to perform the entire simulation activity. These are custom files that are created by the users utilizing scenario definition language (SDL). Users can create as many event files as required and may save them with any name acceptable to DOS.

All of the events occur as a function of distance from the start of the simulation run, and different events have a different number of parameters associated with them. It is possible to activate a number of events at a time to create complex decision-making and situation awareness scenarios. This is accomplished by inserting a function/ subroutine program to events files. This special SDL command is called 'Previously Defined Event' (PDE). This allows the user to work out complex scenarios as the equivalent of subroutines in a main events file.

The SDL allows two forms of data collection that will store data in the STISIM Data file. This data file is earmarked in the GAINS file; otherwise, the data goes automatically to a file that is saved as data XXXX, where XXXX is a number between 0001 and 9999. The first form of data collection, evoked using the RMSB/ RMSE events, computes the standard deviation of a range of variables in the steering and speed control tasks over a specified distance. The second form of data collection is evoked using BSAV/ ESAV events. This form is much more useful in analyzing data saved from the simulation run. This form also allows the user to save data with a number of events parameters. The standard deviation of positioning the vehicle in terms of the centre line of the road can also be calculated for any defined length on the alignment.

4.2.1.4 Other Relevant STISIM Files

There are other program files for the STISIM program, including the main system files. The other program files are *. OVL files, *.BAT files, *.VOC files, *.EXE files, *.HLP files, *.FNT files, and *.PDE files. These files are designated for different common functions required for any simulation. The .OVL files simulate any display of lateral objects, text, signs, etc. in the STISIM program. .BAT files are general DOS batch files and help to execute the program. VOC files produce sound effects during the simulation run. .EXE files help run the program, and .HLP and .FNT files provide the user with help tips and set the requisite font for the program. These are built in files and cannot be modified by the user. Hence, these files are considered unchangeable files.

4.2.2 Developing Methodology to Control Visual Occlusion Spectacle

The visual occlusion spectacles, supplied by 'Translucent Technologies Inc. of Toronto, Canada,' for the experiments, was a corporate donation to help carry out the experimentation. Both glasses of the spectacles remain opaque in normal conditions and are connected to a control box through wires. The control box has two switches that control the opening of the right and left eyes individually. The control box has a provision to accommodate a 9V battery or it can be connected to any power source to make it function to control the opening of the glasses.

To control the opening of glasses from some external source without using the control box switches, an electrical signal must be passed to the control box, which subsequently passes the input signal to open either of the glasses. ToTal Control software, developed by Translucent Technologies Inc. of Toronto, Canada, on activation by any pulse from an external sync, can pass an active signal individually to either of the glasses to make it open for a given duration.

This software was also a corporate donation made by the developers to assist in carrying out this experiment. The files that can be generated to operate the software have an extension *.gl. The .gl file can be programmed to control the opening time of the glasses as well as the total period of each pulse. Thus, it helps to open the glasses individually on receipt of an electrical signal passed by the software. The program also controls the input delay between the time to initiate signal from the source and the time of opening the glasses. The input to the ToTal Control software can be given in two forms. One of them is from 'Internal Sync' and the other is from 'External Sync.' When the internal sync mode is set with looping, the signal keeps generating in a loop from the software itself, and the glasses keep opening as per the given time (generally in milliseconds). When the external sync mode is set, the glasses open on passing an external signal from outside through the software.

To register the signal by the software, an external pulse generator was provided as an external sync. The generator was connected to the computer through the input cable and acted as an input source to the ToTal Control software. ToTal Control was programmed to generate pulses with a zero delay, which can make both the glasses open simultaneously for 500 milliseconds with a total pulse width of 600 milliseconds.

Hence, when an external pulse from the pulse generator is produced, it opens both the glasses simultaneously for a period of 500 milliseconds and closes both within another 100 milliseconds. The glasses of the spectacles open without any delay from the time of generating the external pulse from the external source. The quality of the pulses was checked for accuracy with an oscilloscope.

The output pulse from the computer was connected to the control box of the Plato Vision Spectacle through a splitter. An output from the splitter was taken back as an input to one of the channels of the oscilloscope to measure the pulse quality. The opening of the glasses exactly followed the sequence of pulse generation. Hence, it became clear that the external pulse generation can control the glasses of the spectacles with the same quality of pulses, including a zero delay. That confirms the opening time of both the glasses simultaneously for the given period of 500 milliseconds immediately upon passing an external signal from an external sync.

4.2.3 Synchronizing Registering Signal by Visual Occlusion Device and STISIM

Once the set up is completed as detailed in 4.2.2, the next step was to register the signal simultaneously by STISIM and the visual occlusion device. This is required to record the exact timing of signal generation by STISIM and by the Visual Occlusion spectacles themselves. The opening time needed to be checked to ensure the best quality results for the experiments. Since the total time of opening of the glasses plays a significant role, the pulse time forms an important parameter.

The pulse generation was done from an external circuit, powered by a 9V battery. A switch connected to the 9V battery was connected to the pulse generator as the power source. Whenever the switch was pressed, the electrical pulse triggered the generator to generate a smooth pulse. The generated pulse traveled to the computer through the input wire and triggered the ToTal Control software. The software immediately generated a signal to the Plato Vision Spectacles to make the glasses open for the given period.

The output of the software was connected to the spectacles through a splitter. One of the outputs was connected to the horn input of the simulator, and whenever the switch was pressed, the Plato Vision Spectacles open for the given period, and the time the switch was pressed was noted by the simulator through the horn input switch. Since the simulator saves data at every $1/10^{th}$ of a second or at each 100 milliseconds, in the case of opening the Plato Vision Spectacles for 500 milliseconds, the simulator output data reflects 5 pulses at each 100 milliseconds.

4.3 Experimentation Process

The entire experiment was carried out after finalizing all prerequisites as detailed earlier. Eighteen alignments had been developed. During the development of these alignments, emphasis was given to fixing lengths of individual parameters, such that all subjects would have sufficient time, which would be much higher than the PRT, to maneuver on and along each component. A sample alignment can be seen in Figure-4. The details of these alignments are given in Appendix 'B.'

The alignments are developed as follows:

- One preceding and following tangent to a simple curve. The turning directions and radii of curvatures were also varied simultaneously. Six of such alignments were developed and simulated.
- One preceding and following tangent to one compound or one reverse curve. Turning directions and radii of curvatures were varied in individual alignments. Four such alignments were developed and simulated.
- Two compound or reverse curves in a series preceded and followed by tangents. Four such alignments were developed and simulated.
- A combination of four complex curves was developed. These complex curves comprised both compound and reverse curves in a series separated by tangents with preceding and following tangents. Two such alignments were developed and simulated.
- Long alignments comprised of seven compound and reverse curves separated by tangents, preceded and followed by approaching and departing tangents, were also developed. Two such alignments were simulated for the experiment.

To develop the scenario in the STISIM simulator, the sight distance analyses were carried out for individual alignments first. The sight distance analysis was done using MARKH software. This software operates on the principle of finite element method and is supposed to produce results more accurately than the usual procedures. The lowest level of required sight distance was kept as 400 meters for complex alignments and 600 meters for simple alignments. These sight distances were then averaged to calculate average available sight distance (AASD) for individual elements. The findings of AASD were then utilized to develop the scenario to be simulated. The portions where the sight distances became more than the required level, AASD had been calculated using the given required sight distance.

All the event files were then developed in the simulator, one after another, using Scenario Development Language (SDL). The road scenario comprised curves of given radii, length, and the point of curvature (PC), point of common or reverse curvature (PCC or PRC), and point of tangency (PT). The rural two-lane highways for all the cases were developed with varying lane widths. No lateral obstructions were provided for any case. The speed of the vehicle was fixed as 80 km/h (22.22 meters/ second) for all the cases.

Once all the eighteen event files were developed, eighteen batch files were prepared to operate and simulate individual scenarios, one after another, where the subject's vehicle travels at a constant speed of 80 km/h during all the simulations. One long alignment was developed in addition to the alignments for experimentation. This alignment was used to give all the subjects a test drive to get acclimatized to driving in a driving simulator.

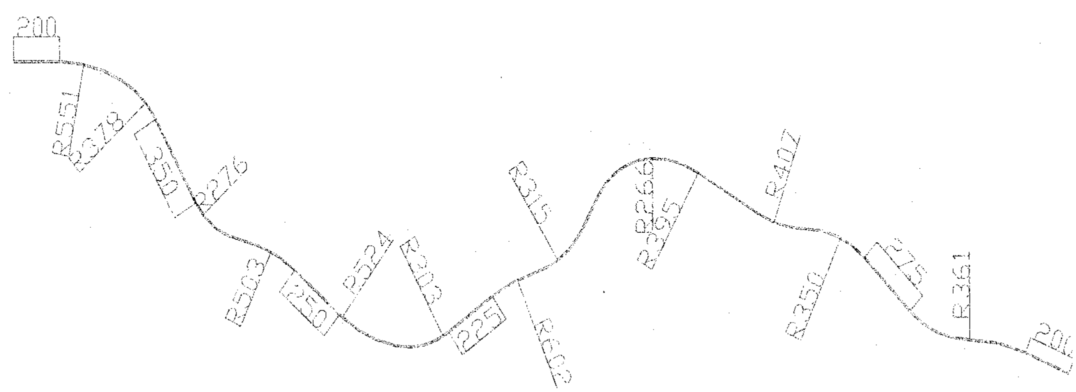

Figure 4 Typical Hypothetical Alignment for Test Curve

Once all such scenarios were developed, individual alignments were simulated, one after another, to oversee the correctness and acceptability as test alignments.

Once the alignments were developed, focus was set on working with visual occlusion spectacles. As discussed earlier, the visual occlusion device was spectacles called Plato Vision Spectacles. It operates through two switches connected to a control box when the box is charged with a power supply source. This charging can be done in two ways. The first one is to put a 9V battery in the control box, and the second one is to connect the control box to an 110V power supply. The second option was adopted to activate the Plato Vision Spectacles.

Opening the glasses by pressing the switch was obvious, but opening the glasses for a given time was accomplished using the ToTal Control software. The software had been designed by the manufacturer of the Plato Vision Spectacles to open the glasses for a given time with a well defined pulse width, such that the glasses open and close periodically, with an electronic pulse simulated by the software. ToTal Control software operates in a Windows operating system.

The software takes input for delay, pulse width, and pulse spacing for both glasses in generating signals to the spectacles' control box to open the glasses. Once these inputs are given, the input file needs to be saved as *.gl file. The input file developed and utilized for this experimentation was given as 0 delay, 500 milliseconds as pulse width for opening both glasses, and 600 milliseconds as the pulse spacing, which meant both the glasses would remain closed for 100 milliseconds.

ToTal Control software operates in two modes. The first one is from internal sync where, if the start button of the input file is hit, the pulses keep generating, within the given parameters, in a loop. So the glasses alternately open and close in a loop for 0.5 second and for 0.1 second respectively. This method is good. It allows the experimenter to control the opening of the glasses on the subjects. The second method for opening the glasses was from external sync. If the preference in the software has been set for opening the glasses from externally generated signals, this mode is used. The external signal can be generated by clicking the external sync in the developed .gl file. The glasses open once on mouse click, and then close. This methodology was adopted to generate pulse from an external sync. This also makes the generated electronic pulses to smooth through a pulse generator and to make the visual occlusion spectacles operate very smoothly with a given period of opening

It was decided to use at least five subjects to drive the eighteen individual alignments, but to obtain more data, nine participants were selected to drive in the driving simulator. Each participant was taken individually. Each was asked to drive on a hypothetical complex alignment first to get familiar with driving in a driving simulator. The test alignment was almost 9.5 km long, and it took almost 8 minutes to drive the whole alignment once. Subjects who were feeling less confident were asked to drive it two or three times to gain confidence in driving in a simulator.

Once the subject showed comfort and confidence, the visual occlusion device was introduced to them. The principle and the operation of the Plato Vision Spectacles were explained clearly to each subject. The subjects were then asked to drive along the same alignment with the Visual Occlusion device on. The opening of the glasses was controlled by the experimenter. The pulse spacing given to an individual subject was long enough, sometimes up to six seconds. Thus, the glasses opened for 500 milliseconds, and then the subject was kept blind for another 5.5 seconds.

The lane extrusion was observed, and again the subjects were provided with lesser pulse spacing. This process was adopted to make the subjects familiar with the alignment to keep glimpses to a minimum. It has been observed that most of the subjects were comfortable with a spacing of 3.5 seconds on the straights, whereas on curves they were going out of the lanes very frequently. Once each subject performed this training to the satisfaction of the experimenter, and they felt comfortable enough to start the experimentation, then the original experiments started.

Before starting the final experimentation, each subject was told how to control opening of glasses as per their requirements: pressing the switch between the throttle and brake pedal. They all were told how it operated, and they were asked to take as few glimpses as possible to remain in the driving lane. Each subject checked the operation and opening of the glasses first, and once they were satisfied with the operation, the main experiments began.

Regarding data collection, all the data were collected for individual runs of each subject through the STISIM database. The eighteen alignments were named as alignment 1 through alignment 18; the prefix of the alignments was "AL." The data were saved in individual data files through the BSAV and ESAV code. All the data were saved for individual runs by individual subject.

The primary focus of saving the data was on recording the time the foot-switch was pressed, termed "Time," along with the pressing information from the foot-switch, termed "Visual Demand Information" (VDI). The distance traveled from the start at each point of time, termed "Distance," and the subject's lateral position at each point of time, termed "Lane Position" (Lane Posi) were also recorded simultaneously. The secondary information collected was the longitudinal speed, lateral speed, lateral acceleration, and the steering angle. The secondary information, especially the longitudinal speed data, reflected the accuracy of the input speed. The other data have not been used for the current study, although it could be used in future to develop expressions for workload and/or performance measures.

The VDI information in the STISIM was generated through the horn input switch of the simulator. This registration operates in a special binary format, i.e., if the signal is registered by the horn switch input, it recorded 0 in the data file; otherwise the information recorded was 1 all the time. Now, since opening of the glasses of the Plato Vision Spectacles had been kept as 0.5 seconds, any time the foot-switch was pressed, the data recorded showed five consecutive zeros. Otherwise, the data showed 1 all the time. The output data files were saved in separate folders with a code representing the names of the subjects and stored in a folder called "Data."

Chapter 5 ANALYSIS RESULTS AND DISCUSSIONS

5.1 Analysis Procedures

The output data generated for individual subjects driving each alignment have been collected in individual files in the database of the STISIM simulator (*.dat files). All eighteen files were stored in one folder for each subject. All these folders were saved in another folder called 'Data.' When commencing the analysis, each data file was opened with Microsoft Excel™ using the requisite formatting for delimited files. The extraction process is briefly described in the Pilot Study chapter. However, it is useful to outline the procedure steps, which are:

- Open the output data file with Microsoft Excel.
- Select the delimited option with separating tab and space.
- The caption for each column of the saved data was put in place (the description of each column was according to the type of data saved using the ESAV option and was found in the STISIM Manual).
- The primary focus was on visual demand information (VDI). This information uses the binary numbers. This data was generated upon receiving/non-receiving signals from the horn input switch. If the horn switch received a signal, generated by pressing the foot-switch for vision, the data recorded by STSIM was 0; otherwise, the data remained as 1. Hence, the entire column of VDI was highlighted, and the filter option was exercised to separate the zeros.
- Once the data on VDI was filtered, it was carried onto another Excel page. The opening time for each glass of the Plato Vision Spectacles was kept as 0.5 second,

and the data was recorded at every 0.1 second, and showed 5 consecutive zeros for each opening of the glasses for vision. The visual demand was then evaluated for each fifth row as per Equation 37.

- As a result, the latest formatted data had visual demand values at every fifth row and zeros in all others. The rows, having calculated visual demands, were then separated and carried over to another Excel page.
- The latest pages show the time at each row when the vision was requested, the corresponding distances traveled, the visual demand figures, and other relevant data including lateral positioning.
- The difference in lateral positioning was then calculated corresponding to the time that vision was requested.
- Visual demand, in the form of VDF (VD_L), was calculated, averaging the visual demand figures obtained on the whole length of the individual element.
- Visual demand, in the form of VDH ($VD_{0.5L}$), was calculated, averaging the visual demand figures obtained on the first half of the full length of each element.
- Visual demand for the first 30 meters, in the form of VD30 (VD_{30}), was calculated, averaging the obtained demand within the first 30 meters of the element under consideration. Where such recording was not found, the method of proportion was applied by summing the total VD, dividing the total VD by the length of the element, and then multiplying by 30. The data obtained for all the elements, mostly show no request for vision within the first 30 meters.
- The standard deviation of lateral positioning (STDVL) was then calculated as follows :

$$STDV(L) = \sqrt{\frac{(LP - LW/2)^2}{N}} \quad (40)$$

where LP = lane position of the subject vehicle at any point of time,

LW = Lane width of the driving lane, and

N = Number of Observations (in this case, the number of times that vision is requested while negotiating the current element.

- The visual demand in VDL, VDH, VD30, and STDV(L) for the stretches was calculated stretchwise, by averaging those for the stretch lengths.
- Once the entire procedure had been done for all 162 output data files, the aggregated data was carried to a new Excel file. The data for all curves were kept in a page of the Excel file.
- A correlation analysis using Excel was carried out for all alignments.
- The development of models was carried out, considering all independent variables with different probability distribution functions. The expectation from the pilot study was that the dependent variable VD does not vary in a normal probability distribution function.
- Different models were compared, and the model which produced the best result for all VDs was considered most suitable, given all other relevant characteristics.
- Since the STDV(L) did not produce an acceptable model, the evaluation of performance measure has not been considered further.

5.2 Calibrated Models

The results of the whole experiment are described under two separate headings visual demand on complex curves and visual demand on tangents. No model on the standard deviation of the lateral positioning could be developed since this, as a dependent variable, did not show any significant relationship with any type of visual demand.

5.2.1 Model of Visual Demand on Complex Curves

Visual demand evaluation forms the primary objective of this research study. The variation of VD was plotted to oversee the effect of curves on visual demand, as shown in Figure 5. It was observed that visual demand rises at the juncture of any change in curvature. It rises higher while negotiating one curve of different radius and direction coming from another curve. However, when entering into a curve from another curve with the same turning direction, the difference in visual demand remains lowest compared to that when the preceding element is a tangent or a curve with the opposite direction. The variability of visual demand shows that the current element is not the only factor in the arousal of VD, but that something else also influences the variation of VD.

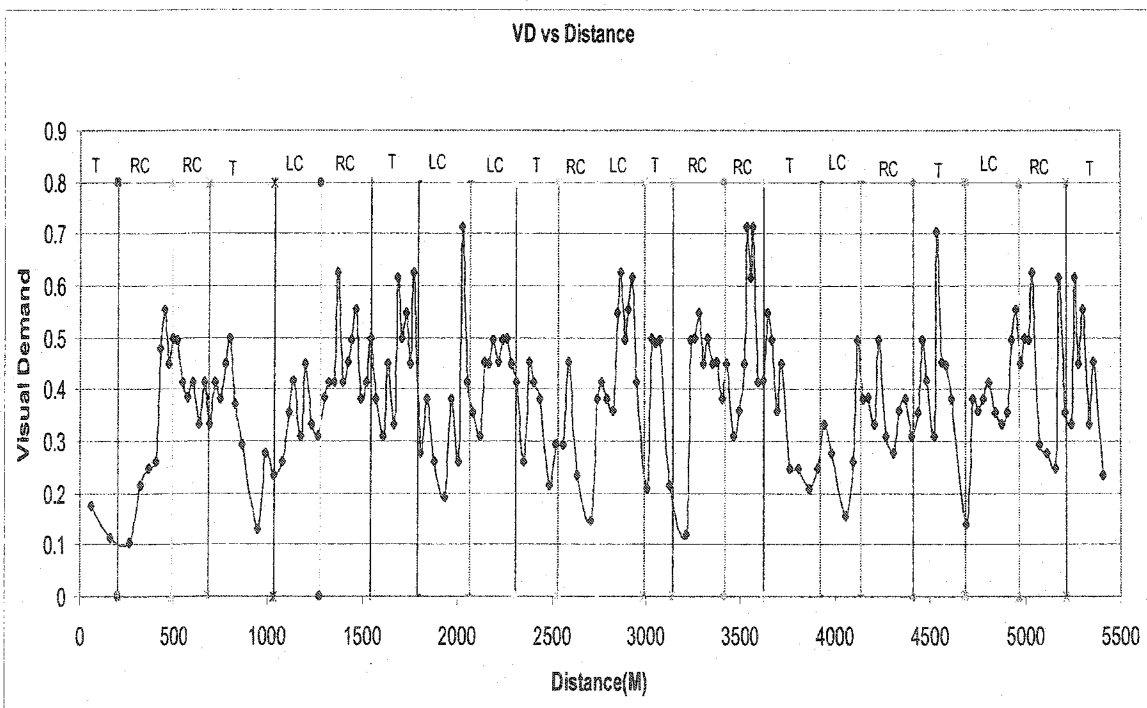

Figure 5 Graph showing variability of Visual Demand on a Continuous Alignment

However, visual demand varies considerably on identical curves, depending on the characteristics of the preceding element. Hence, an in-depth study on the relationship of the preceding element (PE) to the current element was carried out. Individual curves were also categorized in three classes, depending on their combination with the preceding element, as follows:

- Preceding curvature in the same turning direction of the current curve has been taken as a nominal character variable CC;
- Straight tangent as a preceding element to any curve, turning in any direction, has been taken as TC;
- Preceding curvature, in the opposite turning direction of the current curve, has been taken as RC.

The *preceding elements* (PE) values, CC, TC and RC, are considered in the analysis as nominal character variables in SAS.

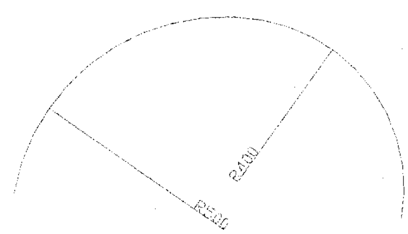

Preceding Element Curve to a Same Directional Curve (PE=CC)

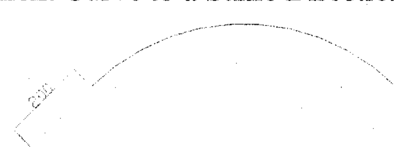

Preceding Element Tangent to a Curve (PE=TC)

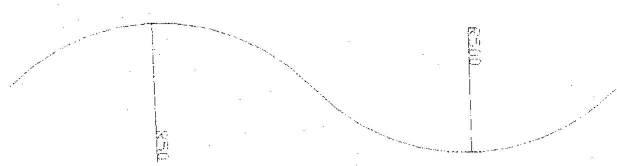

Preceding Element Curve to an Opposite Directional Curve (PE=RC)

Figure 6 Sketches showing Characteristics of Preceding Element

The models developed for VDF, VDH, and VD30 are given in Appendix D. The best of the models are as follows:

$$\text{Log (VDF)} = -\ 0.7885 + 63.6379\ \text{PEINVR*CC} + 49.1648\ \text{INVR} + 67.0418\ \text{PEINVR*RC} - 0.0901\ \text{LW} \quad (41)$$

(Pearson ChiSq / DF = 0.0101)

$$\text{Log (VDH)} = -\ 0.6544 + 110.9792\text{PEINVR*CC} - 0.1397\text{LW} + 124.7537\ \text{PEINVR*RC} + 0.3188\text{INVR*DELTA} \quad (42)$$

(Pearson ChiSq / DF = 0.0127)

$$\text{Log (VD30)} = -\ 0.8617 + 136.2555\ \text{PEINVR*CC} - 0.1112\ \text{LW} + 149.7696\ \text{PEINVR*RC} + 34.9016\ \text{INVR} \quad (43)$$

(Pearson ChiSq / DF = 0.0220)

where

VDF, VDH, and VD30 = visual demand for full, half, and first 30 meters length,

PEINVR = Inverse of radius of curvature of the preceding element, where radius is in meters,

INVR = Inverse of radius of the current element, where radius is in meters,

LW = Lane width of the driving lane, (in meters),

DELTA = Angle of deviation for the current curve element (in degree), and

CC and RC = Nominal character variables, as described above. These take a value of 1, when the preceding curve forms a compound curve (CC) or a reverse curve (RC), with the current curve. Otherwise, the value is 0, implying that the preceding element is a tangent.

Table 2 Parameter Estimates on VDF on Curves

Variable	DF	Estimate	Std Error	ChiSq	Pr >ChiSq
Intercept	1	-0.7885	0.1432	30.3039	<0.0001
PEINVR*CC	1	63.6379	10.2641	38.4406	<0.0001
PEINVR*RC	1	67.0418	7.5320	79.2273	<0.0001
PEINVR*TC	0	0.0000	0.0000	-	-
LW	1	-0.0901	0.0451	3.9950	0.0456
INVR	1	49.1648	12.1218	16.4503	<0.0001

All independent variables were tested with null hypothesis H_0, whereas the PEINVR*PE was observed as the most statistically significant variable for all types of visual demand in all the models developed. Turning directions of curve showed no significance in variation of visual demand.

5.2.2 Model of Visual Demand on Tangents

The second part focuses on the evaluation of visual demand on tangents. It was observed that visual demand varies on tangents, depending on their positioning on the given alignment. The preceding curve characteristics in the form of PETD (Preceding Element Turning Directions) were also considered as nominal character variables in evaluating visual demand on tangents. The PE in the case of tangents was always a curve, whereas the turning direction of the preceding curve (PETD) was taken as:

- PETD = PETD (L), when the preceding element is a curve and turning to left before the current tangent
- PETD = PETD (R), when the preceding element is a curve and turning to the right before the current tangent

The obtained models on visual demand are as follows:

$$\text{Log (VDF)} = - 0.9973 - 0.0002\ \text{PEDEL*LW} + 46.5084\ \text{PEINVR*PETD(L)} + 36.5381\ \text{PEINVR*PETD(R)} \quad (44)$$

(Pearson ChiSq/DF = 0.0115)

$$\text{Log (VDH)} = - 1.0129 - 0.0003\text{PEDEL*LW} + 74.5767\ \text{PEINVR*PETD(L)} + 75.4603\ \text{PEINVR*PETD(R)} \quad (45)$$

(Pearson ChiSq/DF = 0.0125)

$$\text{Log (VD30)} = -1.0526 - 0.0005\ \text{PEDEL*LW} + 78.2150\ \text{PEINVR*PETD(L)} + 80.2572\ \text{PEINVR*PETD(R)} \quad (46)$$

(Pearson ChiSq = 0.0242)

where all other variables, e.g. PEINVR, LW are defined previously, and

PEDEL represents the deviation angle of the preceding curve element,

PETD (L) or PETD (R) variables take a value = 1 when the preceding element is a left or right curve, respectively. Otherwise, the values are zero.

The models developed for VD with respect to the standard deviation on lateral position were not satisfactory, since the independent variable STDV(L) did not show a statistically significant relationship with any of the VD measures and highway geometric parameters. Hence this, as a performance measure, was not considered further.

Table 3 Parameter Estimates on VDF on Tangents

Variable	DF	Estimate	Std Error	ChiSq	Pr >ChiSq
Intercept	1	-0.9973	0.0467	455.5481	<0.0001
PEDEL*LW	1	-0.0002	0.0001	2.6937	0.1007
PEINVR*PETD(L)	1	46.5084	19.8692	5.4790	0.0192
PEINVR*PETD(R)	0	36.5381	23.2646	2.4666	0.1163

The reliability of all the independent variables considered for evaluation of individual classes of VD, as obtained from the analysis, is given with the individual model information in Appendix D. However, Table-2 and Table-3 reflect the statistical significance of the independent variables considered for evaluating VDF on curves and on tangents, respectively. The analysis results show that all variables, except LW (Lane width) have reliability greater than 99.99% for curves, and around 90% for tangent elements. However, it was observed that the sign of LW is negative, which shows that VD values decrease with more available lane width, as was expected.

5.3 Discussions

The variability of VD on complex curves and tangents was established using the developed model. The radius of curvature of the current curve has been varied for different preceding elements to understand the impact of current radius and provision of such curves with the preceding curve or tangent on visual demand on curve. Besides, graphs showing the variation in visual demand on tangents were developed to understand the effect of the preceding element characteristics on tangents. Figure 7, 8, and 9 show the variation of VD with respect to INVR of the current curve. Figures 10, 11, 12, and Figures 18, 19, and 20 show that, with the change of the preceding element characteristics?, the calculated visual demand varies considerably. The VD values for curves associated with a reverse curve show the highest visual demand of all combinations. The VD values depend solely on the preceding features, and reflect the sense of expectancy that is developed by any driver negotiating a long roadway alignment.

5.3.1 Visual Demand on Curves and Impact of Complex Curvature

This primary objective was accomplished with the development of models, while preceding element (PE) characteristics, including radius of the preceding element crossed with TC, CC, or RC, showed a statistically significant relationship with visual demand. However, the PEINVR variable shows the highest influence on evaluation of visual demand. The PE variable individually was not that significant, but when crossed with PEINVR, it showed a high statistical significance. Figures 10, 11, and 12 show that a little variation of radius in the proceeding curve provides much more influence on visual demand in the current curve than that provided by the radius of the current curve (refer to Figures 7, 8, and 9).

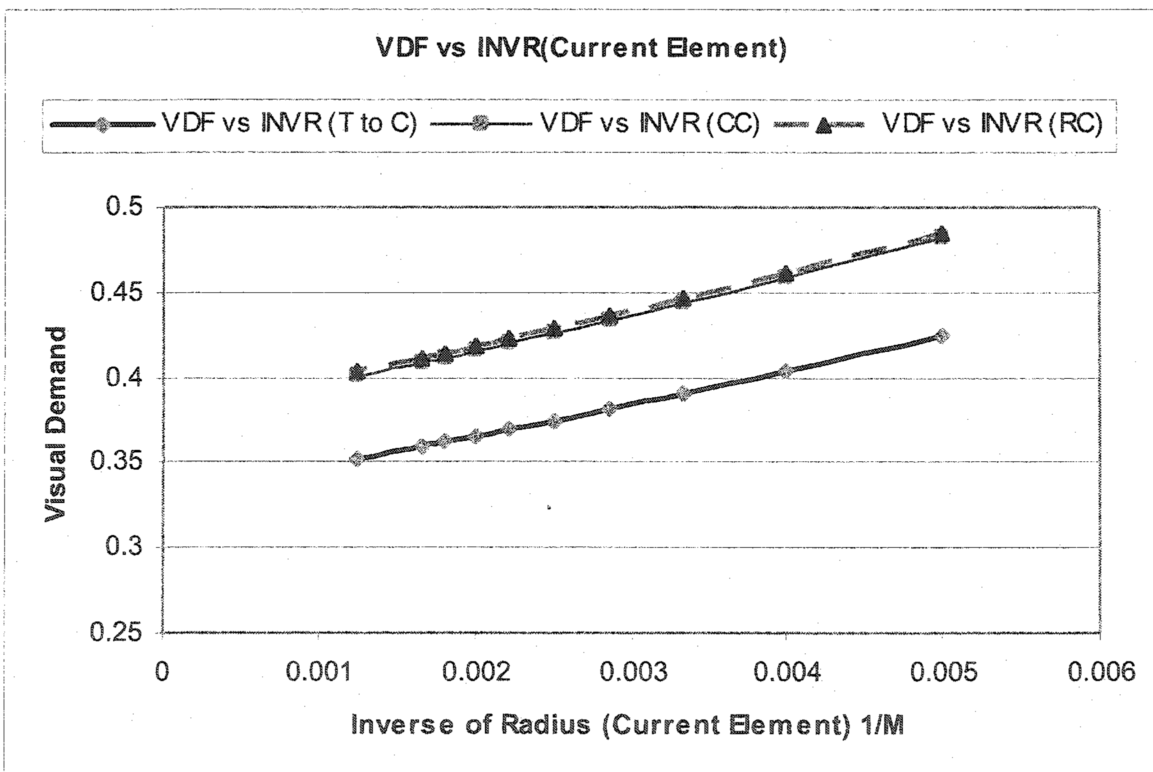

Figure 7 Sensitivity of VDF with varying Inverse of Radius of the Current Curve

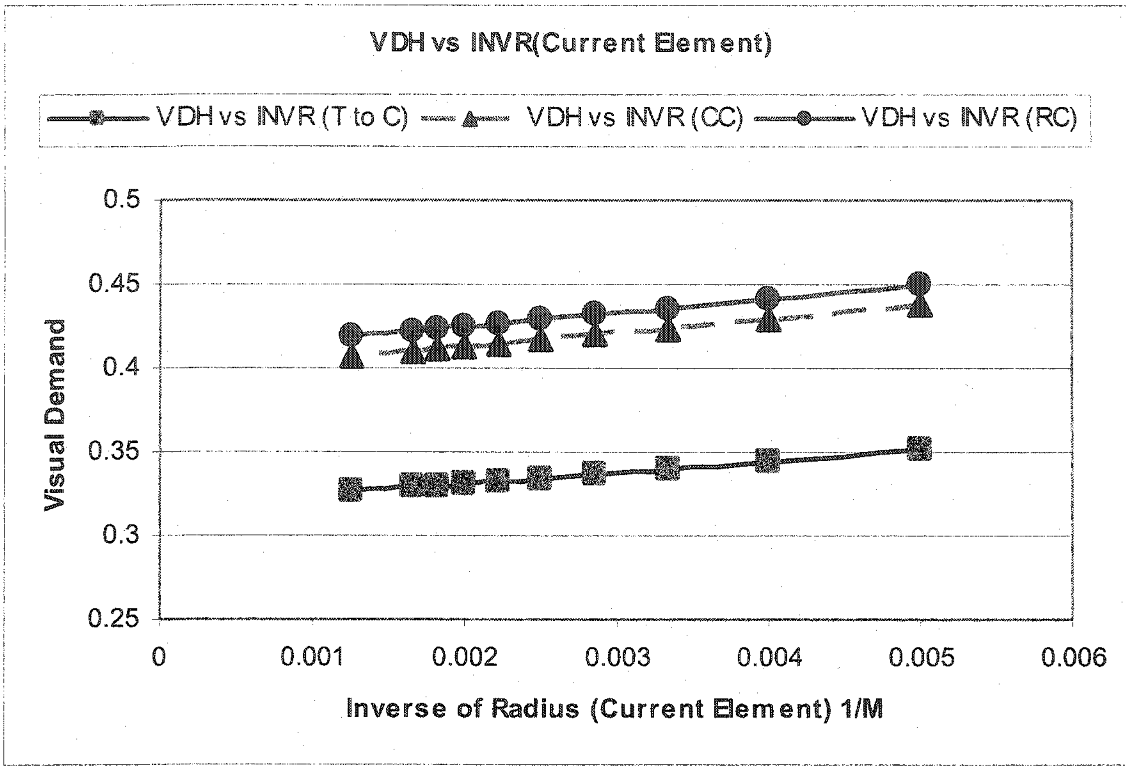

Figure 8 Sensitivity of VDH with varying Inverse of Radius of the Current Curve

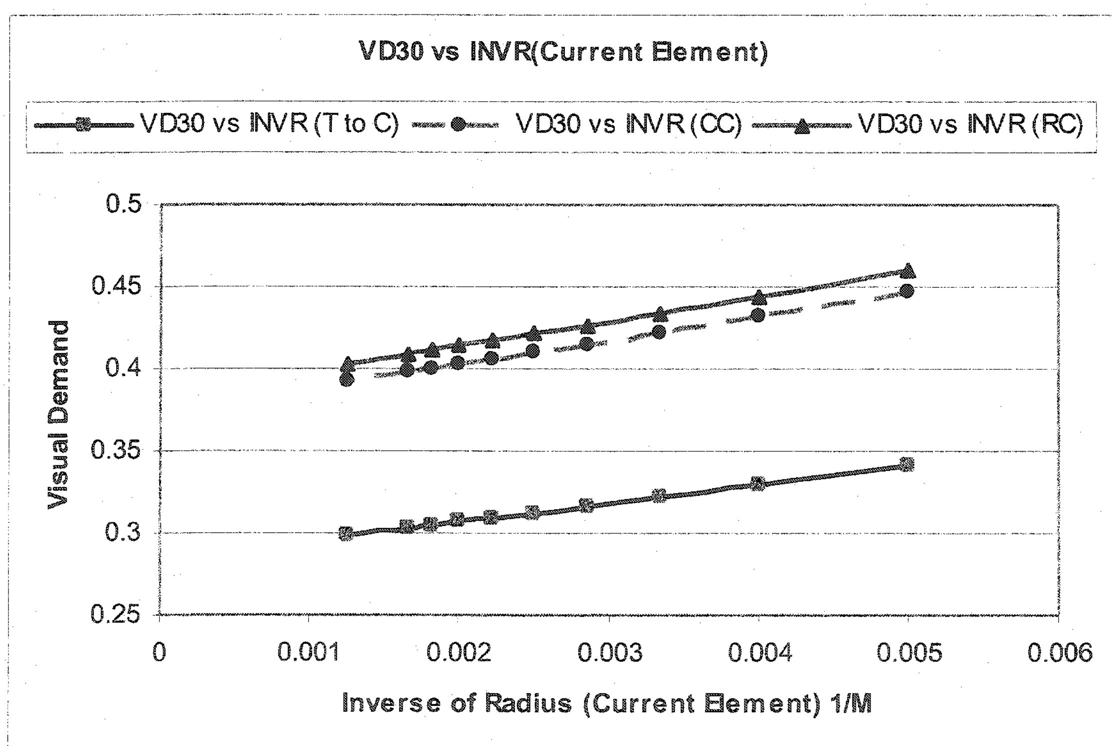

Figure 9 Sensitivity of VD30 with varying Inverse of Radius of the Current Curve

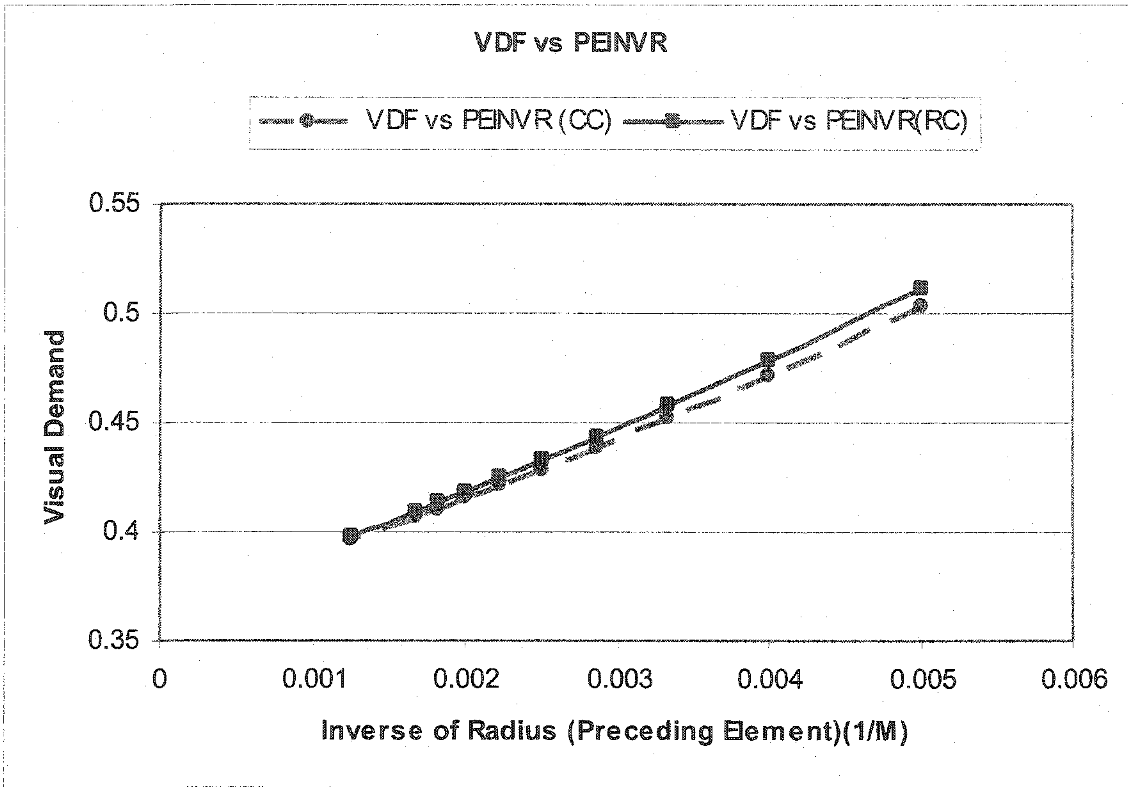

Figure 10 Sensitivity of VDF on Curves with varying Preceding Curve Radius

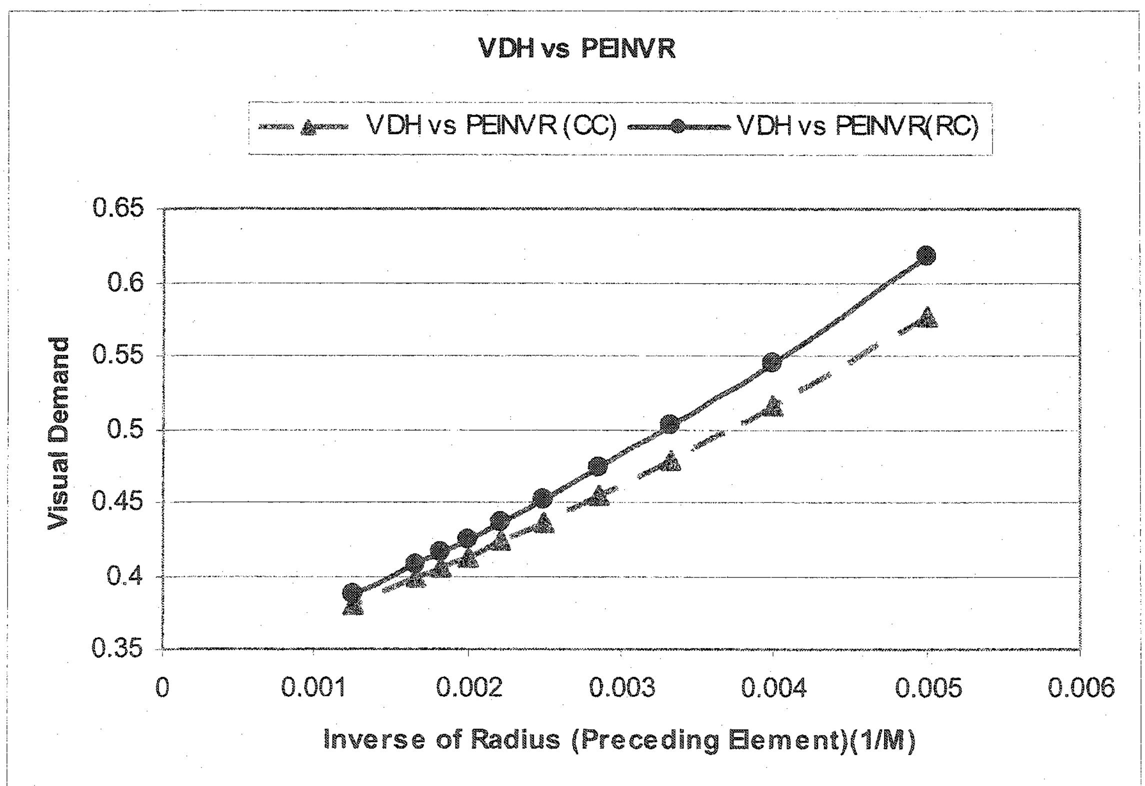

Figure 11 Sensitivity of VDH on Curves with varying Preceding Curve Radius

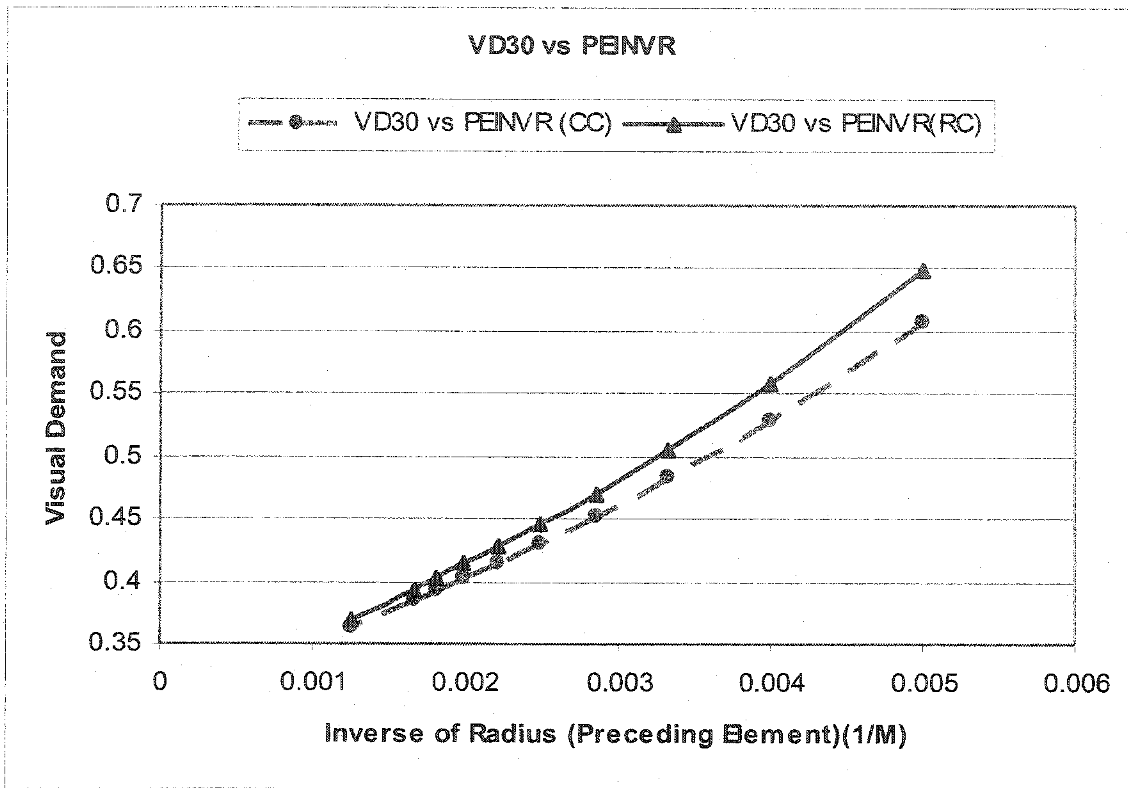

Figure 12 Sensitivity of VD30 on Curves with varying Preceding Curve Radius

The signs of PEINVR and INVR clearly reflect that VD values are directly proportional to these radii, and the coefficients of those clearly show that the PEINVR has always the highest influence in all types of VD. The rate of change of visual demand due to the influence of PEINVR is highest for VD30, decreased for VDH, and lowest in VDF. These clearly reflect the concept ad hoc expectancy.

The reverse and compound curvature effect fades with reduction of PEINVR. Thus, it becomes very clear that visual demand on curves is strongly influenced by the composite effect of the preceding element. The influence of PEINVR has a major effect on VD, and the rate of change of VD is much more dependent on PEINVR than on INVR. The effect of the reverse curve is always higher than that of the compound curve and the tangent–to–curve arrangement in visual demand evaluation, whereas VD on the compound curve remains much higher than that on the curve preceded by a tangent.

However, it is observed that the VDF measure always increases with a higher rate than that of VDH and VD30, as the radius of the current element varies. Figures 13, 14, and 15 clearly illustrate such variation and the comparison of all individual VD measures. The rate of change of VDF is highest while coming from a tangent to a following curve, while this rate decreases when coming from another curve, and reaches a minimum value when negotiating a compound curve.

The influence of varying PEINVR reaches its maximum on VD30, followed by VDH, and then by VDF. However, as clearly reflected from Figures 16 and 17, the influence of reverse curvature is much greater than the influence of compound curvature in the evaluation of visual demand.

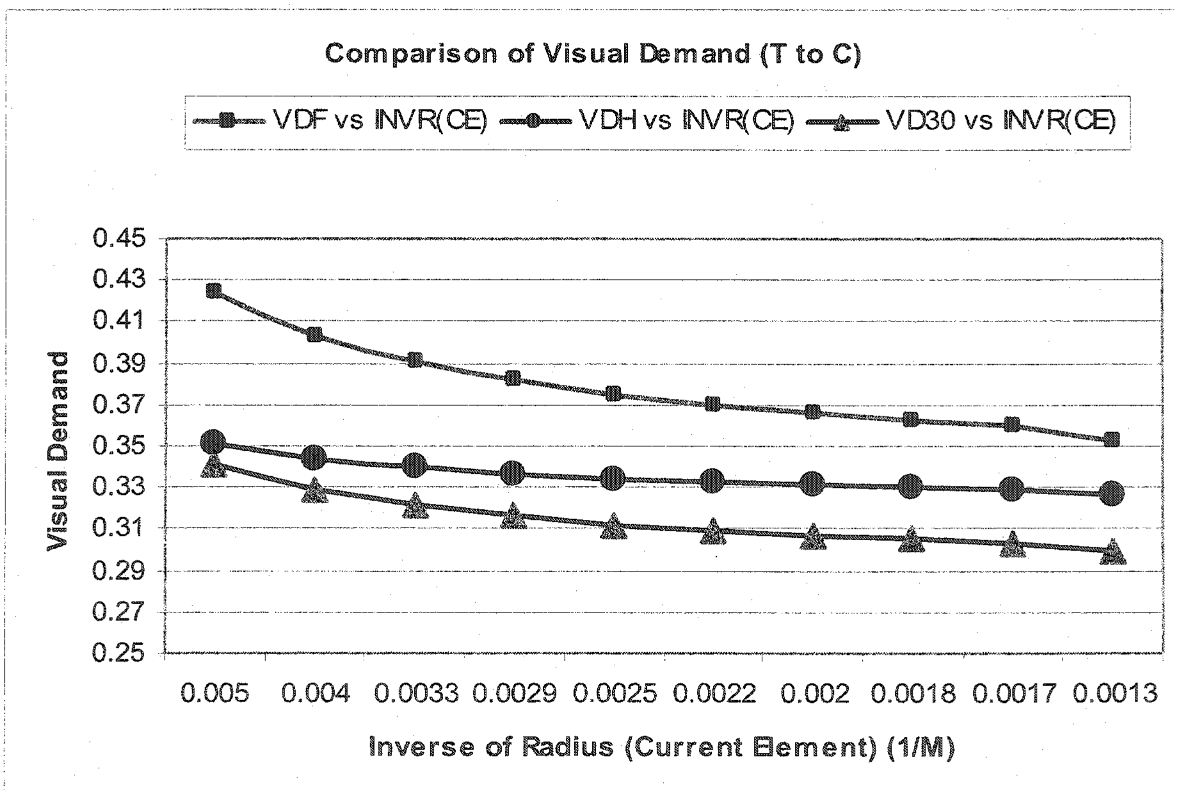

Figure 13 Sensitivity of Visual Demand to INVR (from Tangent to Curve)

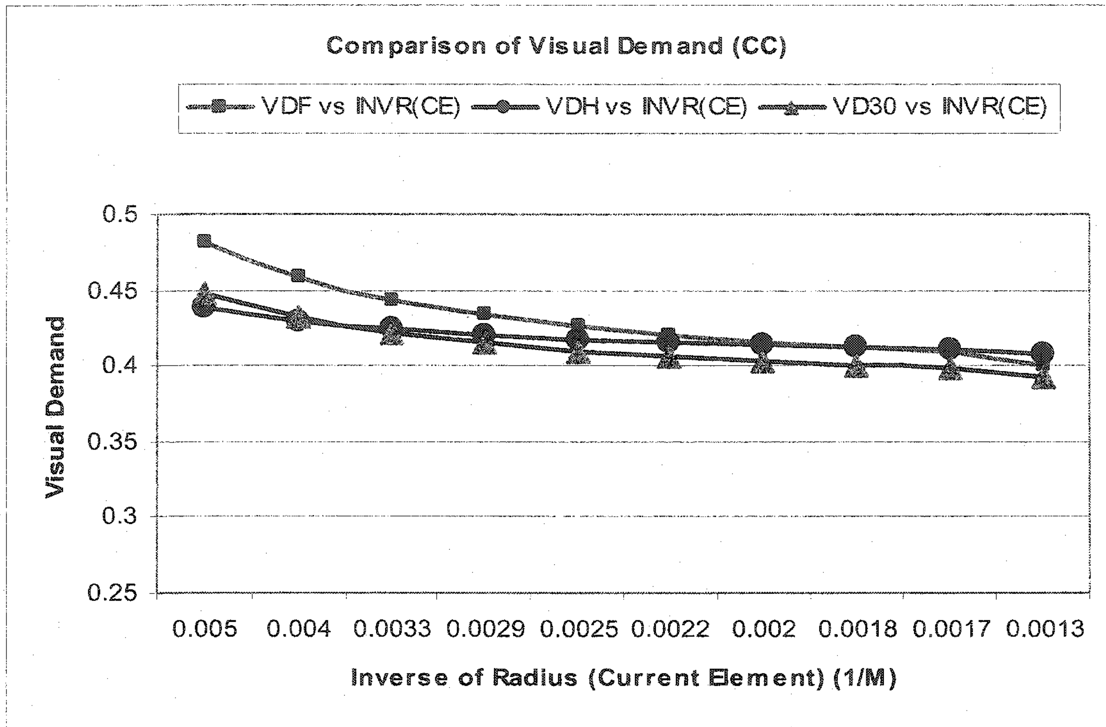

Figure 14 Sensitivity of Visual Demand to INVR (Compound Curve)

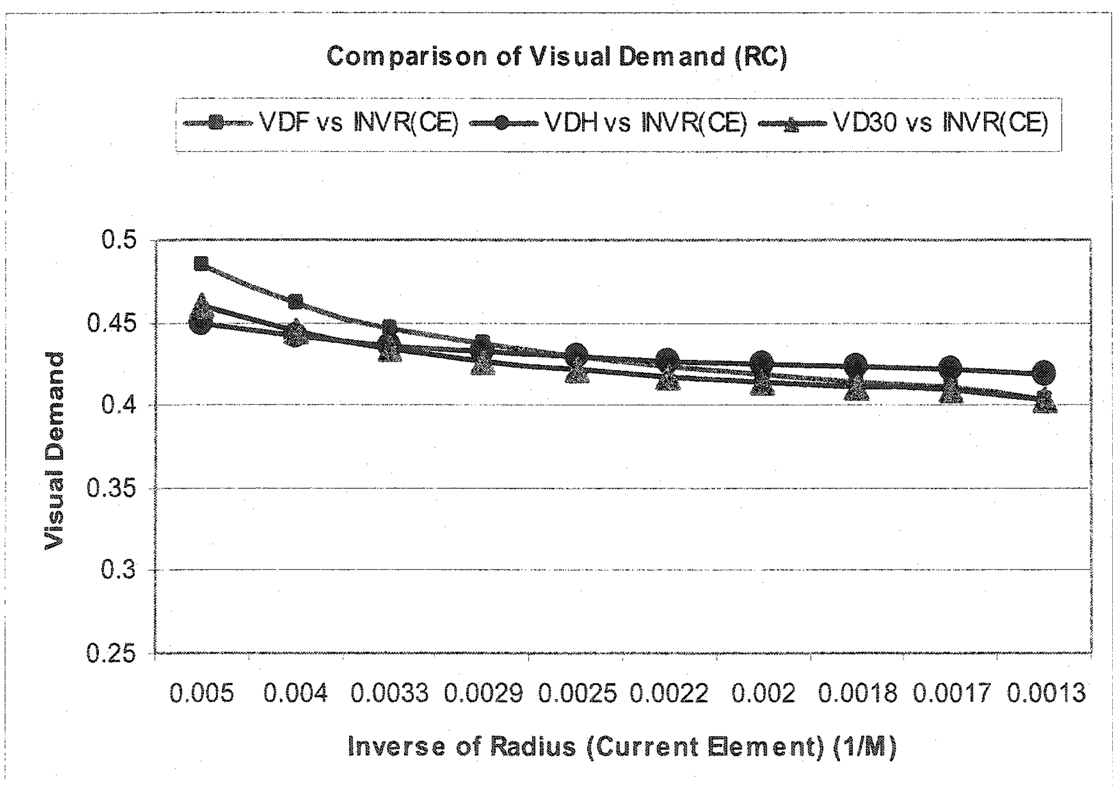

Figure 15 Sensitivity of Visual Demand to INVR (Reverse Curve)

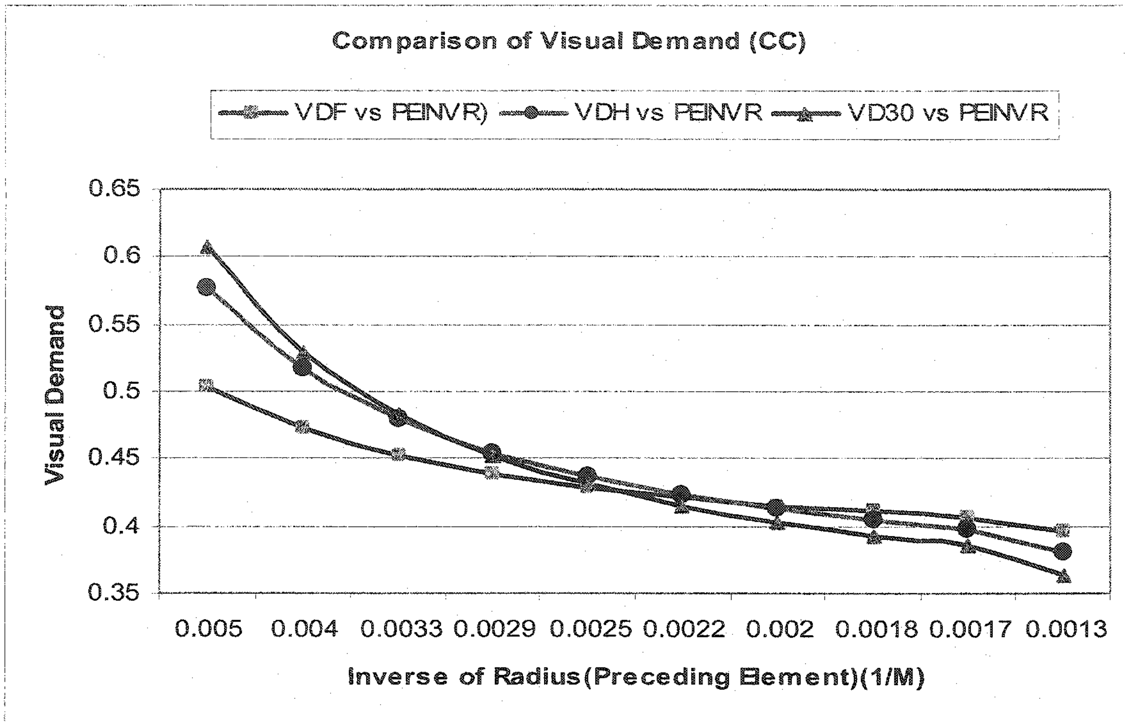

Figure 16 Sensitivity of Visual Demand to PEINVR (Compound Curve)

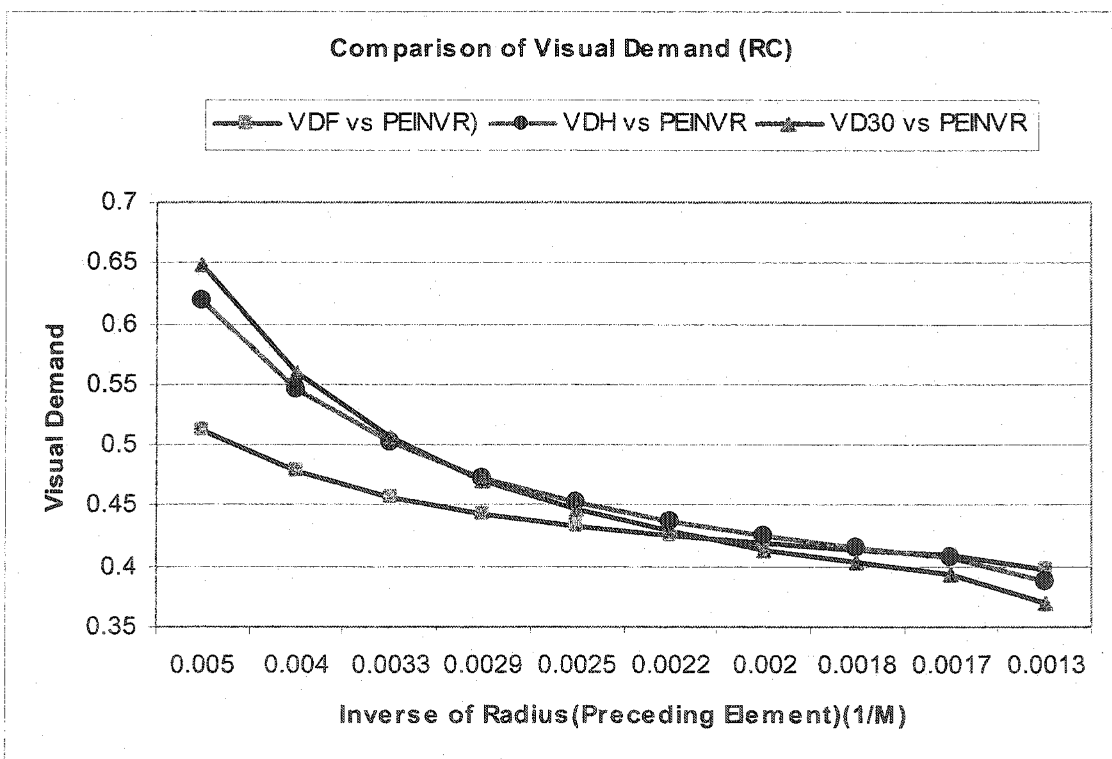

Figure 17 Sensitivity of Visual Demand to PEINVR (Reverse Curve)

5.3.2 Visual Demand on Tangents and Impact of Complex Curvature

The impact of complex curvature on the visual demand of tangents has also become clear from the results of this study. The model developed reflects the impact of the variables PEINVR and PE on the evaluation of all types of VD measures. Especially in developing models of VD on tangents, it has been observed that the PE variable individually causes a significant impact on the evaluation and possesses a high correlation with the obtained/ calculated VD values.

The PE variable, in the case of tangents, was taken as CT (tangent preceded by a curve). In addition, the turning direction of the preceding curve has an immense impact on the evaluation of visual demand of tangents. Thus, this variable has been divided into two categories, PETD (R), and PETD (L), which indicate the directions of the preceding curve as right turning and left turning respectively. Figures 18, 19, and 20 clearly show the impact of turning directions on VDF, VDH, and VD30. It was seen that VD30 remains higher in the current element while coming from a right turning curve. In VDH, the effect of both the directions remains the same but almost becomes identical, whereas in the VDF, the left turning direction was more significant.

It is likely that this effect on VD30 and VDH results from the available sight distance factors, since available sight distance for a given right turning curve always becomes less than for a left turning curve. The reason for the influence of the turning direction on VDF is not clear, although it was observed that VDF goes higher for a tangent preceded by a left curve. A comparison of all VD measures is presented in Figures 21 and 22 for both right turning and left turning curves, where VDH remains almost identical for both directions.

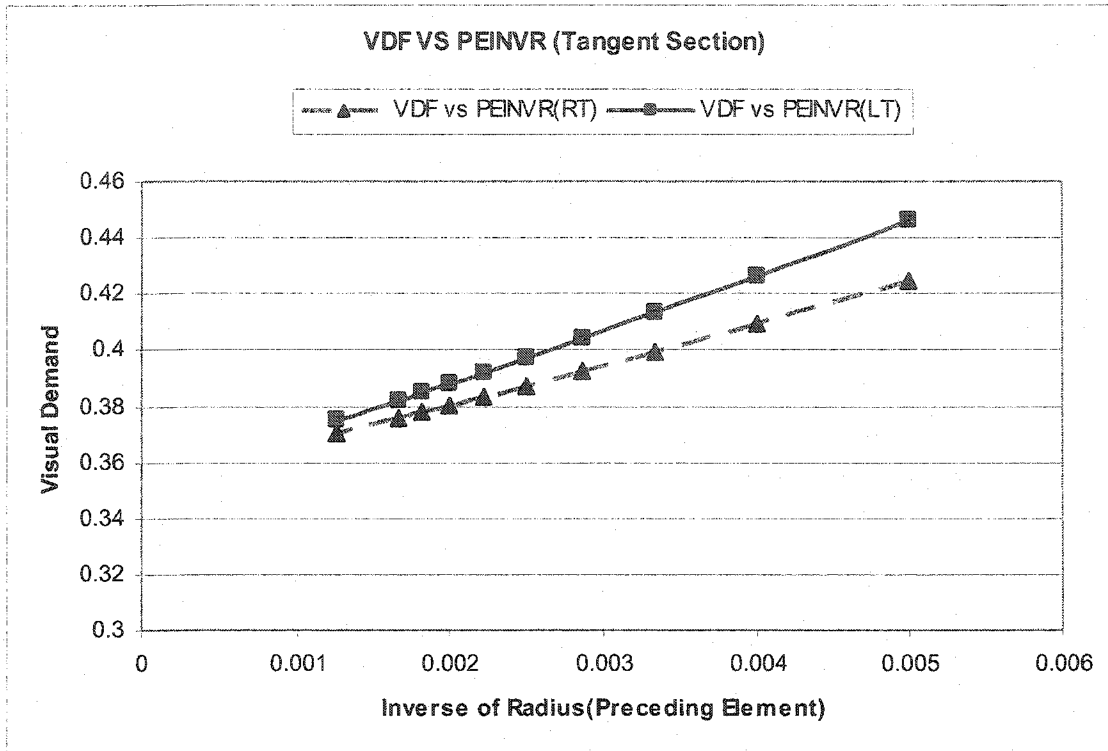

Figure 18 Variability of VDF with varying Inverse of Radius of the Preceding Curve

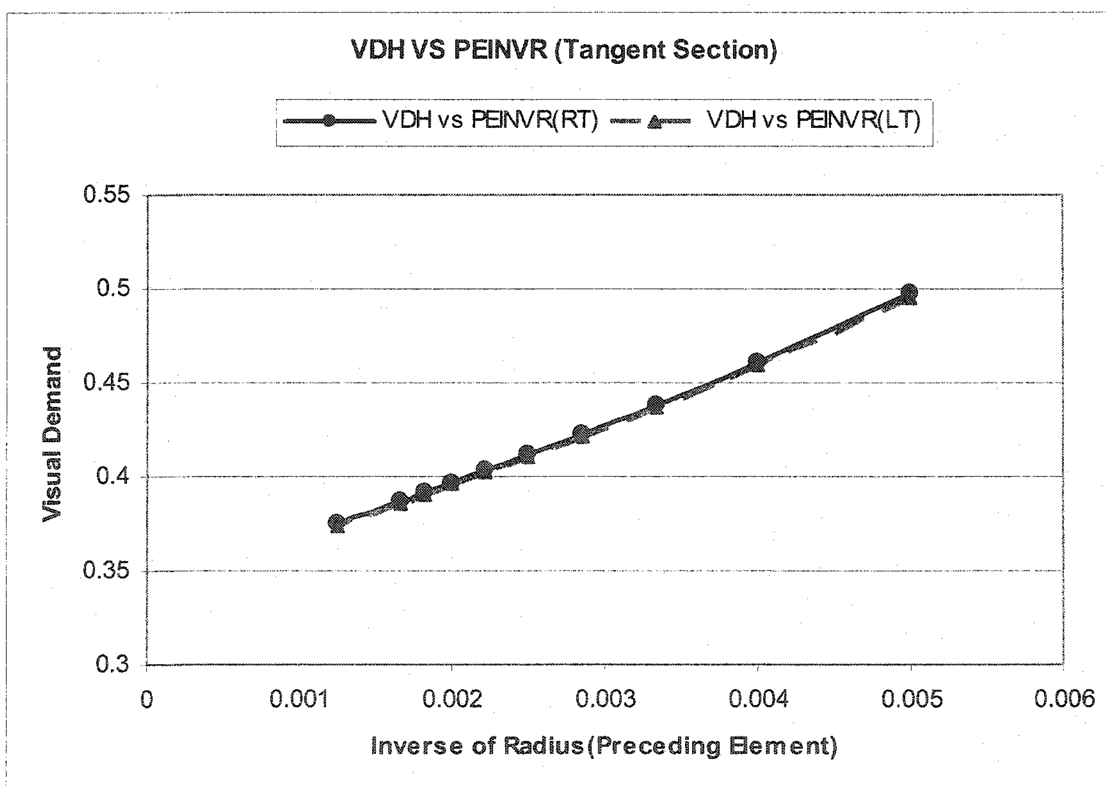

Figure 19 Variability of VDH with varying Inverse of Radius of the Preceding Curve

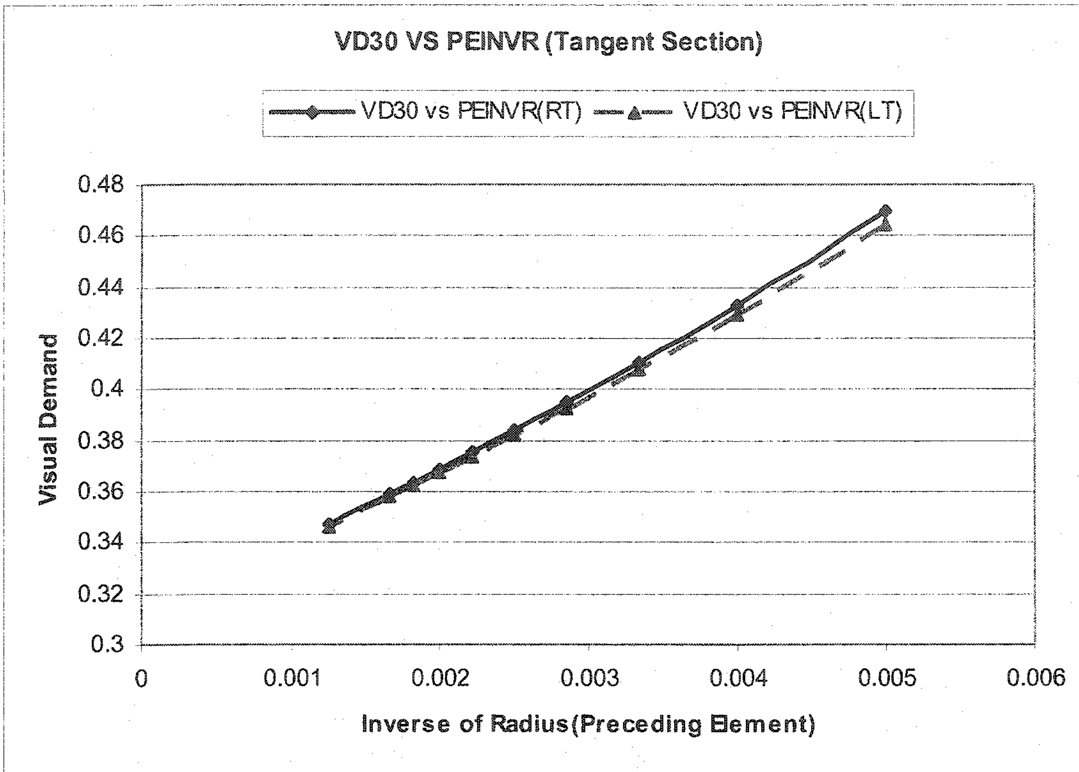

Figure 20 Variability of VD30 with varying Inverse of Radius of the Preceding Curve

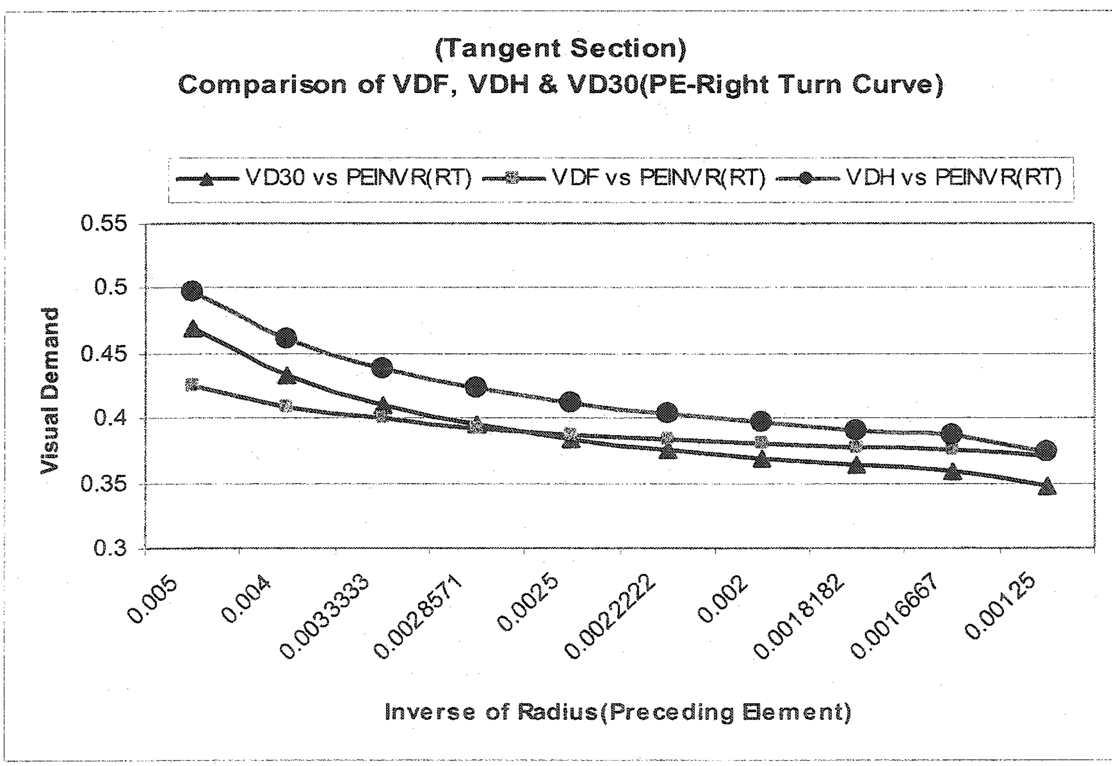

Figure 21 Comparison of VD measures for varying PEINVR (Right Turning Curve)

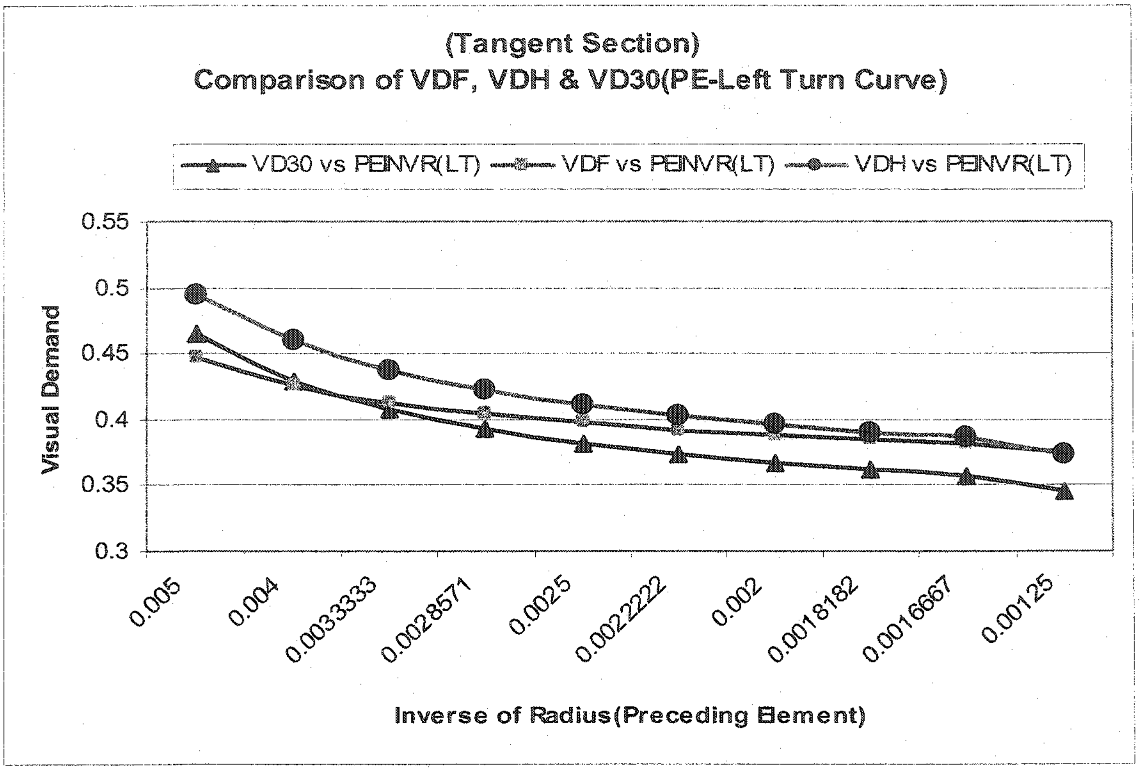

Figure 22 Comparison of VD measures for varying PEINVR (Left Turning Curve)

A comparative study was carried out to consider the goodness of fit of the developed models, for both the curves and for the tangents. The visual demand, obtained in test Alignment 1 from all the subjects during the experimentation, was averaged for all the individual elements. The visual demand for the individual elements of Alignment 1 was calculated using the model equations developed for evaluating VDF, VDH, and VD30. These visual demands were calculated for all curves and tangents. The objective of this study was to understand the effectiveness of applying the developed models in evaluating visual demand in any highway alignment. The comparison graph is presented below to illustrate the goodness of fit of the VDF. The graphs of VDH and VD30 models show similar trends. The RC and LC represent right turning and left turning curves, respectively, and the combination of unidirectional curves constitutes a compound curve,

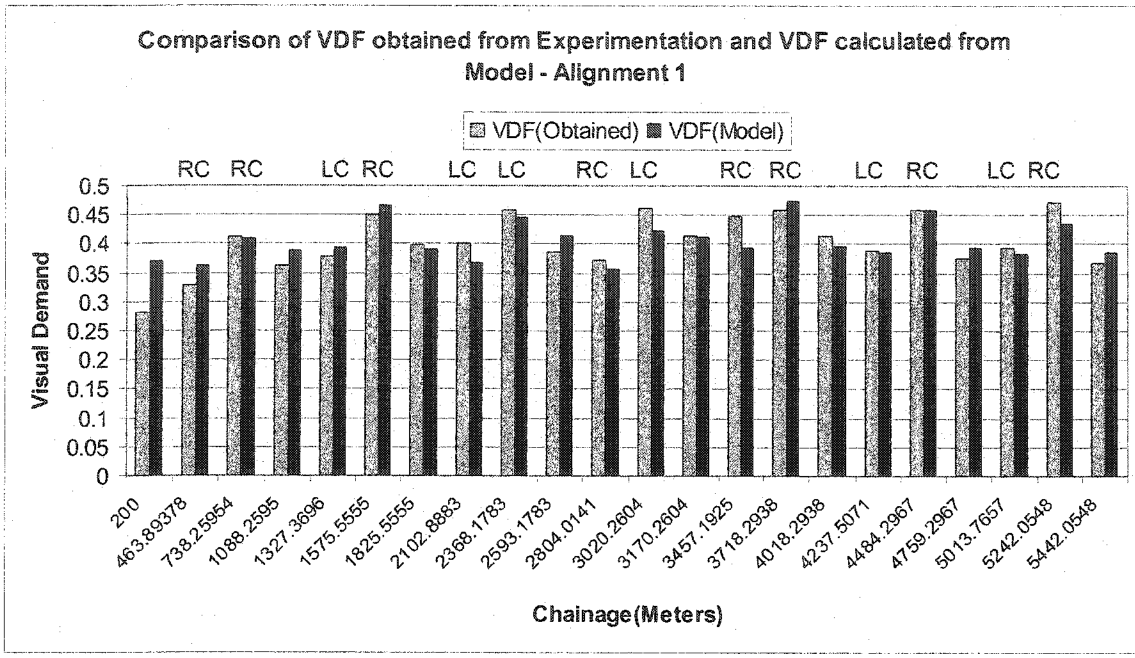

Figure 23 Comparative Study on Goodness of Fit of VDF Model

whereas opposite directional curve combination gives rise to reverse curves.

From the comparative study, it becomes evident that the visual demand calculated from the model very well represents the obtained data from the simulator experimentation. It also becomes evident that both compound curvature and reverse curvature have significant impact on evaluating visual demand in the second curve, whereas the first curve and the tangent have a significant effect of the preceding tangent and any curve respectively. Thus, the primary and main objectives of this research work have successfully been accomplished. All the independent variables were considered in developing the models for visual demand, and those that did not show significant relationship with visual demand measures were not included in the model.

It was expected that the average available sight distance (AASD) would exhibit a fair relationship with visual demand measures, but this variable became insignificant during development of the models. One of the primary reasons for its insignificance might be because of the high correlation of AASD with the radius of curvature, turning directions of curves, deflection angle, and the lane width. Since INVR and LW in all models became significant, the influence of AASD decreased and became ultimately insignificant. A null hypothesis has been carried out during the development of all models, and the variables that became less than 90% significant were generally rejected.

Considering VD30 as an important factor in measuring the change in visual demand did not hold up well at all times. Since the STISIM simulator was a more cost-effective simulator than providing a more realistic experience of on-road driving for the subjects, the results may vary, if identical research is carried out using a more sophisticated and realistic driving simulator.

Due to the absence of the gravity force, none of the subjects felt the sensation of real world driving. The presence of gravity force may cause considerable variance in visual demand, because the subjects understand the effect of lateral friction. On straight portions of road alignment, drivers always asked for a minimum glimpses, whereas on curves, they ask for more, and that may be due to the sensation of the gravity force. That is probably the only reason for the researchers of TTI to consider VD30, but in a simulator experiment, especially at STISIM, this consideration was not considered realistic. Most of the VD30 was calculated based on the proportionate length, which clearly shows that VD30 does not play an important role in a driving simulator where the force of gravity is absent. It has also been understood that all such VD measures possess their own importance. Hence, it is understood that a visual demand profile should be developed when analyzing the consistency of a given alignment, and the corresponding changes from VD30 to VDH and then to VDF may account for an abrupt change in visual demand measure.

5.3.3 Estimation of Performance Measures

The secondary task of evaluating visual demand relative to performance measures did not produce an acceptable result that could be used to fix an upper and lower limit as thresholds of visual demand for any given element. The variability of STDVL does not show any acceptable relationship with VD or with any other relevant geometric features. It also does not prove to be one important parameter in fixing upper or lower limits as the threshold values of VD evaluation.

The model developed to estimate VD has also shown a very close agreement with the model for estimating mental workload as developed by Messer et al. (1979). Visual information is supposed to be the main source of developing mental workload (MWL). Other sources of information during driving include, for example, auditory information. Hence, this could easily be anticipated that VD works as the cause of MWL, whereas MWL is the result of processing all such consecutive information.

The ad hoc expectancy factor, as detailed by Lunenfeld (1990), is reflected by the independent variable PE. This variable complies the concept of carryover workload, as cited by Messer (1979). Hence, the model developed for evaluating VD appears to be an effective start in estimating VD with respect to highway geometric parameters only.

Chapter 6 APPLICATION AND IMPLEMENTATION

6.1 Background

The models developed for visual demand in the form of VDF, VDH, and VD30 reflect their acceptability and their promising application for evaluating design consistency issues. These models may be used to evaluate VD for individual elements as well as for defined stretches comprising a composite curve with preceding and following tangents. The applicability of the developed models was tested by applying these models to different combinations of elements and stretches. In addition, a comparative study was carried out with respect to the established principles of evaluating design consistency issues

The design guide by the Transportation Association of Canada has a revised chapter on Design Consistency (Easa 2003). This chapter deals with a number of given procedures to evaluate design consistency. The detailed literature review in Chapter 2 covers most of the contents of these guidelines. The Design Consistency chapter in TAC divides the evaluation of such design consistency into three major parts: system consistency, local consistency, and safety and consistency. Evaluation of design consistency by the visual demand method falls within the purview of system consistency. Thus, the application of visual demand has been demonstrated considering this area only. Each of the given criteria for evaluating system design consistency has, therefore, been revisited, to demonstrate the accuracy and acceptability of the developed models on visual demand.

6.2 Description of Test Alignments

Three hypothetical alignments are established as follows:

i. An alignment having a simple curve with preceding and following tangents

ii. A mediocre complex alignment comprising one reverse curve with tangents. The radii of individual curves have been kept equal.

iii. A complex alignment comprising a reverse curve, a compound curve, and a simple curve, with preceding, following, and in between tangents.

Simple Alignment

The simple alignment consists of a simple curve as well as the preceding and following tangents. Figure 24 shows the plan view of the simple alignment. The design parameters of this alignment are shown in Table 4.

Mediocre Complex Alignment

Table 5 shows the design parameters of the second alignment, which comprises a reverse curve and the tangents. The radii of both the curves are equal to 500 meters. Figure 25 shows the plan view of the mediocre alignment.

Table 4 Simple Alignment

Feature	Tangent		Curve Turning	Horizontal Curve				
	L_T	Azimuth Nd^{0}E		PC	PT	L_c	R (M)	Delta
Tangent	950	180	-	0	0	0	-	0
Curve	0	80	L	950	1735.398	785.3982	450	100
Tangent	950	80	-	0	0	0	-	0

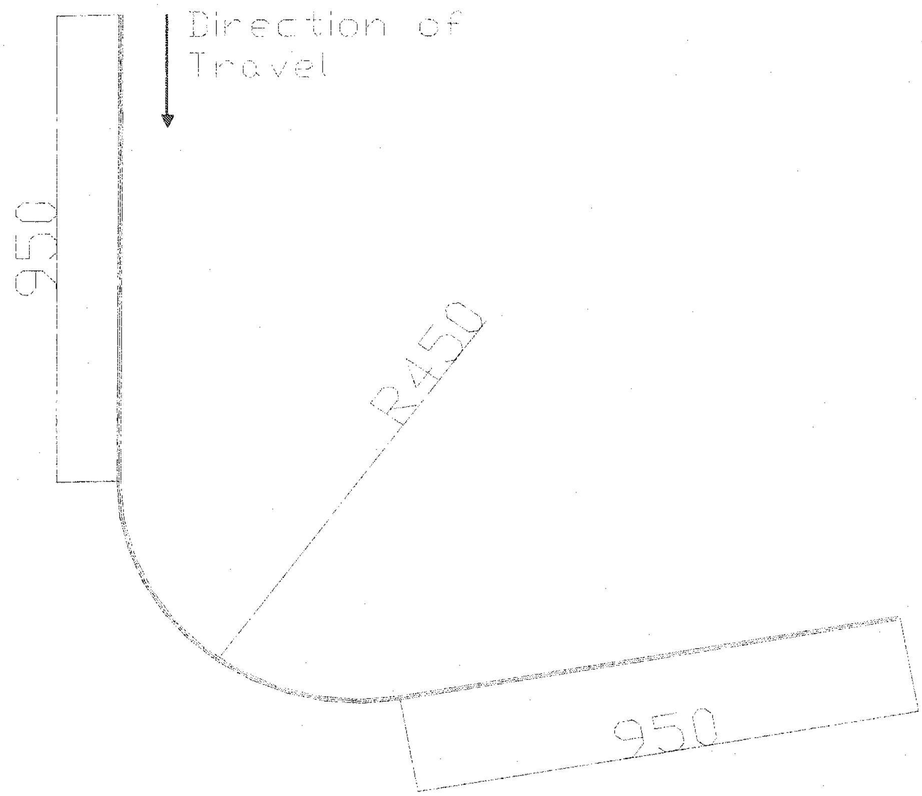

Figure 24 Hypothetical Test Alignment with Simple Curve (Simple Alignment)

Table 5 Mediocre Alignment with Reverse Curve

Feature	Tangent		Curve Turning	Horizontal Curve				
	L_T	Azimuth Nd^0E		PC	PT	L_c	R (M)	Delta
Tangent	500	180	-	0	0	0	-	0
Curve	-	90	L	500	1285.398	785.398	500	90
Curve	-	160	R	1285.398	1896.263	610.865	500	70
Tangent	500	160	-	0	0	0	-	0

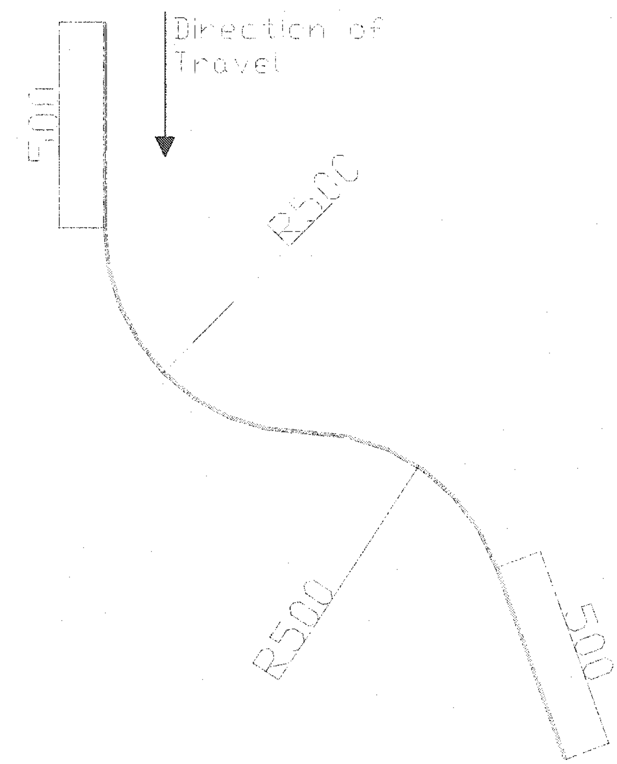

Figure 25 Hypothetical Test Alignment with Reverse Curve (Mediocre Curve)

Table 6 Complex Alignment with Reverse and Compound Curves

Feature	Tangent		Curve Turning	Horizontal Curve				
	L_T	Azimuth Nd^0E		PC	PT	L_c	R (M)	Delta
Tangent	200	90	-	0	0	0	-	0
Curve	-	45	L	200	671.2389	471.2389	600	45
Curve	-	90	R	671.2389	906.8583	235.6194	300	45
Tangent	200	90	-	0	0	0	-	0
Curve	-	30	L	1106.858	1421.018	314.1593	300	60
Curve	-	0	L	1421.018	1656.637	235.6194	450	30
Tangent	225	0	-	0	0	0	-	0
Curve	-	90	R	1881.637	2110.973	229.3363	146	90

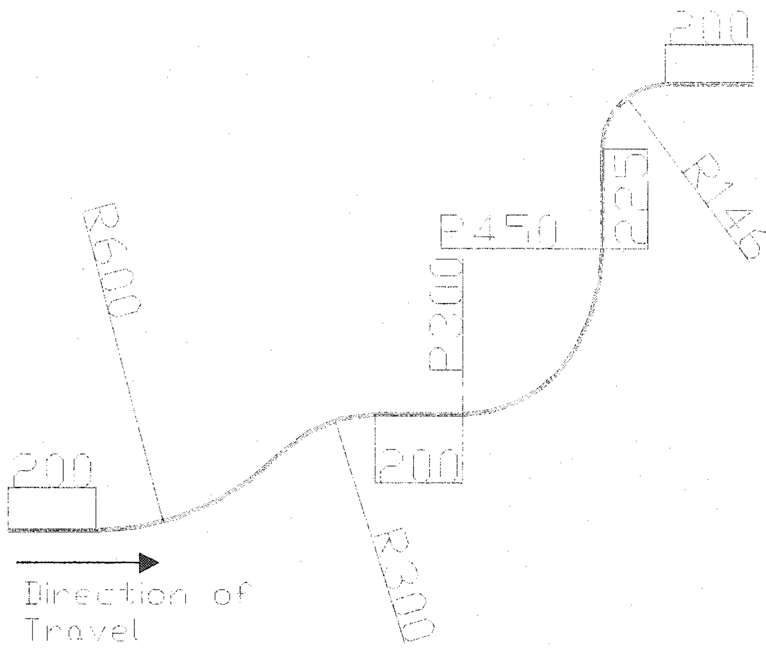

Figure 26 Hypothetical Test Alignment with Reverse and Compound Curve (Complex Alignment)

Complex Alignment

Table 6 shows the design parameter of the complex alignment, and Figure 26 shows the plan view. This alignment consists of a reverse curve, a compound curve, and a simple curve with preceding, following, and in-between tangents.

6.3 Design Consistency Method Evaluated

As discussed in section 6.1, system consistency forms the main category of design consistency, and was evaluated primarily by applying the following three methods:

- Operating speed
- Alignment indices
- Mental workload

Easa (2003) suggests that system consistency of any existing or proposed alignment should be evaluated using the operating speed/speed profile method and/or the alignment indices method. In the section related to driver workload consistency, it clearly states that, due to the absence of a comprehensive analytical model, the application of workload consistency to practical evaluation of highway design is limited. Previous models relating to the three methods of design consistency are discussed in detail in Chapter 2. However, it is useful to present a brief discussion of the individual methods, as follows:

Operating Speed

The operating speed consistency measure suggests that the speed difference between two consecutive elements should not be more than 20 km/h. Otherwise the corresponding element needs to be redesigned such that the speed difference is brought within a difference of 20 km/h and preferably within a difference of 10 km/h.

Alignment Indices

This method of evaluating design consistency suggests checking the average radius of all the radii used in a stretch of any alignment, and comparing the ratio of an individual radius to the average radius. In addition, there are a number of suggestions given by different researchers, but no threshold criteria has been given to detect a specific inconsistency in proposed or existing alignments, where this measure can be applied independently. Hence, this method always forms a secondary check in consistency evaluation.

Visual Demand

There is currently no established method. Some models have been developed and might be applied in a disaggregated manner, but there is nothing that can be applied to measure visual demand for a highway stretch. The models developed in this study shed some light in this area and may be used to determine visual demand for any element as well as for a defined stretch of any alignment.

6.4 Results

6.4.1 Simple Alignment

This is one of the alignments of a 2-lane rural highway used in the simulator study. The operating speed model of TAC has mainly dealt with a design speed of 100 km/h (Easa, 2003). The operating speed on the tangents is calculated using Equation 47 and assuming an equivalent radius (R) of 800 meters, as suggested by TAC. This operating speed model applies for a flat terrain.

$$V_{85} = 104.82 - 3574.51/R \quad (47)$$

The operating speed results are shown in Table 7. The difference in operating speeds between the tangent and the curve was 3.5 km/h, which is well within the acceptable limit of 10 km/h. This shows, according to the accepted principle of operating speed, that the given alignment is consistent.

Table 7 Calculated Operating Speed and Visual Demand on Individual Element (Simple Curve)

Element	Length (M)	Radius (M)	Operating Speed (V_{85}) Consistency in Km/h		Visual Demand Evaluated (VDF)
			V_{85} (Km/h)	$V_{85}1-V_{85}2$ (Km/h)	
Tangent	950	0	100.4	-	0.368
Curve	785.398	450	96.9	3.5	0.369
Tangent	950	0	100.4	3.5	0.381

The alignment indices method does not apply to a single curve alignment. Applying the current model developed on VDF (Equations 41 and 44) the VDF on the curve and tangent, respectively, were calculated as shown in Table 7.

6.4.2 Mediocre Alignment

The difference in operating speeds between the tangents and the curves, in the mediocre alignment, shows a very good and consistent alignment (Table 8). This is especially true since the difference between the operating speeds on the consecutive opposite curves becomes zero. The concept of critical tangent length does not apply to only one reverse curve alignment; hence, it is not discussed here. The alignment indices method applies here since this alignment has an average radius (AR) and comparative radius to average (CRR).

Table 9 shows the results of the analysis using the alignment indices method. The results show that this alignment is perfect, since the percentage difference in CRRi becomes zero. Applying the visual demand method, we have the results as in Table 10. This method points out the difference in visual demand required for the individual element of the alignment, which, in turn, indicates the effect of composite curvatures.

Table 8 Difference of Operating Speed on Consecutive Elements (Mediocre Curve)

Feature	Length (M)	Radius (M)	Operating Speed Consistency	
			V_{85} (Km/h)	$V_{85}1-V_{85}2$ (Km/h)
Tangent	500	800	100.4	-
Curve	785.398	500	97.7	2.681
Curve	610.865	500	97.7	0
Tangent	500	800	100.4	2.681

6.4.3 Complex Alignment

This hypothetical alignment was considered for comparative studies. The radii of some curves have been considered strictly for calculation, which does not comply with any guidelines of either TAC or AASHTO. Again, the disaggregated model of estimating operating speed is applied, as discussed in the previous example. The desirable speed, however, is considered to be 100 km/h. The critical length for connecting tangents has also been worked out to check the consistency of the tangent lengths to accommodate varying speeds between one curve and another; this applies only to the second and third tangents of the given alignment.

The results obtained by applying operating speed consistency are shown in Table 11. These results show that the overall alignment is very good. The consecutive individual elements in this alignment are consistent since the difference in operating speed is less than 10 km/ hour. The last right curve is not useful for consideration since the operating speed difference exceeds 20 km/h.

Table 9 Difference of CRRi on Individual Elements (Mediocre Curve)

Feature	Length (M)	Radius (M)	Operating Speed Consistency		
			AR	CRRi	% difference
Tangent	500	800	000	-	-
Curve	785.398	500	500	1	0
Curve	610.865	500	500	1	0
Tangent	500	800	000	-	-

Table 10 Difference of Visual Demand on Consecutive Elements (Mediocre Curve)

Feature	Length (M)	Radius (M)	Turning	VDF	%difference
Tangent	500	-	-	0.368	-
Curve	785.398	500	L	0.366	0.819
Curve	610.865	500	R	0.418	14.349
Tangent	500	-	-	0.378	9.68

Table 11 Difference of Operating Speed on Consecutive Elements (Complex Curve)

Feature	Length (M)	Radius (M)	Operating Speed Consistency		
			V_{85} (Km/h)	T_{LC} (M)	$V_{85}1-V_{85}2$ (Km/h)
Tangent	200	800	100.4	-	-
Curve	471.2389	600	98.9	-	1.5
Curve	235.6194	300	92.9	-	6.0
Tangent	200	800	100.4	111.05	7.5
Curve	314.1593	300	92.9	-	7.5
Curve	314.1593	450	96.9	-	4.0
Tangent	225	800	100.4	165.97	3.5
Curve	229.3363	146	80.3	-	20.1

Table 12 Difference of CRRi on Individual Elements (Complex Curve)

Feature	Length (M)	Radius (M)	AR (M)	CRRi	%difference
Tangent	200	800	524.5	1.525	-
Curve	471.2389	600	524.5	1.144	25
Curve	235.6194	300	524.5	0.572	50
Tangent	200	800	524.5	1.525	-
Curve	314.1593	300	524.5	0.572	62.5
Curve	314.1593	450	524.5	0.858	50
Tangent	225	800	524.5	1.525	-
Curve	229.3363	146	524.5	0.278	81.75

Table 13 Difference of Visual Demand on Consecutive Elements (Complex Curve)

Feature	Length (M)	Radius (M)	Turning	VDF	%difference
Tangent	200	800	-	0.368	-
Curve	471.2389	600	L	0.360	2.431
Curve	235.6194	300	R	0.437	21.37
Tangent	200	800	-	0.404	7.57
Curve	314.1593	300	L	0.391	1.217
Curve	314.1593	450	L	0.462	18.394
Tangent	225	800	-	0.400	13.396
Curve	229.3363	146	R	0.464	15.933

As pointed out earlier, the radii of some curves do not comply with the AASHTO and/or TAC guidelines, since the minimum radius for a two-lane rural highway having a design speed of 100 km/h should be 438 meters. Two radii of the present alignment do not satisfy that criterion. However, only the last curve of the complex alignment is proven to be an inconsistent element when analyzed with the operating speed consistency model.

6.5 Discussion on Results

For simple curves, the results clearly show that visual demand increases from the preceding tangent to the following tangent through the left curve. Although all established measures in evaluating design consistency show that the following tangent and preceding tangent bear no difference in undertaking design consideration, the visual demand on the following tangent remains at a higher level with the carryover effect of the preceding curve. Higher demand causes higher lateral deviation by the driver, and chances of lane extrusion are high. Hence, individual precautions in designing the tangents should be applied. Since visual demand decreases slowly with the length of the tangent, the lane width of the tangent should be identical to that of the curve for a considerable length. The visual demand should, however, be evaluated considering approaches from either direction for any highway stretch. Since the threshold values for visual demand could not be established, it is possible to comment on workload design consistency only based on strict engineering sense. If a variation of visual demand within a well-defined limit produces an acceptable design, this alignment may be considered consistent as well. In addition, for implementing proper design consistency for a continuous stretch, the stretch as a whole needs to be considered, and consistency measures should be applied from whole to part.

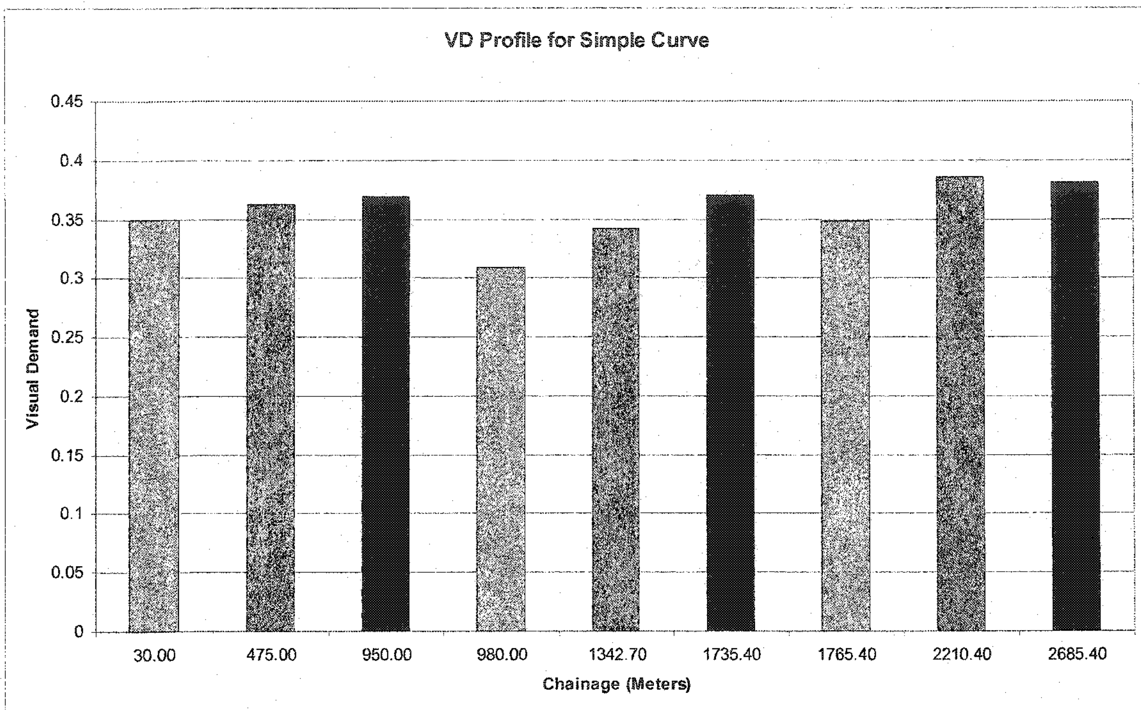

Figure 27 Visual Demand Profile for Simple Curve Alignment

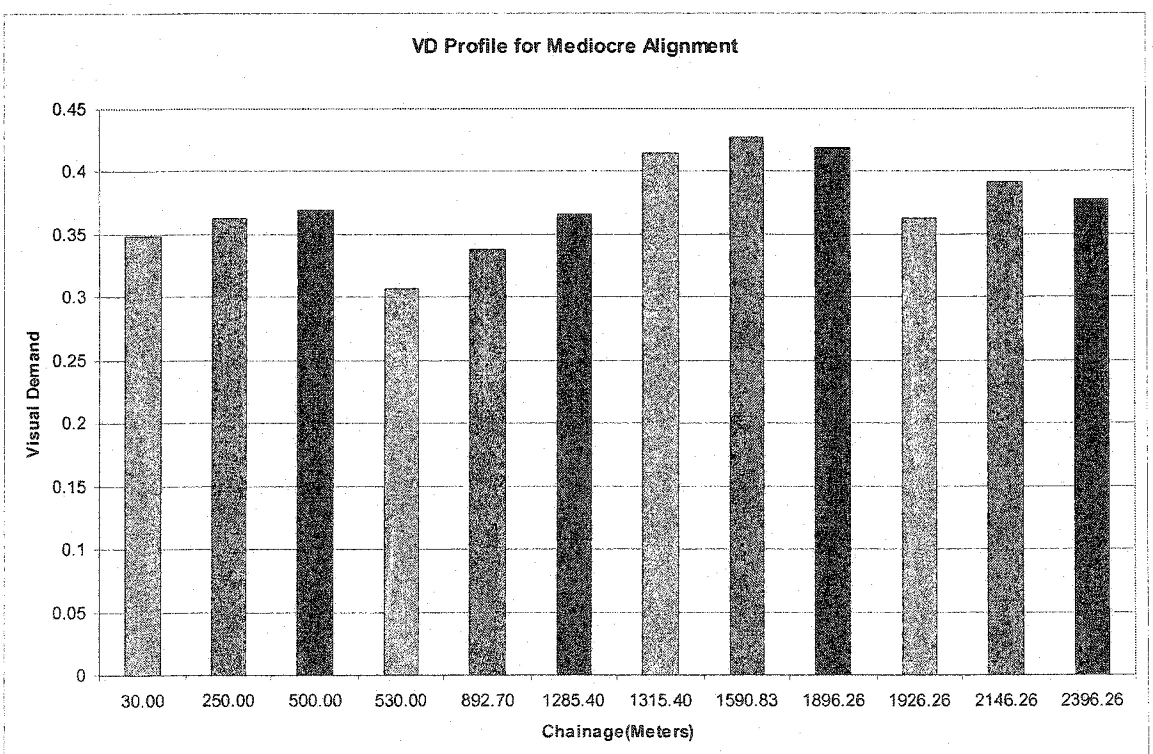

Figure 28 Visual Demand Profile for Mediocre Alignment

The mediocre alignment results (operating speed, or alignment indices) show that the given alignment is consistent and that no discrepancy exists between the consecutive elements. However, the analysis by visual demand clearly shows that the demand goes very high while negotiating a following curve that comes after a preceding curve of the opposite direction. This depicts the importance of reverse curvature effect on mental demand.

The complex alignment analysis clearly shows that the visual demand produces more sensitive result with respect to other methods, as it considers directly the feature characteristics and the turning direction. The result of the application of the model of alignment indices is given in Table 12. This alignment indices consistency evaluation does not provide any threshold values to comment on design inconsistencies of individual elements in and along any given alignment.

The developed visual demand model was applied to the same alignment, and the results are given in Table 13. An overall comparison of the results obtained from the three methods for the complex alignment is given in Table 14.Thus, it may be inferred from the above discussion that:

- This VD method highlights the discrepancy by considering the effect of the previous element in terms of carryover expectancy, which remained hidden in other models used to evaluate design consistency.
- This is the only method that takes into consideration all the individual elements characteristics in terms of tangents and/or curves in a given alignment and, thus, produces a continuous check on visual demand on each of the segments.
- The VD profile will form the best check for evaluating VD consistency.

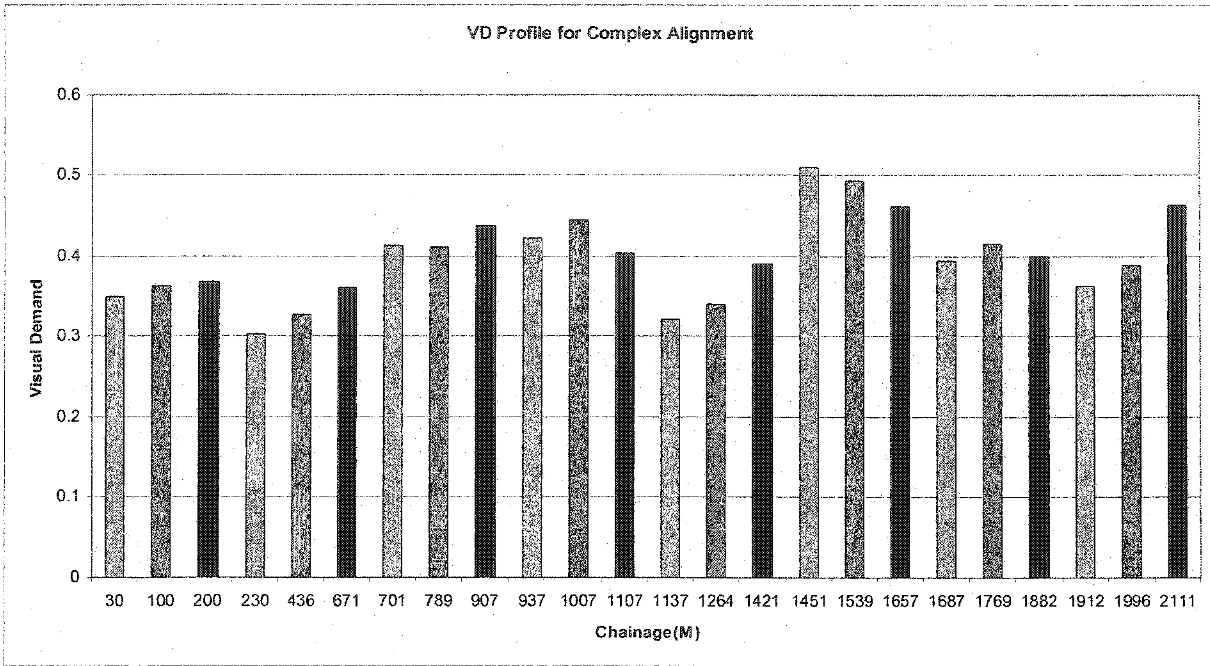

Figure 29 Visual Demand Profile for Complex Alignment

Table 14 Comparison of Operating Speed, Alignment Indices and Visual Demand (Complex Curve)

Feature	Radius (M)	Turning	Operating Speed (Km/h)		Alignment Indices		Visual Demand	
			V_{85}	$V_{85}1-V_{85}2$	CRRi	% Difference	VDF	% Difference
Tangent	-	-	100.4	-	1.525	-	0.368	-
Curve	600	L	98.9	1.5	1.143	25	0.360	2.431
Curve	300	R	92.9	6.0	0.572	50	0.437	21.37
Tangent	-	-	100.4	7.5	1.525	-	0.404	7.57
Curve	300	L	92.9	7.5	0.572	62.5	0.391	1.217
Curve	450	L	96.9	4.0	0.858	50	0.462	18.394
Tangent	-	-	100.4	3.5	1.525	-	0.400	13.396
Curve	146	R	80.3	20.1	0.278	81.75	0.464	15.933

Chapter 7 CONCLUSIONS AND RECOMMENDATIONS

7.1 Conclusions

The purpose of this research was to examine the effects of complex curves (reverse and compound curves) on the driver's visual demand. The design of experiments and the methodology adopted in this research have been developed through a number of steps during the course of this study. The initial simulation of complex alignments clearly showed that the tangent length between two curves or between a pair of curves plays a vital role in evaluating VD. The minimum length of tangents should be such that it provides drivers with a different feeling from the feeling on a curve.

If the in-between tangent length (between a pair of simple curves or complex curves) is too small or the travel time on such tangent is less than PRT, no driver can understand that element as a tangent. Instead, drivers may negotiate the element as a curve. This is a serious source of inconsistency in highway design. The alignments, therefore, were developed in this study keeping in mind that any subject driver had almost same span of time with a little variance to negotiate individual elements of any alignment.

It has also been observed that most of the subjects requested more visual information at the beginning, whereas the demand kept lessening as they continued driving. This criterion satisfies the concept of acclimatization, which should be given due consideration when developing a highway design. Once a driver gets acclimatized with the first phase of driving, he or she might pay more attention to solving complex problems, paying less attention to negotiating highway geometric elements.

Hence, in conclusion, the following points are highlighted:

- The visual demand model needs to be applied from each direction of travel. This would ensure that the proposed radius of each curve of a reverse curve would be designed to provide the best and most consistent alignment.
- All composite curves have a positive impact on visual demand. The preceding element (PE), and its characteristic plays an important role in evaluating visual demand.
- The probability distribution function of VD is a skewed normal distribution, and 'Log Normal' distribution shows good matching and goodness of fit.
- Disaggregate statistical models could be developed with different geometric parameters, but the radius of the current element and the preceding element, including the preceding element characteristics, have been proven to be the most significant exogenous variables in developing expressions for VD.
- The estimation of threshold values of VD will play an important role in evaluating the consistency of a design along any highway alignment. However, it is understood that a great deal of variance in VD in consecutive elements will indicate inconsistent design. However, such threshold cannot be established in this study, since no reliable performance measures could be developed.
- This visual demand evaluation model could prove to be the most acceptable model for pointing out inconsistencies that may have been overlooked, by applying the established model of operating speed, when evaluating design consistency.

- Since threshold values have not yet been established, visual demand should be applied as a secondary check on the alignment design subsequent to applying the operating speed design consistency model to evaluate design consistency.

7.2 Recommendations

- The visual demand models have been developed for an operating speed of 80 km/h. Hence, the developed model should be verified using a rural 2-lane highway in a flat terrain with an operating speed of 80 km/h.
- The variation of cruising speed is expected to have an immense impact on VD. Verifying this may easily be accomplished by conducting the experiment with different speeds.
- This research finding is a start at assessing the impact of composite alignment when considered alone as a highway geometric parameter, without any traffic parameters. Traffic parameters are also expected to have a considerable impact on VD. Hence, a visual demand study should include traffic volume, in both directions, to examine the impact of traffic flow.
- Visual demand should be evaluated with other relevant complex highway geometric elements, including intersections, lane drops, and merging lanes.
- Urban complexities, like pedestrian crossings, should also be incorporated to arrive at a complete model to evaluate visual demand.
- Lane width and turning direction play an important role in the final modeling of visual demand. On the other hand, for consistent road design, the normal criteria should be adopted in widening lanes at curves as per the guidelines provided by TAC or AASHTO.

- The entire experiment has been carried out for two-dimensional, 2 lane rural highway alignments. Visual demand models needs to be developed in a three-dimensional perspective, which will be more useful in application to the real world of highway design. Multilane highways should also be simulated to determine the impact on visual demand in evaluating design consistency.
- After VD thresholds are developed, the visual demand model could be applied in problem prone areas or in accident-prone areas. These areas may possess inconsistencies among consecutive highway elements as far as visual demand is concerned. However, the visual demand model should be applied with VD profile to identify inconsistencies in the alignment under consideration.

References

1. AASHTO (2001). A Policy of Geometric Design on Highways and Streets 2001. Exhibit 2-26 and 2-27. 51 - 52.
2. Anderson, I.B., Bauer, K.M., Harwood, D.W. and Fitzpatrick, K. (1999). Relationship to Safety of Geometric Design Consistency Measure for Rural Two-Lane Highways.- Transportation Research Record 1658 , 43 – 51
3. Al-Masaeid, H.R., Hamed, Mohammad, Aboul-Ela, Mohammad and Ghannam, Adnan G. (1995). Consistency of Horizontal Alignment for Different Vehicle Classes. Transportation Research Record 1500, 178 - 183
4. Alm, H., and Nilsson, L. (1994). Changes in driver behaviour as a function of hands free mobile phones: A simulator study. Accident Analysis and Prevention 26(4), 441-451
5. Alexander, G.J and Lunenfeld, H. (1986). Driver Expectancy in Highway Design and Traffic, Operations. U.S. Department of Transportation, Federal Highway Administration, Washington, D.C.
6. Bernac, T. (1996). Safety at Curves and Road Geometry Standards in some European Countries. Transportation Research Record 1523, 99 – 105
7. Binns, Cw; Knowles, Ss; Blaze-Temple, D (1987). Taking Risks: The Drinking and Driving Practices Of 17-30 Year Old Males. Technology
8. Brown, I. D., and Poulton, E. C. (1961). Measuring The Spare Mental Capacity of Car Drivers by a Subsidiary Task. Ergonomics 4(1), 35-40.
9. Briem, V., and Hedman, L. R. (1995). Behavioral Effects of Mobile Telephone Use During Simulated Driving. Ergonomics 38(12), 2536-2562.

10. Brown, I. D. (1965). Effect of car radio on driving in traffic. Ergonomics 8(4). 475 - 479.

11. Cleveland, D.E., Kostyniuk, L.P., Waissi, G.R., Olson, P.L. and Fancher, P.S. (1985). Stopping Sight Distance Parameters. Transportation Research Record 1026, 13 – 23.

12. Choureiri, E.M., Lamm, R., Kloeckner, J.H., and Mailaender, T. (1994). Safety Aspects of Individual Design Elements and their interaction on Two-Lane Rural Highways: International perspective. Transportation Research Record 1445, 34 – 46

13. Cha, Doo Won and Park, Peom (1997). Simulator-Based Mental Workload Assessment of the In-Vehicle Navigation System Driver Using Revision of NASA-TLX. Internet Resources - http://www.humanfactors.co.kr/paper/97-ie-interface.pdf

14. Denton, G. G. (1969). The use made of the speedometer as an aid to driving. Ergonomics 12(3), 447-452

15. De Waard, D., Jessurun, M., Steyvers, F. J. J. M., Raggatt, P. T. F., and Brookhuis, K. A. (1995). The effect of road layout and road environment on driving performance, drivers physiology and road appreciation. Ergonomics 38(7), 1395-1407.

16. De Waard, Dick (1996). The measurement of drivers mental workload. PhD Thesis, University of Groningen, Netherlands

17. Dingus, T. Hulse, M., Foss, J., Confer, S, Rice A., Roberts, I., Hanowski, R, Sorenson, D., (1996). Development of Human Factor Guidelines for Advance Travellers Information System (ATIS). Literature Review Publication No. FHWA-RD-95-153 under Driver Information Processing Demands: Attention and Workload – Internet Resources – http://www.fhwa.dot.gov/////tfhrc/safety/pubs/95153/index.html

18. Easa, Said (2003). 2003-Design Consistency-In Geometric Design Guide For Canadian Roads. Chapter 1.4, Transportation Association of Canada, Ottawa, Ontario

19. Eggemeier, T. G. (1988). Properties of workload assessment techniques. In P. A. Hancock and N. Meshkati (Eds.). Human Mental Workload North-Holland: Elsevier Science, 41-62

20. Fitzpatrick, K., Wooldridge, M. D., Tsimhoni, O., Collins, J. M., Green P., Bauer, K. M., Parma, K., Koppa, R., Harwood, D., Anderson, I, Krammes, R. A., and Poggioli, B. (2000). Alternative Design Consistency Rating Methods For Two-Lane Rural Highways. FHWA-RD-99-173, www.tfhrc.gov/safety/ihsdm.ihsdm.htm

21. Ford Motor Company (2000). New Lab to Investigate **Driver** Distraction. www.ford.com/en/ourCompany/safetyAndSecurity/vehicleSafetyFeatures/investigatingDriverDistraction.htm

22. Fitzpatrick, K., Elefteriadou, L., Harwood, D.W., Collins, J.M., Mcfadden, J., Vizarry N.I., Perma, K.D., Bauer, K.M., and Anderson, I.B. (1985). Speed Prediction for Rural Two-Lane Highways. Final Report of Contract No. DTFH61 – 195 – C – 00084, Texas Transportation Institute.

23. Fink, K.L. and Krammes, R.A. (1995). Tangent Length and Sight Distance Effects on Accident Rate at Horizontal Curves on Two-Lane Highways. Transportation Research Record 1500, 162 - 166

24. Gibreel, G.M., Easa, S.M., Hassan, Y. and Al-Dimeery, I.A. (1999). State of the Art of Highway Geometric Design Consistency. Journal of Transportation Engineering, 305 – 313

25. Godley. S (1999). A Driving Simulator Investigation Of Perceptual Countermeasures to Speeding. PhD Thesis - www.psych.usyd.edu.au/staff/stuartg/GodleyThesis.pdf

26. Glenon, J.C., Neuman/ T.R. and Leisch/ J.E. (1984). Safety and Operational Considerations for Design of Rural Highway Curves. Report FHWA/RD-36/035 - Federal Highway Administration, U.S. Department of Transportation – Washington D.C.

27. Gordon, D. A. (1965). Static and dynamic visual fields in human space perception. Journal of the Optical Society of America 55(10), 1296-1303.

28. Gibson, J. J. (1950). The Perception of the Visual World. Boston, USA - Houghton Mifflin Company

29. Hassan, Y., Sayed, T. and Tabernero, V. (2001). Establishing Practical Approach for Design Consistency Evaluation. Journal of Transportation Engineering, 295 – 302

30. Hassan, Y., Gibreel, G. and Easa, S.M. (2000). Evaluation of Highway Consistency and Safety: Practical Application. Journal of Transportation Engineering, 193 – 201

31. Heger, Ralf (1998). Driving Behavior and Driver Mental Workload as criteria of Highway Geometric Design Quality. Technical University of Dresden, 43-1– 43-10. http://www.nationalacademies.org/trb/publications/geom/ch43.pdf

32. Hartman, E. (1970). Driver Vision Requirements. Proceedings of the International Automobile Safety Conference, 629 – 630

33. Hills, B. L. (1980). Vision, Visibility, and Perception In Driving. Perception. *9*(2), 183 - 216.

34. Harms, L. (1991). Variation in drivers cognitive load. Effects of driving through village areas and rural junctions. Ergonomics 34(2), 151-160.

35. Hicks, T. G., and Wierwille, W. W. (1979). Comparison of five mental workload assessment procedures in a moving-base driving simulator. Human Factors 21(2), 129 - 143.

36. Hart, S. G., and Staveland, L. E. (1988). Development of the NASA-TLX (Task Load Index). Results of the empirical and theoretical research. In P. A. Hancock and N Meshkati (Eds.), Human Mental Workload North-Holland, Elsevier Science 139 - 184

37. Janssen, W., and Tenkink, E. (1988). Risk homeostasis theory and its critics - Time for an agreement. Ergonomics 31(4), 429 - 433.

38. Johanssen, G. (1992). Workload and Workload Measurements in N. Moray (ed) Mental Workload. Plenum Publishing, New York, 3-12

39. Janssen, W. H., and Tenkink, E. (1988). Considerations on speed selection and risk homeostasis in driving. Accident Analysis and Prevention 20(2), 137-142.

40. Krammes, R.A. (2000). Design Speed and Operating Speed in Rural Highway Alignment Design. Transportation Research Record 1701, 68 – 75

41. Krammes, Raymond A. and Glasscock, Stephen W. (1992). Geometric Inconsistencies and Accident Experience on Two-Lane rural Highways. Transportation Research Record 1356, 1 – 10

42. Kanellaidis, G., Golias, J., and Efstathiadis, S. (1986). Drivers Speed Behaviour on Rural Road Curves. Traffic Engineering and Control, London 31(7/8), 414 – 415

43. Kahneman, D. (1973). Attention and Effort. Englewood Cliffs, NJ: Prentice-Hall.

44. Krammes, R., Brackett R.O., Shafer, M., Ottesen, J., Anderson, I., Fink, K., Collins, K., Pendleton, O., and Messer, C. (1995). Horizontal Alignment Design Consistency

for Rural two-lane Highways. FHWA-RD-94-034. Federal Highway Administration - Washington D.C

45. Lamm, R., Psarianos, B., and Mailaender, T. (2000). Highway Design and Traffic Safety Engineering Handbook. McGraw-Hill New York.

46. Lunenfeld, H. and Alexander, G.J. (1990). A Users Guide to Positive Guidance. Report FHWA-SA-90-017. FHWA, U.S. Department of Transportation.

47. Lamm, R., Choueiri, E.M. and Hayward, J.C. (1988). Tangent as an Independent Design Element. Transportation Research Record 1195, 123 – 131

48. Lamm, R., Choueiri, E.M., Hayward, J.C and Paluri, A. (1988). Possible Design Procedure to Promote Design Consistency in Highway Geometric Design on Two - Lane Rural Roads. Transportation Research Record 1195, 111 – 122

49. Leisch, J.E. and Leisch, J.P. (1977). New Concepts in Design Speed Application. Transportation Research Record 631, 5 - 14

50. Lay, M. G. (1986). Handbook of Road Technology Vol. 2. New York: Gordon and Breach Science Publishers.

51. Lenné, M. G., Triggs, T. J., and Redman, J. R. (1997). Time of day variations in driving performance. Accident Analysis and Prevention 29(4), 431-437.

52. Morrall, J. and Talarico, R.J. (1994). Side Friction Demanded and Margins of Safety on Horizontal Curves. Transportation Research Record 1435, 145 – 152.

53. McCormick, Ernest, J., Mark, S., Sanders (1992). Human Factors Engineering and Design, Seventh Edition, McGRAW-HILL, NC, 82 -83.

54. Messer, C.J., Mounce, J.M. and Brackett, R.Q. (1979). Highway Geometric Design Consistency Related to Drivers Expectancy, Volume III. Methodology for Evaluating

Geometric Design Consistency. Report FHWA/RD-81/037. FHWA, U.S. Department of Transportation.

55. McDonald, L. B., and Ellis, N. C. (1975). Driver workload for various turn radii and speeds. Transportation Research Record 530, 18-30.

56. Meshkati, N., and Loewenthal, A. (1988). An eclectic and critical review of four primary mental workload assessment methods: A guide for developing a comprehensive model. In P. A. Hancock and N. Meshkati (Eds) Human Mental Workload, North Holland: Elsevier Science, 251 – 288.

57. McLean, J. R., and Hoffmann, E. R. (1975). Steering reversals as a measure of driver performance and steering task difficulty. Human Factors 17(3), 248-256.

58. Naatanen, R., and Summala, H. (1974). A model for the role of motivational factors in drivers decision-making. Accident Analysis and Prevention 6(3/4), 243-261.

59. Neuman, T.R. (1989). New Approach to Design for Stopping Sight Distance. Transportation Research Record 1208, 14 – 22

60. Neuman, T.R., Glenon, J.C., and Leisch, J.E. (1983). Functional Analysis of Stopping Sight Distance Requirements. Transportation Research Record 923, 57 – 64.

61. Navon, D., and Gopher, D. (1979). On the economy of the human-processing system. Psychological Review 86, 214-255.

62. Ottesen, J.L. and Krammes, R.A. (2000). Speed-Profile Model for a Design-Consistency Evaluation Procedure in the United States. Transportation Research Record 1701, 76 – 85

63. Olson, P. L. (1993). Vision and Perception. In B. Peacock and W. Karwowski (Eds.), Automotive Ergonomics London, Taylor and Francis, 161-183

64. Passetti, K.A. and Fambro, D.B. (1999). Operating Speeds on Curves with and without Spiral Transitions. Transportation Research Record 1658, 9 – 16

65. Pauzié, Annie., Anne, Sarpedon., Gaël, Saulnier. (1995). Ergonomic Evaluation of a Prototype Guidance System in an Urban Area. IEEE-IEE Vehicle Navigation and Information Systems Conference, 390-396

66. Polus, A. and Dagan, D (1987). Models for Evaluating the Consistency of Highway Alignment. Transportation Research Record 1122, 47 – 56

67. Pignataro, L.J.(1975). Traffic Engineering Theory and Practice, Prentice Hall, N.J.

68. Rockwell, T. (1972). Skills, judgement and information acquisition in driving. Human Factors in Highway Traffic Safety Research, New York: Wiley, 133- 134

69. Recarte, M. A., and Nunes, L. M. (1996). Perception of speed in an automobile: Estimation and production. Journal of Experimental Psychology Applied 2(4), 291-304.

70. Shafer, M.A. (1994). Driver Mental Workload Requirements on Horizontal Curves Based on Occluded Vision Test Measurements. Masters Thesis, Civil Engineering Department, Texas A & M University, College Station, Texas.

71. Smiley Alison (1989). Mental Workload and Information Management. IEEE CH2789, 6/89/0000-0435, 435 – 438

72. Segal, D.J. and Banney, T.A. (1979). Evaluation of Horizontal Curve Design. Report FHWA, RD – 79-48 – Federal Highway Administration, U.S. Department of Transportation, Washington D.C.

73. Senders, J. W. (1998). Analysis of an intersection. Ergonomics in Design 6(2), 4-6.

74. Sivak, M (1996). The information that drivers use: Is it indeed 90% visual?. Perception 25(9), 1081-1090

75. Schlegel, R. E. (1993). Driver mental workload In B. Peacock and W. Karwowski (Eds.). Automotive Ergonomics, London: Taylor and Francis, 359-382

76. Senders, J. W., Kristofferson, A. B., Levison, W., Dietrich, C. W., and Ward, J. L. (1966). An Investigation of Automobile Driver Information Processing (Report No. 1335). Washington, DC: Bureau of Public Roads, US Department of Commerce.

77. Senders, J.W., Kristofferson, A.B., Levison, W.H., Dietrich, C.W., and Ward, J.L. (1967). The Attention Demand of Automobile Driving, HRR 195, Road User Characteristics, 15-33.

78. Shinar, D. (1978). Psychology on the Road. The Human Factors in Traffic Safety. New York: Wiley.

79. Shafer, M.A. (1996). Driver Mental Workload Requirements on Horizontal Curves Based on Occluded Vision Test Measurements. Report Number – 04690 – 2 – August 1996

80. Urbanik, II T., Hinshaw, W. and Fambro, D.B. (1989). Safety Effects of Limited Sight Distance on Vertical Curves. Transportation Research Record 1208, 23 – 35

81. Woodridge, M.D., Fitzpatrick, K., Koppa, R. and Bauer, K. (2000). Effects of Horizontal Curvature on Driver Visual Demand. Transportation Research Record 1737, 71 – 82

82. Walker, M., Burnham, D., and Borland, R. (1994). Psychology (2nd ed). Brisbane, Australia: John Wiley and Son.

83. Wierwille, W.W. and Eggemeier, F.T. (1993). Recommendations for Mental Workload Measurement in a Test and Evaluation Environment. Human Factors Vol. 35 No. 2, 263-281.

84. Wilde, G. J. S. (1982). The theory of risk homeostasis: Implications for safety and health. Risk Analysis – 2, 209-225.

85. Wilde, G. J. S. (1982). Critical issues in risk homeostasis theory. Risk Analysis – 2, 249-258.

86. Wilde, G. J. S. (1988). Risk homeostasis theory and traffic accidents: Propositions, deductions and discussions of dissension in recent reactions. Ergonomics 31(4), 441 - 468.

87. Wierwille, W. W., and Gutmann, J. C. (1978). Comparison of Primary and Secondary Task Measures as a Function of Simulated Vehicle Dynamics and Driving Conditions. Human Factors 20(2), 233-244.

88. Wickens, C. D. (1980). The Structure of Attention Resources. In R. S. Nickerson (Ed.), - Attention and Performance VIII - Hillsdale, NJ: Lawrence, Edbaum, 239 - 257

89. .Wickens, C. D. (1984). Processing Resources in Attention. In R. Parasuraman and D. R. Davies (Eds), Varieties of Attention- Orlando, FL, USA: Academic, 63 -102

90. Zeitlin, L.R. (1995). Estimates of Driver Mental Workload: A Long-Term Field Trial of Two Subsidiary Tasks. Human Factors 37(3), 611-621.

Appendix A

DATA AND RESULT OF FIELD PILOT STUDY ON DVP

Table-17 Extracted Data of DVP from Maps in 1:5000 scale

Original Data as Extracted from 1:5000													
Sl #	E	Degree	Minute	Second	ΔC	R	T	LC	Av. LW	Av. SW	Av. CW	R	Ave R
1	4	5	49	52.56	5.831	3086.0333	157.1759	314.0804	3.545	2.315	14.6	3086.033	2315.892
2	17.5	12	40	49.38	12.680	2843.7232	315.9692	629.357	3.4	2.425	14.35	2843.723	
3	5	8	31	50.76	8.531	1800.2182	134.2653	268.0344	3.425	2.425	14.55	1800.218	
4	7.5	11	18	35.76	11.310	1533.5935	151.8557	302.7246	3.48	3.85	15.2	1533.594	
5	10	11	2	3.15	11.034	2148.6811	207.5419	413.8	3.4	2.4	14.7	2148.681	3774.668
6	15	8	31	50.76	8.531	5400.6547	402.796	804.1033	3.425	2.425	14.55	5400.655	
7	55	30	57	49.52	30.964	1460.775	404.6112	789.4313	3.545	2.315	14.6	1460.775	668.2723
8	120	74	3	16.57	74.055	475.08653	358.3584	614.0478	3.4	2.425	14.35	475.0865	
9	20	35	42	24.09	35.707	395.31999	127.3295	246.3632	3.425	2.425	14.55	395.32	
10	55	53	7	48.37	53.130	465.96747	232.9837	432.0894	3.48	3.85	15.2	465.9675	
11	10	21	48	5.07	21.801	544.21278	104.8058	207.0764	3.4	2.4	14.7	544.2128	
12	75	61	49	17.08	61.821	453.0535	271.2619	488.8389	3.425	2.425	14.55	453.0535	678.4615
13	80	62	43	49.9	62.731	467.44466	284.9406	511.7838	3.48	3.85	15.2	467.4447	
14	60	39	21	6.31	39.352	967.61529	345.9969	664.5753	3.45	3.25	16.25	967.6153	
15	10	17	44	40.82	17.745	825.7325	128.8978	255.7318	3.45	2.3	15.1	825.7325	

Table-18 Calculation of Mental Workload by NASA TLX

Mental Workload	Mental Demand	Weight age	Physical Demand	Weight age	Temporal Demand	Weight age
1	Stretch1	Stretch2	Stretch3	Stretch4		
38	5	6	6	1	1	2
47	5	6	1	1	4	4
25	2	6	1	1	4	3
41	6	6	1	1	2	2
2	Stretch1	Stretch2	Stretch3	Stretch4		
72	6	5	4	6	6	3
71	4	5	6	6	5	3
103	8	5	8	6	5	3
108	9	5	8	6	5	3
3	Stretch1	Stretch2	Stretch3	Stretch4		
42	5	6	2	1	2	5
8	1	5	1	3	0	5
3	0	6	0	2	1	3
64	6	6	4	4	3	4
4	Stretch1	Stretch2	Stretch3	Stretch4		
15	3	3	2	0	3	2
23	5	2	2	2	3	3
40	4	4	3	3	5	3
35	4	5	3	3	3	2
5	Stretch1	Stretch2	Stretch3	Stretch4		
-	-	-	-	-	-	-
81	4	4	5	4	9	5
109	6	4	8	5	9	5
154	9	6	8	5	10	6
6	Stretch1	Stretch2	Stretch3	Stretch4		
60	4	5	5	4	5	4
97	8	6	7	5	7	2
110	8	6	7	6	5	4
109	9	6	7	5	5	4

Mental Workload	Mental Demand	Weight age	Physical Demand	Weight age	Temporal Demand	Weight age
7						
71	3	6	7	5	3	6
56	3	6	4	5	3	6
81	6	6	6	5	3	5
92	7	6	7	5	3	5
8	Stretch1	Stretch2	Stretch3	Stretch4		
66	5	5	6	6	1	5
112	7	6	8	5	6	5
110	8	5	7	5	7	5
122	9	6	8	5	7	4

Table-19 Aggregated Data on Mental Workload and DVP Geometric Parameters

MWL	R	Grade	BTB	CF	LW	SW	LatObs	OhObs	Aesth	Length	RegDr
38	2315.89	-2.64	3	1	3.46	2.75	0	0	2	2100	0
47	3774.67	0.1	1	1	3.41	2.41	0	1	1	2700	0
25	668.270	0.58	4	0	3.45	2.68	1	1	3	3000	0
41	678.460	0.71	2	1	3.45	2.96	3	3	2	3000	0
72	2315.89	-2.64	3	1	3.46	2.75	0	0	2	2100	1
71	3774.67	0.1	1	1	3.41	2.41	0	1	1	2700	1
103	668.270	0.58	4	0	3.45	2.68	1	1	3	3000	1
108	678.460	0.71	2	1	3.45	2.96	3	3	2	3000	1
42	2315.89	-2.64	3	1	3.46	2.75	0	0	2	2100	0
8	3774.67	0.1	1	1	3.41	2.41	0	1	1	2700	0
3	668.270	0.58	4	0	3.45	2.68	1	1	3	3000	0
64	678.460	0.71	2	1	3.45	2.96	3	3	2	3000	0
15	2315.89	-2.64	3	1	3.46	2.75	0	0	2	2100	1
23	3774.67	0.1	1	1	3.41	2.41	0	1	1	2700	1
40	668.270	0.58	4	0	3.45	2.68	1	1	3	3000	1
35	678.460	0.71	2	1	3.45	2.96	3	3	2	3000	1
81	3774.67	0.1	1	1	3.41	2.41	0	1	1	2700	0
109	668.270	0.58	4	0	3.45	2.68	1	1	3	3000	0
154	678.460	0.71	2	1	3.45	2.96	3	3	2	3000	0
60	2315.89	-2.64	3	1	3.46	2.75	0	0	2	2100	0
97	3774.67	0.1	1	1	3.41	2.41	0	1	1	2700	0
110	668.270	0.58	4	0	3.45	2.68	1	1	3	3000	0
109	678.460	0.71	2	1	3.45	2.96	3	3	2	3000	0
71	2315.89	-2.64	3	1	3.46	2.75	0	0	2	2100	1
56	3774.67	0.1	1	1	3.41	2.41	0	1	1	2700	1
81	668.270	0.58	4	0	3.45	2.68	1	1	3	3000	1
92	678.460	0.71	2	1	3.45	2.96	3	3	2	3000	1
66	2315.89	-2.64	3	1	3.46	2.75	0	0	2	2100	0
112	3774.67	0.1	1	1	3.41	2.41	0	1	1	2700	0
110	668.270	0.58	4	0	3.45	2.68	1	1	3	3000	0
122	678.460	0.71	2	1	3.45	2.96	3	3	2	3000	0

Table-20 Correlation Analysis of all variables from Aggregated Data

	MWL	R	Grade	BTB	CF	LW	SW	LatObs	OhObs	Aesth	Length	RegDr
MWL	1											
R	-0.265	1										
Grade	0.299	-0.359	1									
BTB	-0.013	-0.673	-0.139	1								
CF	-0.044	0.529	-0.366	-0.790	1							
LW	0.051	-0.743	-0.357	0.753	-0.241	1						
SW	0.238	-0.808	0.025	0.340	0.054	0.805	1					
LatObs	0.367	-0.747	0.582	0.012	0.015	0.348	0.805	1				
OhObs	0.366	-0.499	0.722	-0.299	0.158	0.001	0.569	0.936	1			
Aesth	0.104	-0.851	0.131	0.952	-0.821	0.742	0.487	0.292	0	1		
Length	0.319	-0.524	0.983	0.025	-0.464	-0.181	0.165	0.659	0.736	0.302	1	
RegDr	-0.126	0.009	-0.045	0.011	0.015	0.015	0.006	-0.021	-0.030	0	-0.043	1

Model Information on Mental Workload

The SAS System 10:26 Saturday, February 8, 2003 1

MWL = R

Response Distribution: Poisson

Link Function: Log

Model Equation

Log (MWL) = 4.4429 - 0.0001 R

Summary of Fit

Mean of Response	69.8387	Deviance	654.1167	Pearson ChiSq	563.3899
SCALE	1.0000	Deviance / DF	22.5557	Pearson ChiSq / DF	19.4272
	.	Scaled Dev	654.1167	Scaled ChiSq	563.3899

Analysis of Deviance

Source	DF	Deviance	Deviance / DF	Scaled Dev	Pr > Scaled Dev
Model	1	44.5180	44.5180	44.5180	<.0001
Error	29	654.1167	22.5557	654.1167	.
C Total	30	698.6347	.	.	.

Type III (Wald) Tests

Source	DF	ChiSq	Pr > ChiSq
R	1	43.1228	<.0001

Parameter Estimates

Variable	DF	Estimate	Std Error	ChiSq	Pr > ChiSq
Intercept	1	4.4429	0.0356	15570.7433	<.0001
R	1	-0.0001	0.0000	43.1228	<.0001

MWL = R GRADE

Response Distribution: Poisson

Link Function: Log

Model Equation

Log (MWL)= 4.3824 - 0.0001 R + 0.1050 GRADE

Summary of Fit

Mean of Response	69.8387	Deviance	624.0971	Pearson ChiSq	517.4545
SCALE	1.0000	Deviance / DF	22.2892	Pearson ChiSq / DF	18.4805
	.	Scaled Dev	624.0971	Scaled ChiSq	517.4545

Analysis of Deviance

Source	DF	Deviance	Deviance / DF	Scaled Dev	Pr > Scaled Dev
Model	2	74.5377	37.2688	74.5377	<.0001
Error	28	624.0971	22.2892	624.0971	.
C Total	30	698.6347	.	.	.

Type III (Wald) Tests

Source	DF	ChiSq	Pr > ChiSq
R	1	14.9530	0.0001
GRADE	1	28.3477	<.0001

Parameter Estimates

Variable	DF	Estimate	Std Error	ChiSq	Pr > ChiSq
Intercept	1	4.3824	0.0367	14224.7029	<.0001
R	1	-0.0001	0.0000	14.9530	0.0001
GRADE	1	0.1050	0.0197	28.3477	<.0001

MWL = R GRADE BTB

Response Distribution: Poisson
Link Function: Log

Model Equation

Log (MWL) = 4.7758 - 0.0001 R + 0.0626 GRADE - 0.1074 BTB

Summary of Fit

Mean of Response	69.8387	Deviance	609.9672	Pearson ChiSq	509.3065
SCALE	1.0000	Deviance / DF	22.5914	Pearson ChiSq / DF	18.8632
	.	Scaled Dev	609.9672	Scaled ChiSq	509.3065

Analysis of Deviance

Source	DF	Deviance	Deviance / DF	Scaled Dev	Pr > Scaled Dev
Model	3	88.6675	29.5558	88.6675	<.0001
Error	27	609.9672	22.5914	609.9672	.
C Total	30	698.6347	.	.	.

Type III (Wald) Tests

Source	DF	ChiSq	Pr > ChiSq
R	1	29.4669	<.0001
GRADE	1	7.5471	0.0060
BTB	1	14.0348	0.0002

Parameter Estimates

Variable	DF	Estimate	Std Error	ChiSq	Pr > ChiSq
Intercept	1	4.7758	0.1098	1892.6392	<.0001
R	1	-0.0001	0.0000	29.4669	<.0001
GRADE	1	0.0626	0.0228	7.5471	0.0060
BTB	1	-0.1074	0.0287	14.0348	0.0002

MWL = R BTB SW

Response Distribution: Poisson

Link Function: Log

Model Equation

Log(MWL) = 6.9401 - 0.0003 R - 0.1986 BTB - 0.6199 SW

Summary of Fit

Mean of Response	69.8387	Deviance	609.9157	Pearson ChiSq	509.1881
SCALE	1.0000	Deviance / DF	22.5895	Pearson ChiSq / DF	18.8588
	.	Scaled Dev	609.9157	Scaled ChiSq	509.1881

Analysis of Deviance

Source	DF	Deviance	Deviance / DF	Scaled Dev	Pr > Scaled Dev
Model	3	88.7190	29.5730	88.7190	<.0001
Error	27	609.9157	22.5895	609.9157	.
C Total	30	698.6347	.	.	.

Type III (Wald) Tests

Source	DF	ChiSq	Pr > ChiSq
R	1	45.2792	<.0001
BTB	1	41.1696	<.0001
SW	1	7.5972	0.0058

Parameter Estimates

Variable	DF	Estimate	Std Error	ChiSq	Pr > ChiSq
Intercept	1	6.9401	0.7286	90.7327	<.0001
R	1	-0.0003	0.0000	45.2792	<.0001
BTB	1	-0.1986	0.0310	41.1696	<.0001
SW	1	-0.6199	0.2249	7.5972	0.0058

MWL = R BTB AESTH

Response Distribution: Poisson
Link Function: Log

Model Equation

Log(MWL)= 3.9690 - 0.0000 R - 0.5017 BTB + 0.7817 AESTH

Summary of Fit

Mean of Response	69.8387	Deviance	609.9722	Pearson ChiSq	509.3149
SCALE	1.0000	Deviance / DF	22.5916	Pearson ChiSq / DF	18.8635
	.	Scaled Dev	609.9722	Scaled ChiSq	509.3149

Analysis of Deviance

Source	DF	Deviance	Deviance / DF	Scaled Dev	Pr > Scaled Dev
Model	3	88.6625	29.5542	88.6625	<.0001
Error	27	609.9722	22.5916	609.9722	.
C Total	30	698.6347	.	.	.

Type III (Wald) Tests

Source	DF	ChiSq	Pr > ChiSq
R	1	0.2873	0.5919
BTB	1	14.5751	0.0001
AESTH	1	7.5422	0.0060

Parameter Estimates

Variable	DF	Estimate	Std Error	ChiSq	Pr > ChiSq
Intercept	1	3.9690	0.3675	116.6423	<.0001
R	1	-0.0000	0.0001	0.2873	0.5919
BTB	1	-0.5017	0.1314	14.5751	0.0001
AESTH	1	0.7817	0.2846	7.5422	0.0060

MWL = R AESTH SW

Response Distribution: Poisson
Link Function: Log

Model Equation

Log(MWL) = 8.8828 - 0.0005 R - 0.5121 AESTH - 1.0247 SW

Summary of Fit

Mean of Response	69.8387	Deviance	609.8799	Pearson ChiSq	509.1241
SCALE	1.0000	Deviance / DF	22.5881	Pearson ChiSq / DF	18.8564
	.	Scaled Dev	609.8799	Scaled ChiSq	509.1241

Analysis of Deviance

Source	DF	Deviance	Deviance / DF	Scaled Dev	Pr > Scaled Dev
Model	3	88.7548	29.5849	88.7548	<.0001
Error	27	609.8799	22.5881	609.8799	.
C Total	30	698.6347	.	.	.

Type III (Wald) Tests

Source	DF	ChiSq	Pr > ChiSq
R	1	49.0785	<.0001
AESTH	1	41.2031	<.0001
SW	1	14.6626	0.0001

Parameter Estimates

Variable	DF	Estimate	Std Error	ChiSq	Pr > ChiSq
Intercept	1	8.8828	0.9622	85.2185	<.0001
R	1	-0.0005	0.0001	49.0785	<.0001
AESTH	1	-0.5121	0.0798	41.2031	<.0001
SW	1	-1.0247	0.2676	14.6626	0.0001

MWL = R BTB CF

Response Distribution: Poisson

Link Function: Log

Model Equation

Log (MWL) = 5.3429 - 0.0002 R - 0.2313 BTB - 0.2392 CF

Summary of Fit

Mean of Response	69.8387	Deviance	609.9722	Pearson ChiSq	509.3149
SCALE	1.0000	Deviance / DF	22.5916	Pearson ChiSq / DF	18.8635
	.	Scaled Dev	609.9722	Scaled ChiSq	509.3149

Analysis of Deviance

Source	DF	Deviance	Deviance / DF	Scaled Dev	Pr > Scaled Dev
Model	3	88.6625	29.5542	88.6625	<.0001
Error	27	609.9722	22.5916	609.9722	.
C Total	30	698.6347	.	.	.

Type III (Wald) Tests

Source	DF	ChiSq	Pr > ChiSq
R	1	85.3848	<.0001
BTB	1	34.5680	<.0001
CF	1	7.5422	0.0060

Parameter Estimates

Variable	DF	Estimate	Std Error	ChiSq	Pr > ChiSq
Intercept	1	5.3429	0.1700	987.9260	<.0001
R	1	-0.0002	0.0000	85.3848	<.0001
BTB	1	-0.2313	0.0393	34.5680	<.0001
CF	1	-0.2392	0.0871	7.5422	0.0060

MWL = R SW LW

Response Distribution: Poisson

Link Function: Log

Model Equation

Log (MWL) = 50.2905 - 0.0002 R + 0.8270 SW - 13.9476 LW

Summary of Fit

Mean of Response	69.8387	Deviance	606.5071	Pearson ChiSq	505.2152
SCALE	1.0000	Deviance / DF	22.4632	Pearson ChiSq / DF	18.7117
	.	Scaled Dev	606.5071	Scaled ChiSq	505.2152

Analysis of Deviance

Source	DF	Deviance	Deviance / DF	Scaled Dev	Pr > Scaled Dev
Model	3	92.1277	30.7092	92.1277	<.0001
Error	27	606.5071	22.4632	606.5071	.
C Total	30	698.6347	.	.	.

Type III (Wald) Tests

Source	DF	ChiSq	Pr > ChiSq
R	1	25.9744	<.0001
SW	1	17.2280	<.0001
LW	1	44.3335	<.0001

Parameter Estimates

Variable	DF	Estimate	Std Error	ChiSq	Pr > ChiSq
Intercept	1	50.2905	7.0161	51.3783	<.0001
R	1	-0.0002	0.0000	25.9744	<.0001
SW	1	0.8270	0.1992	17.2280	<.0001
LW	1	-13.9476	2.0948	44.3335	<.0001

Appendix B

DATA, TABLES AND FIGURES

RELATING EXPERIMENTATION

Table- 21 Detail Geometric Information on Test Alignment-1

1										
Design Speed(Km/H)		SSD(M)	R_{min}(M)	Min Distance(M)		Total Length(M)		Driving Time(sec)		
80		106.2295	265.23	72.62		5413.26		243.60		
Feature	Tangent		Curve Turning	Horizontal Curve					Cross Sectional Details	Available Sight Distance
	L_T	Azimuth Nd^0E		PC	PT	L_c	R (M)	Δ_c^0	Lane Wd (M)	
Tangent	200	90	-	0	0	0	-	0	3.6	203.34
Curve	0	120	R	200	488.5029	288.5029	551	30	3.6	138.63
Curve	0	150	R	488.5029	686.4233	197.9203	378	30	3.6	229.73
Tangent	350	150	-	0	0	0	-	0	3.6	400.00
Curve	0	100	L	1036.423	1277.279	240.8554	276	50	3.6	400.00
Curve	0	130	R	1277.279	1540.649	263.3702	503	30	3.6	226.08
Tangent	250	130	-	0	0	0	-	0	3.6	400.00
Curve	0	100	L	1790.649	2065.015	274.3658	524	30	3.6	400.00
Curve	0	55	L	2065.015	2302.99	237.9756	303	45	3.6	400.00
Tangent	225	55	-	0	0	0	-	0	3.6	214.24
Curve	0	75	R	2527.99	2738.128	210.1376	602	20	3.6	310.94
Curve	0	30	L	2738.128	2985.528	247.4004	315	45	3.6	400.00
Tangent	150	30	-	0	0	0	-	0	3.6	139.09
Curve	0	90	R	3135.528	3414.083	278.5545	266	60	3.6	106.13
Curve	0	120	R	3414.083	3620.904	206.8215	395	30	3.6	238.97
Tangent	300	120	-	0	0	0	-	0	3.6	400.00
Curve	0	90	L	3920.904	4134.009	213.1047	407	30	3.6	400.00
Curve	0	135	R	4134.009	4408.898	274.8894	350	45	3.6	184.64
Tangent	275	135	-	0	0	0	-	0	3.6	400.00
Curve	0	90	L	4683.898	4967.427	283.5287	361	45	3.6	400.00
Curve	0	112.5	R	4967.427	5213.257	245.8296	626	22.5	3.6	255.81
Tangent	200	112.5	-	0	0	0	-	0	3.6	400.00

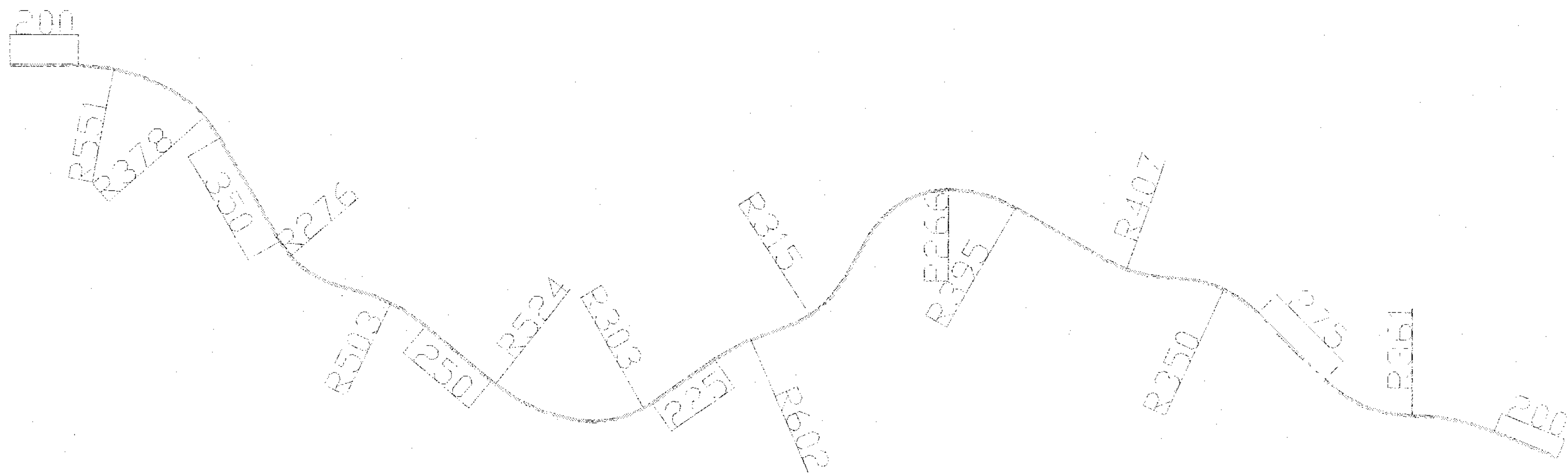

Figure 11 Test Alignment – 1

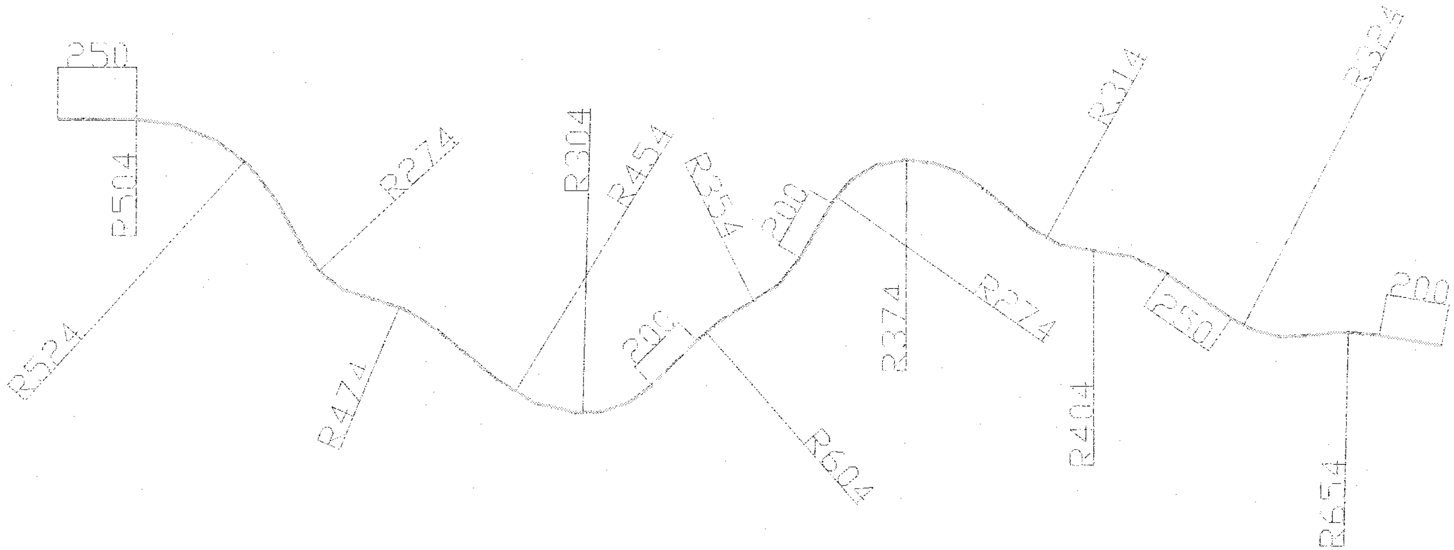

Figure 12 Test Alignment – 2

Table- 22 Detail Geometric Information on Test Alignment-2

2											
Design Speed(Km/H)		SSD(M)	R_{min}(M)	Min Distance(M)		Total Length(M)		Driving Time(sec)			
80		106.2295	265.23	72.62		5242.05		235.89			
Feature	Tangent		Curve Turning	Horizontal Curve					Cross Sectional Details	Available Sight Distance
	L_T	Azimuth Nd^0E		PC	PT	L_c	R (M)	Δ_c^0	Lane Wd (M)	
Tangent	250	90	-	0	0	0	-	0	3.05	219.32
Curve	0	120	R	250	513.8938	263.8938	504	30	3.05	135.41
Curve	0	150	R	513.8938	788.2595	274.3658	524	30	3.05	225.15
Tangent	200	150	-	0	0	0	-	0	3.05	400.00
Curve	0	100	L	988.2595	1227.37	239.1101	274	50	3.05	400.00
Curve	0	130	R	1227.37	1475.555	248.1858	474	30	3.05	227.63
Tangent	250	130	-	0	0	0	-	0	3.05	400.00
Curve	0	95	L	1725.555	2002.888	277.3328	454	35	3.05	400.00
Curve	0	45	L	2002.888	2268.178	265.29	304	50	3.05	400.00
Tangent	200	45	-	0	0	0	-	0	3.05	198.09
Curve	0	65	R	2468.178	2679.014	210.8358	604	20	3.05	331.08
Curve	0	30	L	2679.014	2895.26	216.2463	354	35	3.05	400.00
Tangent	200	30	-	0	0	0	-	0	3.05	155.18
Curve	0	90	R	3095.26	3382.193	286.9321	274	60	3.05	102.94
Curve	0	130	R	3382.193	3643.294	261.1013	374	40	3.05	226.88
Tangent	200	130	-	0	0	0	-	0	3.05	400.00
Curve	0	90	L	3843.294	4062.507	219.2134	314	40	3.05	400.00
Curve	0	125	R	4062.507	4309.297	246.7896	404	35	3.05	217.44
Tangent	250	125	-	0	0	0	-	0	3.05	400.00
Curve	0	80	L	4559.297	4813.766	254.469	324	45	3.05	400.00
Curve	0	100	R	4813.766	5042.055	228.2891	654	20	3.05	278.57
Tangent	200	100	-	0	0	0	-	0	3.05	400.00

Table- 23 Detail Geometric Information on Test Alignment-3

3										
Design Speed(Km/H)		SSD(M)	R_{min}(M)	Min Distance(M)		Total Length(M)		Driving Time(sec)		
80		106.2295	265.23	72.62		3087.62		138.94		
Feature	Tangent		Curve Turning	Horizontal Curve					Cross Sectional Details	Available Sight Distance
	L_T	Azimuth Nd^0E		PC	PT	L_c	R (M)	Δ_c^0	Lane Wd (M)	
Tangent	300	90	-	0	0	0	-	0	3.15	400.00
Curve	0	60	L	300	512.5811	212.5811	406	30	3.15	400.00
Curve	0	82.5	R	512.5811	719.1408	206.5597	526	22.5	3.15	260.14
Tangent	200	82.5	-	0	0	0	-	0	3.15	400.00
Curve	0	30	L	919.1408	1172.039	252.8982	276	52.5	3.15	400.00
Curve	0	60	R	1172.039	1436.98	264.941	506	30	3.15	232.41
Tangent	225	60	-	0	0	0	-	0	3.15	400.00
Curve	0	20	L	1661.98	1924.478	262.4975	376	40	3.15	400.00
Curve	0	0	L	1924.478	2125.539	201.0619	576	20	3.15	400.00
Tangent	250	0	-	0	0	0	-	0	3.15	182.32
Curve	0	60	R	2375.539	2664.566	289.0265	276	60	3.15	186.76
Curve	0	30	L	2664.566	2887.619	223.0531	426	30	3.15	400.00
Tangent	200	30	-	0	0	0	-	0	3.15	400.00

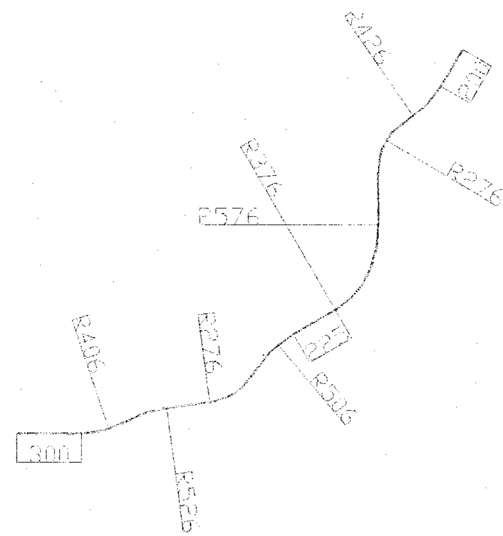

Figure 13 Test Alignment – 3

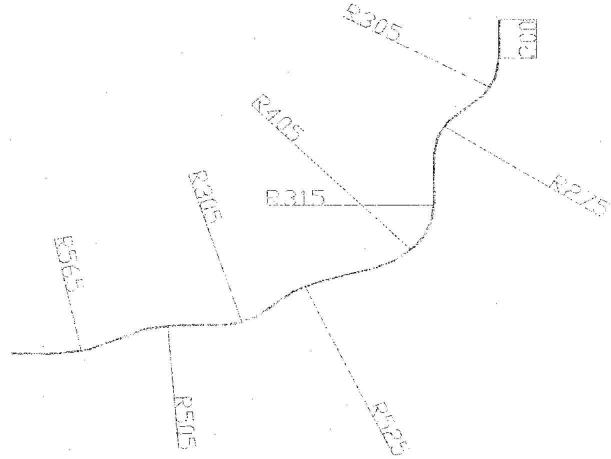

Figure 14 Test Alignment – 4

Table- 24 Detail Geometric Information on Test Alignment-4

4										
Design Speed(Km/H)		SSD(M)	R_{min}(M)	Min Distance(M)		Total Length(M)		Driving Time(sec)		
80		106.2295	265.23	72.62		3216.52		144.74		
Feature	Tangent		Curve Turning	Horizontal Curve					Cross Sectional Details	Available Sight Distance
	L_T	Azimuth Nd^0E		PC	PT	L_c	R (M)	Δ_c^0	Lane Wd (M)	
Tangent	200	90	-	0	0	0	-	0	3.25	400.00
Curve	0	60	L	200	495.8333	295.8333	565	30	3.25	400.00
Curve	0	90	R	495.8333	760.2507	264.4174	505	30	3.25	222.96
Tangent	200	90	-	0	0	0	-	0	3.25	400.00
Curve	0	45	L	960.2507	1199.797	239.5464	305	45	3.25	400.00
Curve	0	75	R	1199.797	1474.686	274.8894	525	30	3.25	229.28
Tangent	225	75	-	0	0	0	-	0	3.25	400.00
Curve	0	45	L	1699.686	1911.744	212.0575	405	30	3.25	400.00
Curve	0	0	L	1911.744	2159.144	247.4004	315	45	3.25	400.00
Tangent	250	0	-	0	0	0	-	0	3.25	193.42
Curve	0	60	R	2409.144	2697.124	287.9793	275	60	3.25	200.49
Curve	0	0	L	2697.124	3016.519	319.3953	305	60	3.25	400.00
Tangent	200	0	-	0	0	0	-	0	3.25	400.00

Table- 25 Detail Geometric Information on Test Alignment-5

5										
Design Speed(Km/H)		SSD(M)	R_{min}(M)	Min Distance(M)		Total Length(M)		Driving Time(sec)			
80		106.2295	265.23	72.62		2757.09		124.07			
Feature	Tangent		Curve Turning	Horizontal Curve					Cross Sectional Details	Available Sight Distance
	L_T	Azimuth Nd^0E		PC	PT	L_c	R (M)	Δ_c^0	Lane Wd (M)	
Tangent	200	90	-	0	0	0	-	0	3.35	400.00
Curve	0	45	L	200	672.0243	472.0243	601	45	3.35	400.00
Curve	0	90	R	672.0243	1104.779	432.7544	551	45	3.35	197.21
Tangent	200	90	-	0	0	0	-	0	3.35	400.00
Curve	0	30	L	1304.779	1850.369	545.5899	521	60	3.35	400.00
Curve	0	90	R	1850.369	2532.094	681.7256	651	60	3.35	161.82
Tangent	225	90	-	0	0	0	-	0	3.35	400.00

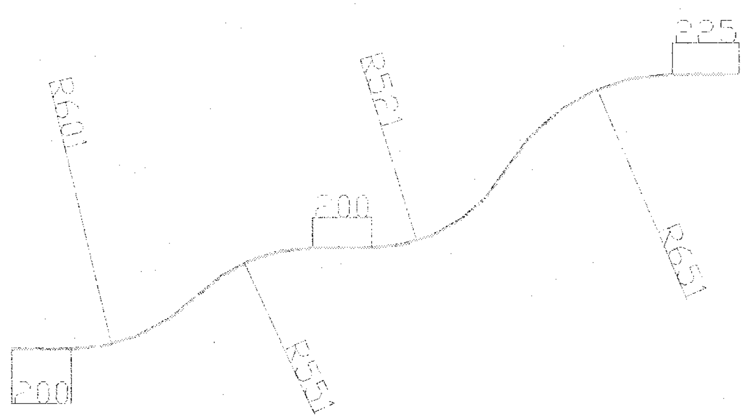

Figure 15 Test Alignment – 5

Table- 26 Detail Geometric Information on Test Alignment-6

6											
Design Speed(Km/H)		SSD(M)	R_{min}(M)	Min Distance(M)		Total Length(M)		Driving Time(sec)			
80		106.2295	265.23	72.62		2934.45		132.05			
Feature	Tangent		Curve Turning	Horizontal Curve					Cross Sectional Details	Available Sight Distance
	L_T	Azimuth Nd^0E		PC	PT	L_c	R (M)	Δ_C^0	Lane Wd (M)	
Tangent	200	0	-	0	0	0	-	0	3.45	197.07
Curve	0	60	R	200	725.6932	525.6932	502	60	3.45	205.75
Curve	0	0	L	725.6932	1303.746	578.053	552	60	3.45	400.00
Tangent	300	0	-	0	0	0	-	0	3.45	276.31
Curve	0	30	R	1603.746	2107.448	503.702	962	30	3.45	193.22
Curve	0	0	L	2107.448	2684.454	577.0059	1102	30	3.45	218.48
Tangent	250	0	-	0	0	0	-	0	3.45	400.00

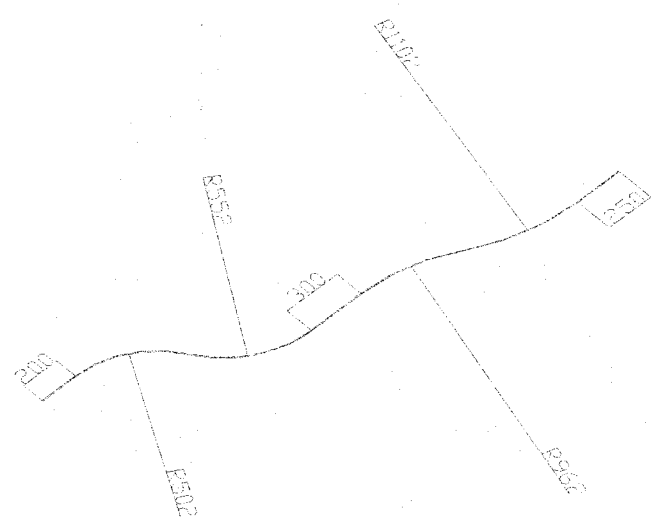

Figure 16 Test Alignment – 6

Table- 27 Detail Geometric Information on Test Alignment-7

7										
Design Speed(Km/H)		SSD(M)	R_{min}(M)	Min Distance(M)		Total Length(M)		Driving Time(sec)		
80		106.2295	265.23	72.62		2881.05		129.65		
Feature	Tangent		Curve Turning	Horizontal Curve					Cross Sectional Details	Available Sight Distance
	L_T	Azimuth Nd^0E		PC	PT	L_c	R (M)	Δ_c^0	Lane Wd (M)	
Tangent	200	-30	-	0	0	0	-	0	3.1	210.52
Curve	0	15	R	200	712.865	512.865	653	45	3.1	155.12
Curve	0	60	R	712.865	1265	552.1349	703	45	3.1	207.14
Tangent	300	60	-	0	0	0	-	0	3.1	400.00
Curve	0	30	L	1565	2074.462	509.4616	973	30	3.1	400.00
Curve	0	0	L	2074.462	2631.047	556.5855	1063	30	3.1	400.00
Tangent	250	0	-	0	0	0	-	0	3.1	400.00

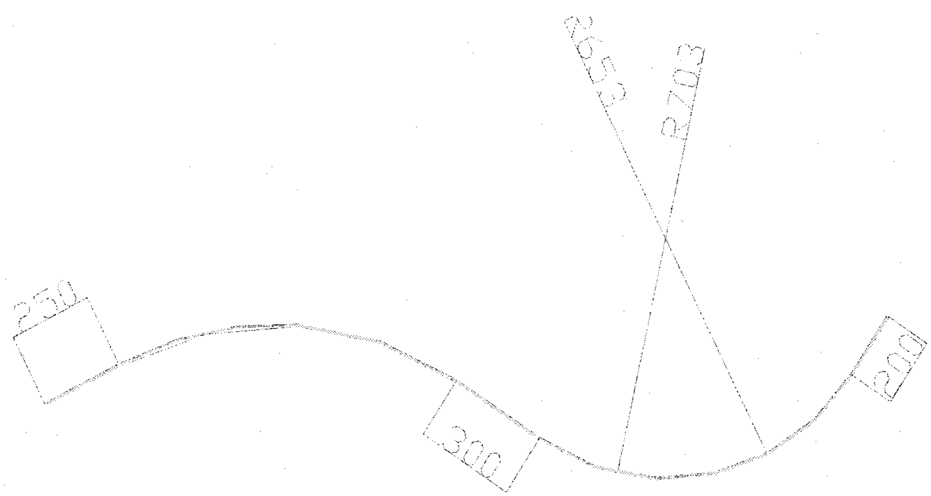

Figure 17 Test Alignment – 7

Table- 28 Detail Geometric Information on Test Alignment-8

8											
Design Speed(Km/H)		SSD(M)	R_{min}(M)	Min Distance(M)		Total Length(M)		Driving Time(sec)			
80		106.2295	265.23	72.62		2927.65		131.74			
Feature	Tangent		Curve Turning	Horizontal Curve					Cross Sectional Details	Available Sight Distance
	L_T	Azimuth Nd^0E		PC	PT	L_c	R (M)	Δ_c^0	Lane Wd (M)	
Tangent	200	180	-	0	0	0	-	0	3.2	
Curve	0	125	L	200	753.8802	553.8802	577	55	3.2	400.00
Curve	0	95	L	753.8802	1265.436	511.556	977	30	3.2	400.00
Tangent	300	95	-	0	0	0	-	0	3.2	284.31
Curve	0	130	R	1565.436	2161.641	596.2045	976	35	3.2	183.52
Curve	0	175	R	2161.641	2677.647	516.0066	657	45	3.2	206.43
Tangent	250	175	-	0	0	0	-	0	3.2	400.00

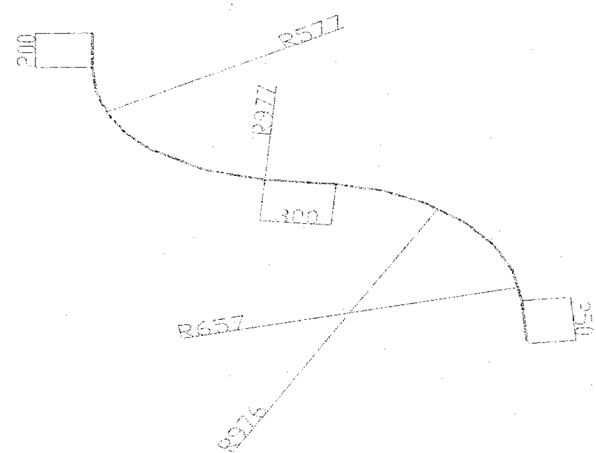

Figure 18 Test Alignment – 8

Table- 29 Detail Geometric Information on Test Alignment-9

9										
Design Speed(Km/H)		SSD(M)	R_{min}(M)	Min Distance(M)		Total Length(M)		Driving Time(sec)		
80		106.2295	265.23	72.62		2887.06		129.92		
Feature	Tangent		Curve Turning	Horizontal Curve					Cross Sectional Details	Available Sight Distance
	L_T	Azimuth Nd^0E		PC	PT	L_c	R (M)	Δ_c^0	Lane Wd (M)	
Tangent	500	180	-	0	0	0	-	0	3.15	600.00
Curve	0	60	L	500	1695.9	1195.9	571	120	3.15	600.00
Curve	0	0	L	1695.9	2587.065	891.1651	851	60	3.15	600.00
Tangent	300	0	-	0	0	0	-	0	3.15	600.00

Table- 30 Detail Geometric Information on Test Alignment-10

10										
Design Speed(Km/H)		SSD(M)	R_{min}(M)	Min Distance(M)		Total Length(M)		Driving Time(sec)		
80		106.2295	265.23	72.62		2946.75		132.60		
Feature	Tangent		Curve Turning	Horizontal Curve					Cross Sectional Details	Available Sight Distance
	L_T	Azimuth Nd^0E		PC	PT	L_c	R (M)	Δ_c^0	Lane Wd (M)	
Tangent	500	0	-	0	0	0	-	0	3.0	357.18
Curve	0	75	R	500	1547.198	1047.198	800	75	3.0	167.68
Curve	0	180	R	1547.198	2646.755	1099.557	600	105	3.0	182.82
Tangent	300	180	-	0	0	0	-	0	3.0	600.00

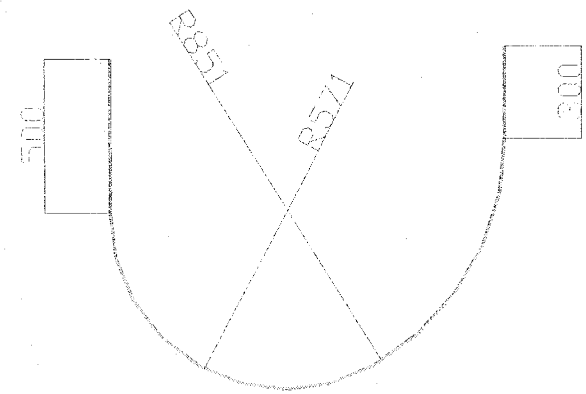

Figure 19 Test Alignment – 9

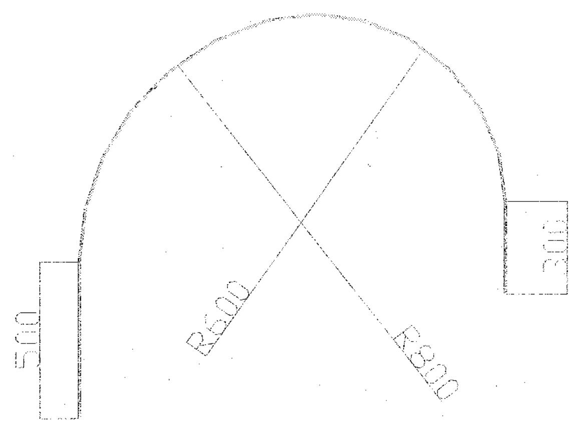

Figure 20 Test Alignment – 10

Table- 31 Detail Geometric Information on Test Alignment-11

11										
Design Speed(Km/H)		SSD(M)	R_{min}(M)	Min Distance(M)		Total Length(M)		Driving Time(sec)		
80		106.2295	265.23	72.62		2879.12		129.56		
Feature	Tangent		Curve Turning	Horizontal Curve					Cross Sectional Details	Available Sight Distance
	L_T	Azimuth Nd^0E		PC	PT	L_c	R (M)	Δ_c^0	Lane Wd (M)	
Tangent	500	0	-	0	0	0	-	0	3.0	356.80
Curve	0	75	R	500	1540.653	1040.653	795	75	3.0	235.42
Curve	0	-10	L	1540.653	2579.123	1038.471	700	85	3.0	600.00
Tangent	300	-10	-	0	0	0	-	0	3.0	600.00

Table- 32 Detail Geometric Information on Test Alignment-12

12										
Design Speed(Km/H)		SSD(M)	R_{min}(M)	Min Distance(M)		Total Length(M)		Driving Time(sec)		
80		106.2295	265.23	72.62		2948.83		132.70		
Feature	Tangent		Curve Turning	Horizontal Curve					Cross Sectional Details	Available Sight Distance
	L_T	Azimuth Nd^0E		PC	PT	L_c	R (M)	Δ_c^0	Lane Wd (M)	
Tangent	500	180	-	0	0	0	-	0	3.0	600.00
Curve	0	90	L	500	1451.903	951.9026	606	90	3.0	600.00
Curve	0	160	R	1451.903	2448.835	996.9321	816	70	3.0	223.65
Tangent	500	160	-	0	0	0	-	0	3.0	600.00

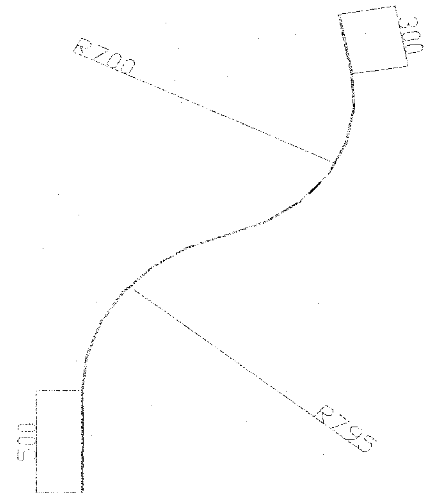

Figure 21 Test Alignment – 11

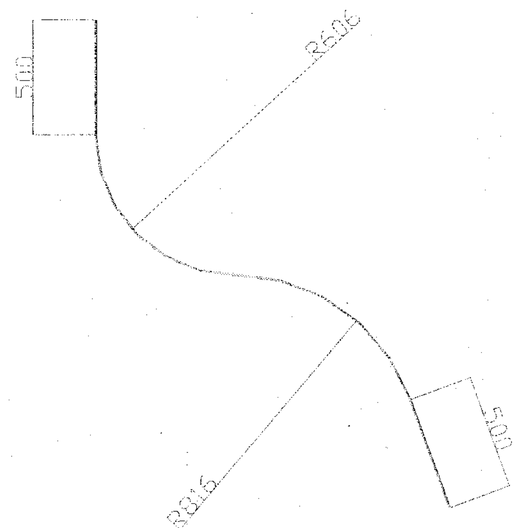

Figure 22 Test Alignment – 12

Table- 33 Detail Geometric Information on Test Alignment-13

13										
Design Speed(Km/H)		SSD(M)	R_{min}(M)	Min Distance(M)		Total Length(M)		Driving Time(sec)		
80		106.2295	265.23	72.62		2778.65		125.04		
Feature	Tangent		Curve Turning	Horizontal Curve					Cross Sectional Details	Available Sight Distance
	L_T	Azimuth Nd^0E		PC	PT	L_c	R (M)	Δ_C^0	Lane Wd (M)	
Tangent	600	180	-	0	0	0	-	0	3.0	600.00
Curve	0	30	L	600	2178.65	1578.65	603	150	3.0	600.00
Tangent	600	30	-	0	0	0	-	0	3.0	600.00

Table- 34 Detail Geometric Information on Test Alignment-14

14										
Design Speed(Km/H)		SSD(M)	R_{min}(M)	Min Distance(M)		Total Length(M)		Driving Time(sec)		
80		106.2295	265.23	72.62		2685.40		120.84		
Feature	Tangent		Curve Turning	Horizontal Curve					Cross Sectional Details	Available Sight Distance
	L_T	Azimuth Nd^0E		PC	PT	L_c	R (M)	Δ_C^0	Lane Wd (M)	
Tangent	950	180	-	0	0	0	-	0	3.1	600.00
Curve	0	80	L	950	1735.398	785.3982	450	100	3.1	600.00
Tangent	950	80	-	0	0	0	-	0	3.1	600.00

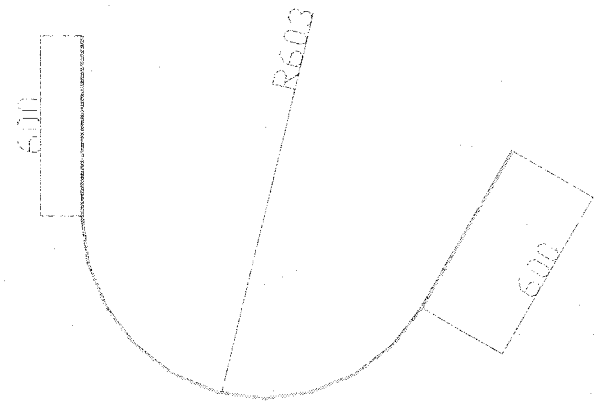

Figure 23 Test Alignment – 13

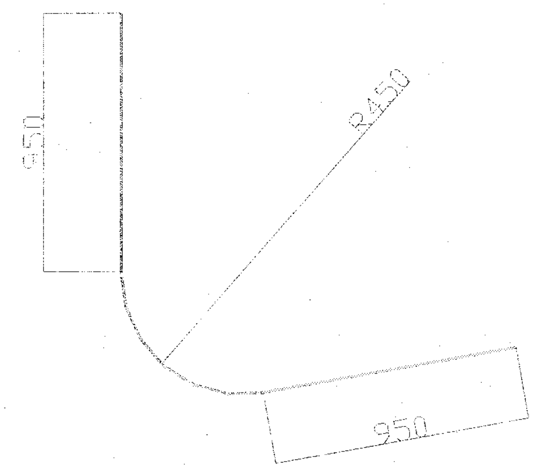

Figure 24 Test Alignment – 14

Table- 35 Detail Geometric Information on Test Alignment-15

15											
Design Speed(Km/H)		SSD(M)	R_{min}(M)	Min Distance(M)		Total Length(M)		Driving Time(sec)			
80		106.2295	265.23	72.62		2623.96		118.08			
Feature	Tangent		Curve Turning	Horizontal Curve					Cross Sectional Details	Available Sight Distance
	L_T	Azimuth Nd^0E		PC	PT	L_c	R (M)	Δ_c^0	Lane Wd (M)	
Tangent	1000	180	-	0	0	0	-	0	3.6	600.00
Curve	0	50	L	1000	1623.955	623.9552	275	130	3.6	600.00
Tangent	1000	50	-	0	0	0	-	0	3.6	600.00

Table- 36 Detail Geometric Information on Test Alignment-16

16											
Design Speed(Km/H)		SSD(M)	R_{min}(M)	Min Distance(M)		Total Length(M)		Driving Time(sec)			
80		106.2295	265.23	72.62		2751.16		123.80			
Feature	Tangent		Curve Turning	Horizontal Curve					Cross Sectional Details	Available Sight Distance
	L_T	Azimuth Nd^0E		PC	PT	L_c	R (M)	Δ_c^0	Lane Wd (M)	
Tangent	600	0	-	0	0	0	-	0	3.0	390.56
Curve	0	125	R	600	2151.161	1551.161	711	125	3.0	193.89
Tangent	600	125	-	0	0	0	-	0	3.0	600.00

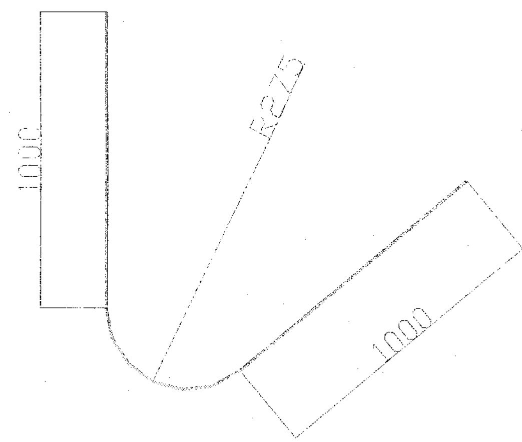

Figure 25 Test Alignment – 15

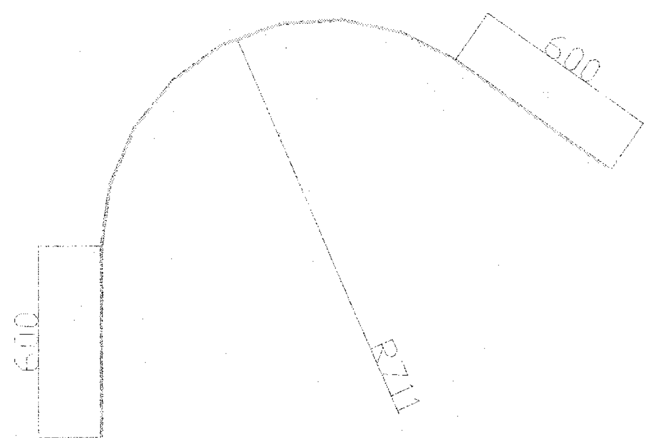

Figure 26 Test Alignment – 16

Table- 37 Detail Geometric Information on Test Alignment-17

17										
Design Speed(Km/H)		SSD(M)	R_{min}(M)	Min Distance(M)		Total Length(M)		Driving Time(sec)		
80		106.2295	265.23	72.62		2567.59		115.54		
Feature	Tangent		Curve Turning	Horizontal Curve					Cross Sectional Details	Available Sight Distance
	L_T	Azimuth Nd^0E		PC	PT	L_c	R (M)	Δ_c^0	Lane Wd (M)	
Tangent	950	0	-	0	0	0	-	0	3.15	449.40
Curve	0	90	R	950	1617.588	667.5884	425	90	3.15	184.73
Tangent	950	90	-	0	0	0	-	0	3.15	600.00

Table- 38 Detail Geometric Information on Test Alignment-18

18										
Design Speed(Km/H)		SSD(M)	R_{min}(M)	Min Distance(M)		Total Length(M)		Driving Time(sec)		
80		106.2295	265.23	72.62		2812.45		126.56		
Feature	Tangent		Curve Turning	Horizontal Curve					Cross Sectional Details	Available Sight Distance
	L_T	Azimuth Nd^0E		PC	PT	L_c	R (M)	Δ_c^0	Lane Wd (M)	
Tangent	1000	0	-	0	0	0	-	0	3.6	448.54
Curve	0	175	R	1000	1812.451	812.4508	266	175	3.6	150.06
Tangent	1000	175	-	0	0	0	-	0	3.6	600.00

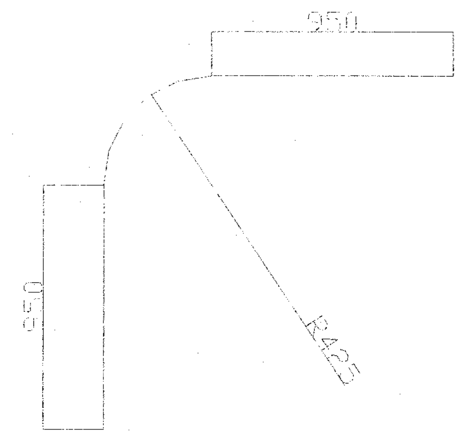

Figure 27 Test Alignment – 17

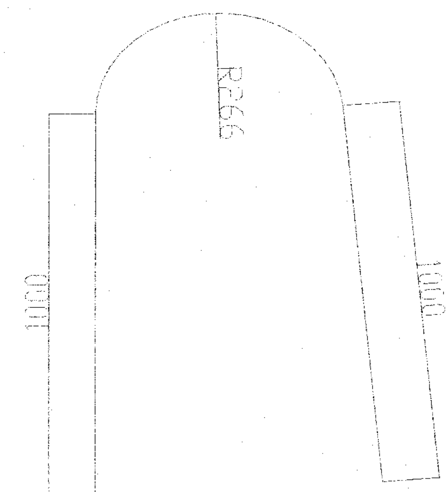

Figure 28 Test Alignment – 18

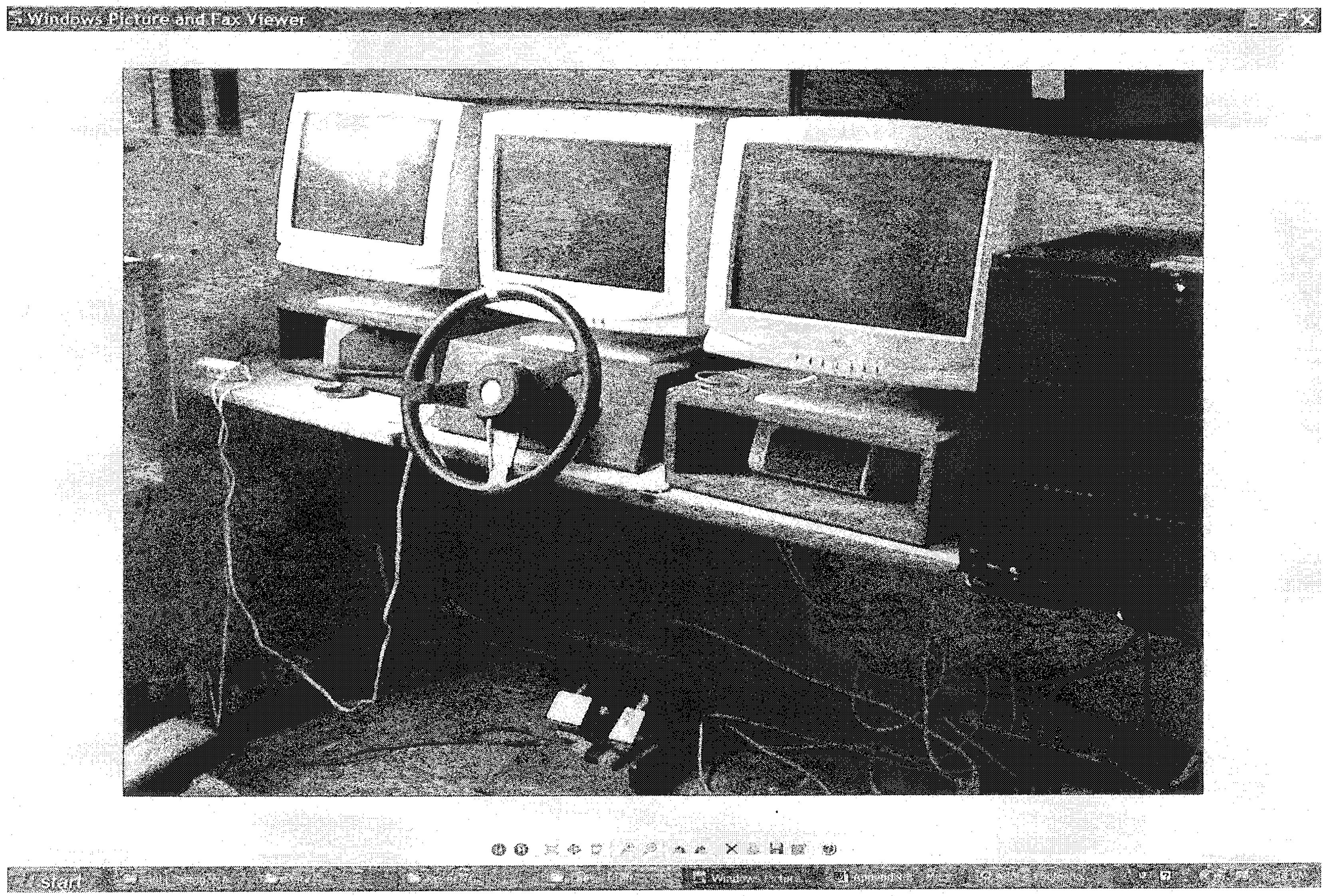

Figure 29 STISIM Simulator at ETC Lab in UFT

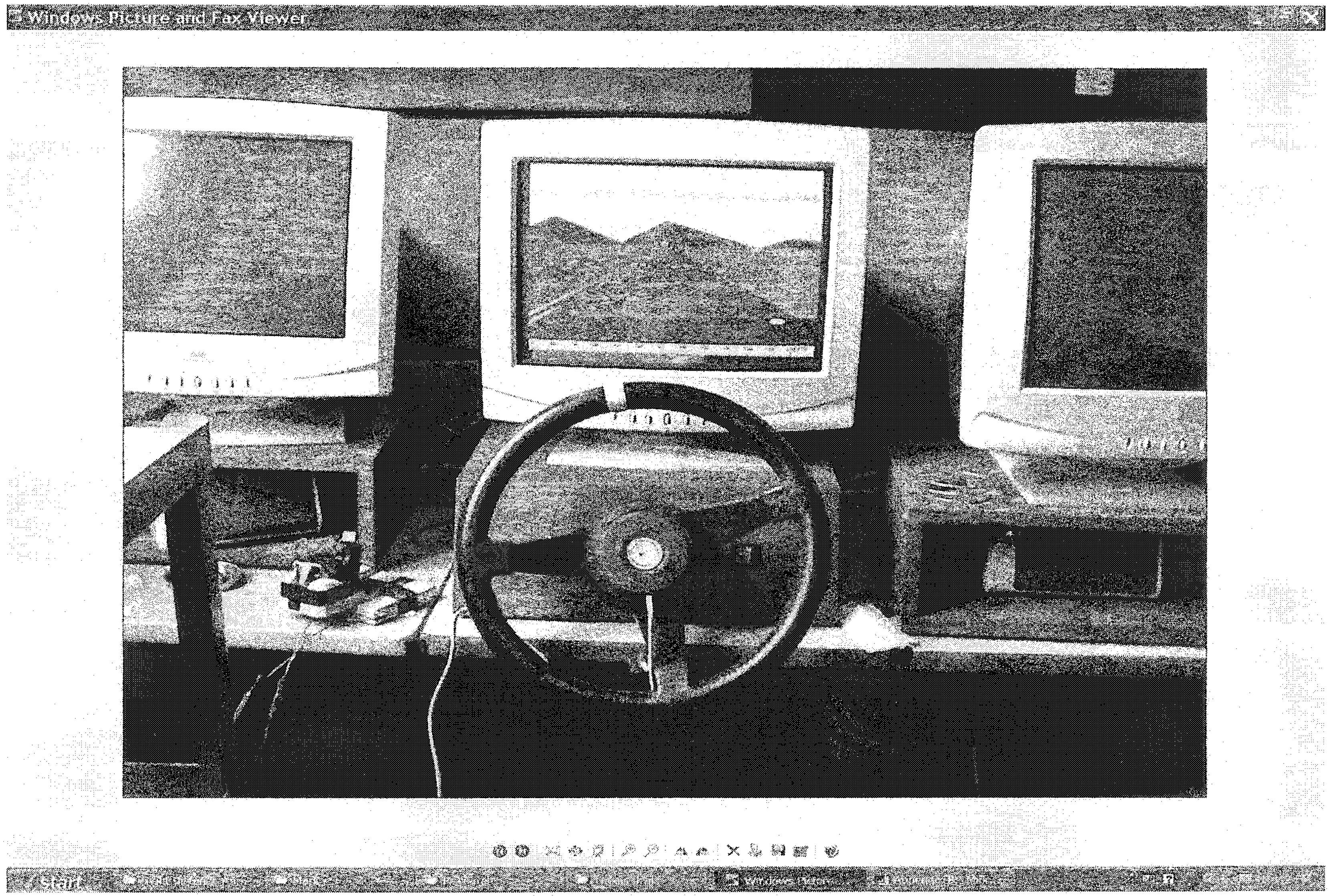

Figure 30 Simulated Alignment in STISIM Simulator

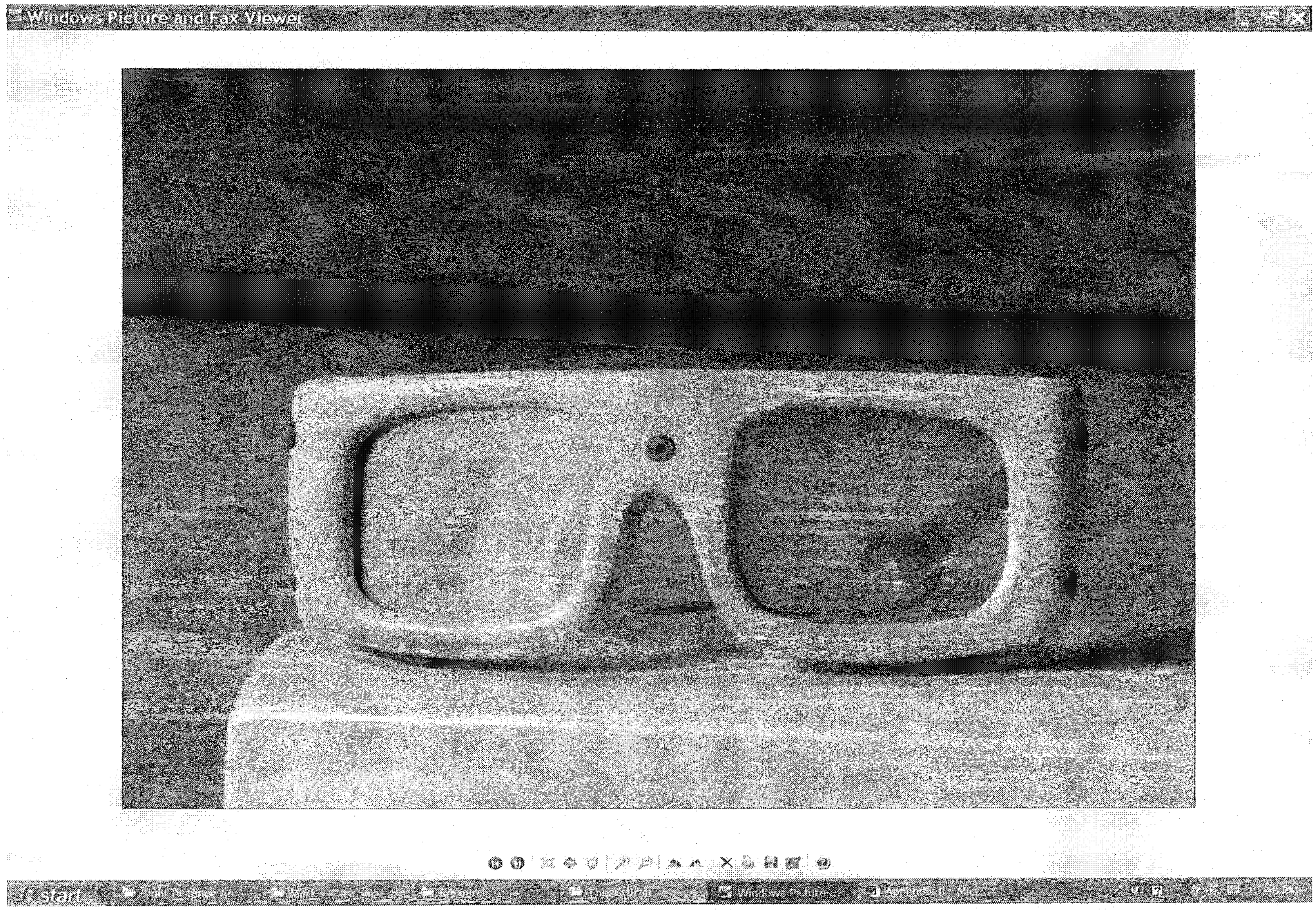

Figure 31 Plato Vision Spectacle Operating with ToTal Control

Appendix C

SUMMARY OUTPUT AND RESULTS ON SIMULATOR PILOT STUDY

SUMMARY OUTPUT	$VD_{0.5L}$							
Regression Statistics								
Multiple R	0.549789568							
R Square	0.30226857							
Adjusted R Square	0.296928788	0.544911725						
Standard Error	0.106677897	**$VD_{0.5L}$=0.519+0.081*PE-0.066*LW-6.34E-05*AASD**						
Observations	396							
ANOVA								
	df	*SS*	*MS*	*F*	*Significance F*			
Regression	3	1.93258972	0.644197	56.60692	2.01853E-30			
Residual	392	4.461028125	0.01138					
Total	395	6.393617845						
	Coefficients	*Standard Error*	*t Stat*	*P-value*	*Lower 95%*	*Upper 95%*	*Lower 95.0%*	*Upper 95.0%*
Intercept	0.519424684	0.084410668	6.153543	1.87E-09	0.35347023	0.685379	0.35347023	0.685379138
PE	0.081285562	0.006449497	12.6034	8.21E-31	0.068605615	0.093966	0.068605615	0.093965509
LW	-0.065958352	0.024960236	-2.64254	0.008558	-0.115031088	-0.01689	-0.115031088	-0.016885616
AASD	-6.34134E-05	3.82587E-05	-1.65749	0.09822	-0.000138631	1.18E-05	-0.000138631	1.18046E-05

Model developed on VDH during Pilot Study

SUMMARY OUTPUT	$VD_{0.5L}$							
Regression Statistics								
Multiple R	0.593870615							
R Square	0.352682308							
Adjusted R Square	0.346060132	0.588268758						
Standard Error	0.102883018	**$VD_{0.5L}$=0.472+0.089*PE-0.070*LW+0.02*Turning+14.117*INVR**						
Observations	396							
ANOVA								
	df	*SS*	*MS*	*F*	*Significance F*			
Regression	4	2.254915898	0.563729	53.25777	8.2842E-36			
Residual	391	4.138701947	0.010585					
Total	395	6.393617845						
	Coefficients	*Standard Error*	*t Stat*	*P-value*	*Lower 95%*	*Upper 95%*	*Lower 95.0%*	*Upper 95.0%*
Intercept	0.472139811	0.078199329	6.037645	3.64E-09	0.318396009	0.625884	0.318396009	0.625883614
PE	0.089823118	0.006351323	14.14243	5.79E-37	0.077336098	0.10231	0.077336098	0.102310139
LW	-0.070465967	0.024086242	-2.92557	0.003639	-0.117820726	-0.02311	-0.117820726	-0.023111207
Turning	0.01737849	0.010541811	1.64853	0.100047	-0.003347239	0.038104	-0.003347239	0.038104218
INVR	14.11744514	7.019835332	2.011079	0.045003	0.31609684	27.91879	0.31609684	27.91879344

Model developed on VDH during Pilot Study

SUMMARY OUTPUT	$VD_{0.5L}$							
Regression Statistics								
Multiple R	0.588206222							
R Square	0.34598656							
Adjusted R Square	0.340981355	0.583936088						
Standard Error	0.103281762	**$VD_{0.5L}$=0.453+0.089*PE-0.063*LW+0.03*Turning**						
Observations	396							
ANOVA								
	df	*SS*	*MS*	*F*	*Significance F*			
Regression	3	2.212105845	0.737369	69.12535	6.69883E-36			
Residual	392	4.181512	0.010667					
Total	395	6.393617845						
	Coefficients	*Standard Error*	*t Stat*	*P-value*	*Lower 95%*	*Upper 95%*	*Lower 95.0%*	*Upper 95.0%*
Intercept	0.452967469	0.07791686	5.813472	1.27E-08	0.299780079	0.606155	0.299780079	0.60615486
PE	0.088897201	0.006359165	13.97938	2.58E-36	0.076394851	0.1014	0.076394851	0.101399552
LW	-0.063378342	0.023919357	-2.64967	0.008383	-0.110404671	-0.01635	-0.110404671	-0.016352012
Turning	0.034324435	0.006359165	5.397632	1.17E-07	0.021822084	0.046827	0.021822084	0.046826786

Model developed on VDH during Pilot Study

SUMMARY OUTPUT	$VD_{0.5L}$							
Regression Statistics								
Multiple R	0.590070434							
R Square	0.348183118							
Adjusted R Square	0.343194723	0.585828237						
Standard Error	0.103108176	**$VD_{0.5L}$=0.489+0.089*PE-0.074*LW+23.367*INVR**						
Observations	396							
ANOVA								
	df	*SS*	*MS*	*F*	*Significance F*			
Regression	3	2.226149794	0.74205	69.79863	3.47523E-36			
Residual	392	4.16746805	0.010631					
Total	395	6.393617845						
	Coefficients	*Standard Error*	*t Stat*	*P-value*	*Lower 95%*	*Upper 95%*	*Lower 95.0%*	*Upper 95.0%*
Intercept	0.489015761	0.077696045	6.29396	8.29E-10	0.336262501	0.641769	0.336262501	0.641769022
PE	0.089170653	0.006352852	14.03632	1.51E-36	0.076680713	0.101661	0.076680713	0.101660593
LW	-0.074486601	0.024014885	-3.10168	0.002063	- 0.121700742	-0.02727	- 0.121700742	-0.02727246
INVR	23.36751815	4.227477277	5.527533	5.94E-08	15.05614349	31.67889	15.05614349	31.67889281

Model developed on VDH during Pilot Study

Appendix D

Model Information on Visual Demand

Model Information on Visual Demand on Complex Curves

VDF = PEINVR*PE LW INVR
Response Distribution: Normal
Link Function: Log

Nominal Variable Information

Level	PE
1	CC
2	RC
3	TC

Parameter Information

Parameter	Variable	PE
1	Intercept	
2	PEINVR*PE	CC
3		RC
4		TC
5	LW	
6	INVR	

Model Equation

Log(VDF)= - 0.7885+ 63.6379 PEINVR*CC+49.1648 INVR+ 67.0418 PEINVR*RC- 0.0901 LW

Summary of Fit

Mean of Response	0.4072	Deviance	6.6671	Pearson ChiSq	6.6671
SCALE (MLE)	0.1001	Deviance / DF	0.0101	Pearson ChiSq / DF	0.0101

Analysis of Deviance

Source	DF	Deviance	Deviance / DF
Model	4	1.0128	0.2532
Error	661	6.6671	0.0101
C Total	665	7.6799	.

Type III (Wald) Tests

Source	DF	ChiSq	Pr > ChiSq
PEINVR*PE	2	93.0931	<.0001
LW	1	3.9950	0.0456
INVR	1	16.4503	<.0001

Parameter Estimates

Variable	PE	DF	Estimate	Std Error	ChiSq	Pr > ChiSq
Intercept		1	-0.7885	0.1432	30.3039	<.0001
PEINVR*PE	CC	1	63.6379	10.2641	38.4406	<.0001
	RC	1	67.0418	7.5320	79.2273	<.0001
	TC	0	0.0000	.	.	.
LW		1	-0.0901	0.0451	3.9950	0.0456
INVR		1	49.1648	12.1218	16.4503	<.0001

VDH = PEINVR*PE INVR*DELTA
Response Distribution: Normal
Link Function: Log

Nominal Variable Information

Level	PE
1	CC
2	RC
3	TC

Parameter Information

Parameter	Variable	PE
1	Intercept	
2	PEINVR*PE	CC
3		RC
4		TC
5	INVR*DELTA	

Model Equation

Log(VDH)= -1.1010+ 109.9361 PEINVR*CC + 123.7533 PEINVR*RC + 0.2663 INVR*DELTA

Summary of Fit

Mean of Response	0.3938	Deviance	8.4609	Pearson ChiSq	8.4609
SCALE (MLE)	0.1127	Deviance / DF	0.0128	Pearson ChiSq / DF	0.0128

Analysis of Deviance

Source	DF	Deviance	Deviance / DF
Model	3	2.7176	0.9059
Error	662	8.4609	0.0128
C Total	665	11.1785	.

Type III (Wald) Tests

Source	DF	ChiSq	Pr > ChiSq
PEINVR*PE	2	226.5422	<.0001
INVR*DELTA	1	4.7767	0.0288

Parameter Estimates

Variable	PE	DF	Estimate	Std Error	ChiSq	Pr > ChiSq
Intercept		1	-1.1010	0.0235	2196.6763	<.0001
PEINVR*PE	CC	1	109.9361	11.6875	88.4790	<.0001
	RC	1	123.7533	8.5771	208.1778	<.0001
	TC	0	0.0000	.	.	.
INVR*DELTA		1	0.2663	0.1219	4.7767	0.0288

VDH = PEINVR*PE INVR*DELTA LW
Response Distribution: Normal
Link Function: Log

Nominal Variable Information

Level	PE
1	CC
2	RC
3	TC

Parameter Information

Parameter	Variable	PE
1	Intercept	
2	PEINVR*PE	CC
3		RC
4		TC
5	INVR*DELTA	
6	LW	

Model Equation

Log(VDH)= -0.6544+110.9792PEINVR*CC-0.1397LW+124.7537 PEINVR*RC+0.3188INVR*DELTA

Summary of Fit

Mean of Response	0.3938	Deviance	8.3676	Pearson ChiSq	8.3676
SCALE (MLE)	0.1121	Deviance / DF	0.0127	Pearson ChiSq / DF	0.0127

Analysis of Deviance

Source	DF	Deviance	Deviance / DF
Model	4	2.8109	0.7027
Error	661	8.3676	0.0127
C Total	665	11.1785	.

Type III (Wald) Tests

Source	DF	ChiSq	Pr > ChiSq
PEINVR*PE	2	232.5291	<.0001
INVR*DELTA	1	6.4676	0.0110
LW	1	7.2890	0.0069

Parameter Estimates

Variable	PE	DF	Estimate	Std Error	ChiSq	Pr > ChiSq
Intercept		1	-0.6544	0.1666	15.4301	<.0001
PEINVR*PE	CC	1	110.9792	11.6761	90.3414	<.0001
	RC	1	124.7537	8.5247	214.1662	<.0001
	TC	0	0.0000	.	.	.
INVR*DELTA		1	0.3188	0.1254	6.4676	0.0110
LW		1	-0.1397	0.0518	7.2890	0.0069

VDH = PEINVR*PE INVR*PETD LW DELTA
Response Distribution: Normal
Link Function: Log

Nominal Variable Information

Level	PE	PETD
1	CC	L
2	RC	R
3	TC	S

Parameter Information

Parameter	Variable	PE	PETD
1	Intercept		
2	PEINVR*PE	CC	
3		RC	
4		TC	
5	INVR*PETD		L
6			R
7			S
8	LW		
9	DELTA		

Model Equation

Log (VDH) = - 0.7409 + 55.7993 PEINVR*CC + 39.1801 INVR*PETD(R) - 27.5422 INVR*PETD(S)- 0.1081 LW + 78.5313 PEINVR*RC + 51.2844 INVR*PETD(L)+ 0.0012 DELTA

Summary of Fit

Mean of Response	0.3938	Deviance	8.1552	Pearson ChiSq	8.1552
SCALE (MLE)	0.1107	Deviance / DF	0.0124	Pearson ChiSq / DF	0.0124

Analysis of Deviance

Source	DF	Deviance	Deviance / DF
Model	7	3.0233	0.4319
Error	658	8.1552	0.0124
C Total	665	11.1785	.

Type III (Wald) Tests

Source	DF	ChiSq	Pr > ChiSq
PEINVR*PE	2	28.0384	<.0001
INVR*PETD	3	14.4257	0.0024
LW	1	4.1791	0.0409
DELTA	1	9.2262	0.0024

Parameter Estimates

Variable	PE	PETD	DF	Estimate	Std Error	ChiSq	Pr > ChiSq
Intercept			1	-0.7409	0.1728	18.3786	<.0001
PEINVR*PE	CC		1	55.7993	21.0776	7.0084	0.0081
	RC		1	78.5313	16.2658	23.3095	<.0001
	TC		0	0.0000	.	.	.
INVR*PETD		L	1	51.2844	22.0698	5.3998	0.0201
		R	1	39.1801	21.4378	3.3402	0.0676
		S	1	-27.5422	15.4128	3.1933	0.0739
LW			1	-0.1081	0.0529	4.1791	0.0409
DELTA			1	0.0012	0.0004	9.2262	0.0024

VDH = PEINVR*PE INVR*PETD
Response Distribution: Normal
Link Function: Log

Nominal Variable Information

Level	PE	PETD
1	CC	L
2	RC	R
3	TC	S

Parameter Information

Parameter	Variable	PE	PETD
1	Intercept		
2	PEINVR*PE	CC	
3		RC	
4		TC	
5	INVR*PETD		L
6			R
7			S

Model Equation

Log(VDH) = - 1.0125 + 47.0189 PEINVR*CC + 37.8843 INVR*PETD(R)- 29.9977 INVR*PETD(S) + 70.0593 PEINVR*RC + 45.6892 INVR*PETD(L)

Summary of Fit

Mean of Response	0.3938	Deviance	8.3477	Pearson ChiSq	8.3477
SCALE (MLE)	0.1120	Deviance / DF	0.0126	Pearson ChiSq / DF	0.0126

Analysis of Deviance

Source	DF	Deviance	Deviance / DF
Model	5	2.8308	0.5662
Error	660	8.3477	0.0126
C Total	665	11.1785	.

Type III (Wald) Tests

Source	DF	ChiSq	Pr > ChiSq
PEINVR*PE	2	23.6137	<.0001
INVR*PETD	3	13.7140	0.0033

Parameter Estimates

Variable	PE	PETD	DF	Estimate	Std Error	ChiSq	Pr > ChiSq
Intercept			1	-1.0125	0.0356	809.2510	<.0001
PEINVR*PE	CC		1	47.0189	20.4332	5.2951	0.0214
	RC		1	70.0593	15.8304	19.5862	<.0001
	TC		0	0.0000	.	.	.
INVR*PETD		L	1	45.6892	21.5109	4.5114	0.0337
		R	1	37.8843	20.6090	3.3791	0.0660
		S	1	-29.9977	15.3552	3.8165	0.0507

VDH = PEINVR*PE LW DELTA PETD

Response Distribution: Normal

Link Function: Log

Nominal Variable Information

Level	PE	PETD
1	CC	L
2	RC	R
3	TC	S

Parameter Information

Parameter	Variable	PE	PETD
1	Intercept		
2	PEINVR*PE	CC	
3		RC	
4		TC	
5	LW		
6	DELTA		
7	PETD		L
8			R
9			S

Model Equation

Log(VDH) = - 0.8421+ 66.1310 PEINVR*CC+ 0.0012 DELTA+ 0.1562 PETD*L+ 0.1360 PETD*R+ 84.8172 PEINVR*RC - 0.0981 LW

Summary of Fit

Mean of Response	0.3938	Deviance	8.1912	Pearson ChiSq	8.1912
SCALE (MLE)	0.1109	Deviance / DF	0.0124	Pearson ChiSq / DF	0.0124

Analysis of Deviance

Source	DF	Deviance	Deviance / DF
Model	6	2.9873	0.4979
Error	659	8.1912	0.0124
C Total	665	11.1785	.

Type III (Wald) Tests

Source	DF	ChiSq	Pr > ChiSq
PEINVR*PE	2	30.7089	<.0001
LW	1	3.7177	0.0538
DELTA	1	9.7658	0.0018
PETD	2	11.4066	0.0033

Parameter Estimates

Variable	PE	PETD	DF	Estimate	Std Error	ChiSq	Pr > ChiSq
Intercept			1	-0.8421	0.1708	24.3034	<.0001
PEINVR*PE	CC		1	66.1310	19.6269	11.3529	0.0008
	RC		1	84.8172	15.7668	28.9386	<.0001
	TC		0	0.0000	.	.	.
LW			1	-0.0981	0.0509	3.7177	0.0538
DELTA			1	0.0012	0.0004	9.7658	0.0018
PETD		L	1	0.1562	0.0466	11.2435	0.0008
		R	1	0.1360	0.0465	8.5613	0.0034
		S	0	0.0000	.	.	.

VD30 = PEINVR*PE INVR LW
Response Distribution: Normal
Link Function: Log

Nominal Variable Information

Level	PE
1	CC
2	RC
3	TC

Parameter Information

Parameter	Variable	PE
1	Intercept	
2	PEINVR*PE	CC
3		RC
4		TC
5	INVR	
6	LW	

Model Equation

Log(VD30)= -0.8617+136.2555 PEINVR*CC-0.1112 LW +149.7696 PEINVR*RC+34.9016 INVR

Summary of Fit

Mean of Response	0.3780	Deviance	14.5607	Pearson ChiSq	14.5607
SCALE (MLE)	0.1479	Deviance / DF	0.0220	Pearson ChiSq / DF	0.0220

Analysis of Deviance

Source	DF	Deviance	Deviance / DF
Model	4	4.0774	1.0193
Error	661	14.5607	0.0220
C Total	665	18.6381	.

Type III (Wald) Tests

Source	DF	ChiSq	Pr > ChiSq
PEINVR*PE	2	202.0667	<.0001
INVR	1	3.0875	0.0789
LW	1	2.4588	0.1169

Parameter Estimates

Variable	PE	DF	Estimate	Std Error	ChiSq	Pr > ChiSq
Intercept		1	-0.8617	0.2262	14.5148	0.0001
PEINVR*PE	CC	1	136.2555	15.2253	80.0902	<.0001
	RC	1	149.7696	11.0318	184.3121	<.0001
	TC	0	0.0000	.	.	.
INVR		1	34.9016	19.8630	3.0875	0.0789
LW		1	-0.1112	0.0709	2.4588	0.1169

VD30 = PEINVR*PE
Response Distribution: Normal
Link Function: Log

Nominal Variable Information

Level	PE
1	CC
2	RC
3	TC

Parameter Information

Parameter	Variable	PE
1	Intercept	
2	PEINVR*PE	CC
3		RC
4		TC

Model Equation

Log(VD30) = - 1.1461 + 137.9472 PEINVR*CC + 149.2060 PEINVR*RC

Summary of Fit

Mean of Response	0.3780	Deviance	14.6613	Pearson ChiSq	14.6613
SCALE (MLE)	0.1484	Deviance / DF	0.0221	Pearson ChiSq / DF	0.0221

Analysis of Deviance

Source	DF	Deviance	Deviance / DF
Model	2	3.9768	1.9884
Error	663	14.6613	0.0221
C Total	665	18.6381	.

Type III (Wald) Tests

Source	DF	ChiSq	Pr > ChiSq
PEINVR*PE	2	197.4992	<.0001

Parameter Estimates

Variable	PE	DF	Estimate	Std Error	ChiSq	Pr > ChiSq
Intercept		1	-1.1461	0.0226	2582.5876	<.0001
PEINVR*PE	CC	1	137.9472	15.3064	81.2228	<.0001
	RC	1	149.2060	11.1453	179.2208	<.0001
	TC	0	0.0000	.	.	.

Model Information on Visual Demand on Tangents

VDF	=	PEDEL*LW	PEINVR*PETD
	Response Distribution:	Normal	
	Link Function:	Log	

Nominal Variable Information

Level	PETD
1	L
2	R

Parameter Information

Parameter	Variable	PETD
1	Intercept	
2	PEDEL*LW	
3	PEINVR*PETD	L
4		R

Model Equation

Log(VDF)= -0.9973 -0.0002PEDEL*LW +46.5084 PEINVR*PETD(L)+36.5381 PEINVR*PETD(R)

Summary of Fit

Mean of Response	0.3879	Deviance	4.0858	Pearson ChiSq	4.0858
SCALE (MLE)	0.1065	Deviance / DF	0.0115	Pearson ChiSq / DF	0.0115

Analysis of Deviance

Source	DF	Deviance	Deviance / DF
Model	3	0.0776	0.0259
Error	356	4.0858	0.0115
C Total	359	4.1634	.

Type III (Wald) Tests

Source	DF	ChiSq	Pr > ChiSq
PEDEL*LW	1	2.6937	0.1007
PEINVR*PETD	2	5.8731	0.0530

Parameter Estimates

Variable	PETD	DF	Estimate	Std Error	ChiSq	Pr > ChiSq
Intercept		1	-0.9973	0.0467	455.5481	<.0001
PEDEL*LW		1	-0.0002	0.0001	2.6937	0.1007
PEINVR*PETD	L	1	46.5084	19.8692	5.4790	0.0192
	R	1	36.5381	23.2646	2.4666	0.1163

VDH = PEDEL*LW PEINVR*PETD
Response Distribution: Normal
Link Function: Log

Nominal Variable Information

Level	PETD
1	L
2	R

Parameter Information

Parameter	Variable	PETD
1	Intercept	
2	PEDEL*LW	
3	PEINVR*PETD	L
4		R

Model Equation

Log(VDH)= -1.0129 -0.0003PEDEL*LW +74.5767 PEINVR*PETD(L)+75.4603 PEINVR*PETD(R)

Summary of Fit

Mean of Response	0.4060	Deviance	4.4605	Pearson ChiSq	4.4605
SCALE (MLE)	0.1113	Deviance / DF	0.0125	Pearson ChiSq / DF	0.0125

Analysis of Deviance

Source	DF	Deviance	Deviance / DF
Model	3	0.1933	0.0644
Error	356	4.4605	0.0125
C Total	359	4.6538	.

Type III (Wald) Tests

Source	DF	ChiSq	Pr > ChiSq
PEDEL*LW	1	4.7298	0.0296
PEINVR*PETD	2	14.1616	0.0008

Parameter Estimates

Variable	PETD	DF	Estimate	Std Error	ChiSq	Pr > ChiSq
Intercept		1	-1.0129	0.0472	460.1599	<.0001
PEDEL*LW		1	-0.0003	0.0001	4.7298	0.0296
PEINVR*PETD	L	1	74.5767	19.8516	14.1129	0.0002
	R	1	75.4603	23.3205	10.4703	0.0012

VD30 = PEDEL*LW PEINVR*PETD
Response Distribution: Normal
Link Function: Log

Nominal Variable Information

Level	PETD
1	L
2	R

Parameter Information

Parameter	Variable	PETD
1	Intercept	
2	PEDEL*LW	
3	PEINVR*PETD	L
4		R

Model Equation

Log(VD30)= -1.0526 - 0.0005PEDEL*LW +78.2150PEINVR*PETD(L)+80.2572PEINVR*PETD(R)

Summary of Fit

Mean of Response	0.3760	Deviance	8.6151	Pearson ChiSq	8.6151
SCALE (MLE)	0.1547	Deviance / DF	0.0242	Pearson ChiSq / DF	0.0242

Analysis of Deviance

Source	DF	Deviance	Deviance / DF
Model	3	0.2792	0.0931
Error	356	8.6151	0.0242
C Total	359	8.8943	.

Type III (Wald) Tests

Source	DF	ChiSq	Pr > ChiSq
PEDEL*LW	1	7.1697	0.0074
PEINVR*PETD	2	6.8087	0.0332

Parameter Estimates

Variable	PETD	DF	Estimate	Std Error	ChiSq	Pr > ChiSq
Intercept		1	-1.0526	0.0727	209.5990	<.0001
PEDEL*LW		1	-0.0005	0.0002	7.1697	0.0074
PEINVR*PETD	L	1	78.2150	30.0474	6.7759	0.0092
	R	1	80.2572	35.4967	5.1120	0.0238

Appendix E

FORMS

Experimental Explanatory Statement for Informed Consent

Project Title: **<u>Evaluation of Highway Design Consistency with respect to Driver's Visual Demand in a 2-D Environment</u>**

My name is Chandi Ganguly and I am studying for my M.A.Sc (Civil Engineering) at Ryerson University. This research project is an important component of my thesis and I am undertaking my research project under the supervision of Dr. Said Easa, Chair of Civil Engineering Department at the Ryerson University in Toronto.

The aim of this research project is to investigate Consistency of existing or proposed highway design with respect to Driver's visual demand and or mental workload. The findings of this research project will be important for the future of road safety in Canada and North America as well. The results will be used for my thesis and may be published in professional publications as well.

I am seeking **people who have held a driving license for at least three years** who are prepared to drive a high-tech driving simulator. The procedure will take approximately one and half hour of your time, and will be undertaken at the **Ergonomics in Tele-operation and Control Laboratory in the Department of Mechanical and Industrial Engineering at University of Toronto**, situated at the **3rd floor of 4, Taddle Creek Road**. For your time, you will be paid $10 per hour. "*None of the procedures used in this study are experimental in nature. The only experimental aspect of this study is the gathering of information for the purpose of analysis.*"

As with all devices of this type, some people have reported feelings of discomfort during or after their drives in the simulator. These effects are usually not serious and last only a short time. Should they occur, you will not be able to carry out the experimentation further in this research study, therefore it is advisable that you let me know if you start feeling any discomfort, and the session will be concluded.

No findings which could identify any individual participant will be published. The anonymity of your participation is assured by our procedure, in which your name will not be associated with your simulator data which is collected. Access to data is restricted to my supervisor, Dr. Paul Milgram (Faculty Mechanical and Industrial Department at University of Toronto), and myself. Coded data will be stored for schedule time, as prescribed by University regulations.

Participation in this research is entirely voluntary, and if you agree to participate, you may withdraw your consent at any time by indicating this to the experimenter. You may also decline to participate in any section of the procedure. Whether or not you participate in the study will not influence your academic performance, academic standing, or future relations with Ryerson.

If you have any queries or would like to be informed of the aggregate research finding, please contact Chandi Ganguly on telephone (416) 979 5000 extension 7043

Should you have any complaint concerning the manner in which this research is conducted, please do not hesitate to contact:

Dr. Said Easa, Chair, Civil Engineering Department,
Ryerson University,
350 Victoria Street, Toronto, ON M5B 2K3
Telephone # (416) 979 5000 Ext: 6451

You may also contact:

Research Ethics Board, c/o Office of Research Services,
Ryerson Polytechnic University,
350 Victoria Street,
Toronto, ON M5B 2K3

Thank you.

Chandi Ganguly

Informed Consent Form

Project Title: Evaluation of Consistency of highway Design with Respect to Driver's Workload

I agree to take part in the above Ryerson University research project. I have had the project explained to me, and I have read and understood the Explanatory Statement, which I retain for my records.

I understand that any information I provide is confidential, and that no information that could lead to the identification of any individual will be disclosed in any reports on the project, or to any other party.

I also understand that my participation is voluntary, that I can choose not to participate, and that I can withdraw my participation at any stage of the project.

Name: ....(please print)

Signature: ....

Date: ....

______________________________ _______________

Signature of Investigator Date